SPATIAL AND TEMPORAL PATTERNS OF OGALLALA FORMATION DEPOSITION REVEALED BY U-PB ZIRCON GEOCHRONOLOGY

BY

JASON ANDREW HALLMAN

Submitted to the graduate degree program in Geology and the Graduate Faculty of the University of Kansas in partial fulfillment of the requirements for the degree of Master of Science.

____
Co-Chairperson Andreas Möller

____
Co-Chairperson Noah M. McLean

____
Greg A. Ludvigson

____
Mary C. Hill

Date Defended: June 28, 2016

The Thesis Committee for JASON ANDREW HALLMAN
certifies that this is the approved version of the following thesis:

SPATIAL AND TEMPORAL PATTERNS OF OGALLALA FORMATION DEPOSITION
REVEALED BY U-PB ZIRCON GEOCHRONOLOGY

Co-Chairperson Andreas Möller

Co-Chairperson Noah M. McLean

Date approved: June 28, 2016

ABSTRACT

Difficulties in correlation within continental clastic basins arise from the common shortage of reliable marker beds, which limits characterization of geological relationships. In the High Plains of the central United States, an improved understanding of the stratigraphic architecture of the terrestrial Ogallala Formation can be used to improve management of depleted groundwater resources, illuminate the causes of fluvial aggradation, enhance the western US climatic record, and strengthen the temporal precision of the North American Land Mammal Ages. Such relationships can be derived from chronostratigraphic information provided by abundant, dateable, volcanogenic zircon in volcanic ashes and fluvial beds, which provide the first high-precision (ca. 1-5% uncertainty) radioisotopic dates for the Ogallala Formation. These zircon-bearing ashes appear to have travelled ~1350 km from their interpreted sources within the Bruneau-Jarbidge and Twin Falls volcanic centers in Idaho, suggesting that volcanogenic zircon has the previously unappreciated potential to time-stamp terrestrial surfaces at great distances from contemporaneous magmatic centers. Volcanic ash depositional ages are consistent with fluvial maximum depositional ages, indicating that deposition of common lithologies within the Ogallala Formation, including sands, paleosols, and volcanic ashes can be reliably dated with modern, high-precision techniques. Zircon U-Pb LA-ICP-MS results suggest diachronous aggradation of the Ogallala Formation in Kansas, particularly deposition of an inferred Norton lobe in northern Kansas that initiated prior to ~12.5 Ma and aggraded to near-modern levels by 11.7 Ma, measurably earlier than the ~8-9.5 Ma deposition of an inferred Ellis lobe over a bedrock high in central Kansas. The observed diachronous relationships predict aquifer anisotropy that could inform efforts to develop numerical groundwater models designed to forecast aquifer response to different conservation strategies.

ACKNOWLEDGEMENTS

This work was initiated and supported by Dr. Greg Ludvigson and Dr. Jon Smith, who graciously encouraged this foray into High Plains geology. The mentorship of Dr. Noah McLean and Dr. Andreas Möller was expert, patient, and tireless, exceeding what could be expected from any adviser. Much time and energy was devoted to the improvement of this work by Dr. J. Douglas Walker and Dr. Joe Andrew, despite many frustrations and setbacks. Insightful comments and critiques from Dr. Mary C. Hill steered this project in a more realistic and fruitful direction, and discussions with Dr. Michael Blum improved the quality of this work. Thanks are owed to Ben Campanaro, Soroush Rezvanbehbahani, Maggie Graham, Ty Tenpenny, Jeff Oalmann, Tyson Berndt, Josh Feldman, Wayne Dickerson, and members of IGL who provided invaluable assistance, training, and guidance. Analytical techniques proposed in the Boise State University IGL Labshare improved the efficiency and success rate of laboratory procedures. Special thanks are owed to Brian Sitek for splitting fieldwork and for sharing unpublished information, as well as to the Calvert Corporation and Mr. Taylor G. Bemis for granting property access. Partial support for this project comes from the University of Kansas, the Kansas Geological Foundation, the Geological Society of America, and the SIPES Foundation. Logistical and financial support from the KGS was made possible by a National Science Foundation grant to Jon Smith and a USGS STATEMAP grant to the KGS.

TABLE OF CONTENTS

INTRODUCTION

Depositional models of fluvial clastic basins are difficult to develop and often incomplete because correlation on a basin-wide scale is barred by frequent irregular lateral and vertical facies changes, common secondary alteration that obscures original depositional features, and indistinguishable lithologies coupled with a shortage and limited extent of distinctive marker beds (Swinehart, 1974; North and Prosser, 1993; Sweet, 1999; Newell, 2001). The lenticular, indistinct units and frequent absence of viable marker beds often hinders detailed stratigraphic investigations in these basins, which is critical to the understanding of depositional causes and timing, stratigraphic context of fossil assemblages, and the three-dimensional extent of contained mineral or water resources. If understanding of a basin's lithostratigraphy is insufficient for analysis of its stratigraphic architecture, then other tools are needed to supply information about depositional processes and timescales.

Investigating the absolute depositional timing of continental deposits might thus be the best means of unravelling the stratigraphic architecture of basins that preserve dateable material. Ashfall zircon is commonly used to measure the depositional age of marine sequences (e.g. Bowring and Schmitz, 2003; Mundil et al., 2004; Furin et al., 2006; Burgess et al., 2014), but because continental basins are often high energy, alternately erosional and depositional environments vulnerable to weathering and alteration, dateable materials like volcanic ash may be locally absent or difficult to recognize. The chronological record of continental basins has therefore enjoyed less study than the marine record, despite the potential existence of dateable and stratigraphically useful material.

Here we suggest that the dating potential for continental clastic basins based on ashfall deposits may be greater than was previously recognized. Silicic volcanic centers yield frequent eruptions of volcanic ash, of which zircon is a common component. Volcanic ash beds are common in Miocene fluvial sequences of the High Plains of the central United States (Carey et al., 1952; Izett and Wilcox, 1982; Ludvigson et al., 2009), making this area a rich testing ground for dating methods of continental strata. The spatial correlation (Fig. 1) between modern volcanic centers and large, fluvial clastic basins termed distributive fluvial systems (DFSs) by Weissmann et al. (2010) indicates that many of these terrestrial basins might also host similarly dateable deposits. Continental clastic basins beyond Miocene or Holocene age may also commonly contain volcanic material.

Volcanic ash can remain aloft in the atmosphere over distances of thousands of kilometers (Rose et al., 2003), yet little research has been devoted to the heavy mineral content of distal volcanic ashes. The density and geometry of zircon crystals implies that long-distance airborne travel should be aerodynamically unfavorable. However, volcanogenic zircon interpreted as distal ash fallout has been recognized in marine sequences up to a few thousand kilometers from its presumed vent (e.g. Santos et al., 2006; Rasmussen and Fletcher, 2010). Even basins separated by thousands of kilometers from very large silicic eruptions may thus preserve significant volumes of volcanic ash. If these ashes include cogenetic, dateable zircons contemporaneous with deposition, then the zircons can be used to accurately and precisely date associated deposits.

The Ogallala Formation is a broad apron of fluvial and aeolian sediments shed from the Rocky Mountains onto the Great Plains in the mid-late Miocene. It defines the modern High Plains, a broad, mostly flat expanse of semi-arid grassland stretching from New Mexico and Texas in the south to Wyoming and South Dakota in the north (Fenneman, 1917). Its inclusion of lenses of zircon-bearing volcanic ash presumably from magmatic centers in the western United

States makes it ideally suited to the exploration of dating methods for continental strata. These units contain abundant, contemporaneous zircon, yet none have been previously analyzed with modern, high-precision techniques (Ludvigson et al., 2009). We apply laser ablation inductively coupled plasma mass spectrometry (LA-ICP-MS) U-Pb zircon geochronology with single-grain uncertainties ca. 5-10% to date common Ogallala Formation lithologies.

The ubiquitous presence of young, evidently syndepositional volcanogenic zircon in common Ogallala Formation deposits like sand, pedogenic calcretes, and altered and unaltered ash beds indicates that accurate depositional or maximum depositional ages can likely be measured within the ~5% analytical uncertainty of single analyses. High-precision radioisotopic dating of the Ogallala Formation and comparison with dated tectonic and marine isotopic events may help to illuminate the causes of Ogallala Formation aggradation, enhance the western US climatic record, and strengthen the temporal precision of the North American Land Mammal Ages (NALMAs). In this work, it is also shown that temporal resolution of LA-ICP-MS dating is adequate for the evaluation of two models of Ogallala Formation aggradation: deposition as an alluvial plain (Johnson, 1901; Smith, 1940; Frye and Leonard, 1964), or aggradation as diachronous, avulsing lobes (Seni, 1980; Skinner and Johnson, 1984; Chapin, 2008; Galloway et al., 2011; Harlow, 2013), termed distributive fluvial systems by Weissmann et al. (2010). These models predict different stratigraphic architectures and three-dimensional arrangements of high and low hydraulic conductivity units, so this information is prerequisite to the planned development by the Kansas Geological Survey (KGS) of more accurate groundwater flow models designed to assess the water resources of the rapidly declining Ogallala-High Plains aquifer.

SETTING

Ogallala Formation

The 350,000 km^2 (Gutentag et al., 1984) Ogallala Formation is a sequence of gravels, sands, and clays of fluvial and aeolian origin (Darton, 1903; Hawley et al., 1976) shed from the Rocky Mountains in the mid-late Miocene (Frye et al., 1956; Ludvigson et al., 2009). Included within the dominant fluvial deposits are pedogenic calcretes and lenses of volcanic ash (Darton, 1903; Swineford et al., 1958), the latter of which may comprise as much as 3% volumetrically of the lower parts of the formation (Swineford et al., 1955). The Ogallala Formation is typically mantled with Quaternary loess and other aeolian sediments (Soller and Reheis, 2004).

Deposition of the Ogallala Formation progressed as a series of fluvial deposits that first filled incised bedrock valleys (Seni, 1980; Swinehart et al., 1985; Gustavson and Winkler, 1988) before overtopping them, eventually forming a broad sheet that may have stretched from the erosional surface of the Rocky Mountains to the Flint Hills topographic barrier in eastern Kansas (Frye et al., 1956; Zeller, 1968). In northwestern Kansas, the Ogallala Formation fills paleovalleys incised into Cretaceous rocks of the Western Interior Seaway (Frye and Leonard, 1949; Neuhauser and Pool, 1988), resulting in up to 100 m of basal relief (Heller et al., 2003). Fluvial valley fill conglomerates and sands are interpreted as longitudinal bar channel deposits from braided streams due to common fining-upward sequences, shallow, wide channels, and a scarcity of overbank deposits (Goodwin and Diffendal, 1987). These streams were probably high energy, braided, and ephemeral, with deposition punctuated by periods of landscape stability and aeolian processes (Gustavson and Winkler, 1988; Fielding et al., 2007; Harlow, 2013). Deposition of the Ogallala Formation south of the Canadian River in Texas may have diverged from the dominant-fluvial aggradation farther north (Holliday, 1991). Following fluvial valley aggradation, a sheet of aeolian-dominated sediments may have blanketed valley fills and interfluves in Texas (Gustavson and Winkler, 1988). Pliocene to modern incision continues to erode the Ogallala Formation from stream valleys and along its margin, including erosion from within ~150 km of the Rocky Mountain front in Colorado and New Mexico (Heller et al., 1988).

Ogallala aggradation has been attributed to late Cenozoic uplift of the Rocky Mountains by many authors (Eaton, 1987; Heller et al., 1988; Wayne et al., 1991; Heller et al., 2003) due to evidence for several hundred meters of regional differential uplift centered under the Rocky Mountains (Trimble, 1980; Leonard, 2002; McMillan et al., 2002; McMillan et al., 2006; Riihimaki et al., 2007; Galloway et al., 2011; Duller et al., 2012). However, this well-documented uplift episode is probably contemporaneous with Pliocene incision in the High Plains, rather than increased deposition of highland-sourced clasts (Leonard, 2002; Galloway et al., 2011; Duller et al., 2012). A middle Miocene global increase in sedimentation that accelerated during the Pliocene (Molnar, 2004), as well as late-Cenozoic conglomerates adjacent to mountain ranges worldwide (Molnar and England, 1990) are attributed to climate change rather than globally-synchronous tectonic upheaval for which there is no evidence (Molnar and England, 1990; Molnar, 2004). Following this line of reasoning, Ogallala aggradation has been attributed to a mid-late Miocene period of aridity that both reduced vegetative cover in the Rocky Mountains and decreased stream capacity in the Great Plains, causing increased erosion in the highlands and deposition in the plains (Chapin, 2008; Galloway et al., 2011). After Ogallala deposition, Pliocene uplift and incision was likely facilitated by a climatically induced transition to increased streamflow (Wobus et al., 2010) from initiation of the North American monsoon ~5-7 Ma (Oskin and Stock, 2003; Chapin, 2008; Galloway et al., 2011). Efforts to discern the relative importance of tectonics and climate on Ogallala deposition and erosion may be informed by high-precision radioisotopic dating and comparison with dated tectonic and marine isotopic events (Harlow, 2013).

The Ogallala Formation preserves a high-fidelity record of the climatic, tectonic, and biological records of the Neogene interior of North America, yet understanding of the interconnections between these diverse data has been impeded by its complex and alteration-prone stratigraphy. Lithologic correlation of clastic units has been hampered by variable degrees of pedogenic calcrete alteration that causes equivalent units to appear dissimilar and obscures original depositional and lithological characteristics (Izett and Wilcox, 1982; Ludvigson et al., 2009; Kreitzer, 2011; Smith and Ludvigson, 2011). Complex fluvial depositional patterns mean that sediments fail to follow a consistent stratigraphic order (Swinehart, 1974), and distinctive units tend to be too limited in extent for use as marker beds (Frye et al., 1956). A further obstacle to lithologic correlation is imposed by the low relief topography of the High Plains, which minimizes the abundance and stratigraphic thickness of surface exposures.

The uncertain lithostratigraphy of the Ogallala Formation led Frye et al. (1956) to conclude that members lack sufficient contrast with neighboring units to be mapped or correlated as rock-stratigraphic units. Correlation must therefore be undertaken chronologically. Most geochronologic study of the Ogallala Formation has focused on the fossil record (e.g. Thomasson, 1979; Bennett, 1983; Thomasson, 1990; Zakrzewski, 1990; Bartley, 2005; Ludvigson et al., 2009), though a handful of attempts have been made via chemical fingerprinting of Ogallala Formation ashes and correlation to dated volcanic eruptions (Perkins, 1998; David, 2006; Ludvigson et al., 2009), or radioisotopic dating of volcanic glass by the K-Ar (Thomasson, 1979) or glass fission-track methods (Boellstorff, 1976; Naeser et al., 1980; Bennett, 1983; Skinner and Johnson, 1984). The most precise and likely most accurate depositional age yet assigned to any part of the Ogallala Formation comes from a single-grain LA-ICP-MS U-Pb zircon date of 11.35 ± 0.44 Ma (Fig. 2) for an ash from Landon Draw in Scott County, KS (personal communication from analyst Brian Sitek, 2014). Existing paleontological, chemical correlation, and radioisotopic data are broadly consistent with Ogallala Formation deposition from the middle Miocene to earliest Pliocene, yet too low in precision to make detailed geological interpretations about depositional processes and timescales. Identification of syndepositional zircons from numerous potentially zircon-bearing volcanic ash beds, fluvial units, and paleosols in the Ogallala Formation provides high-precision (ca. 1-5% uncertainty) dates that facilitate these goals.

The presence of dateable material in the Ogallala Formation, along with its complex and diachronous depositional history, makes it an excellent location to test the use of radioisotopic dating methods for geologic characterization of these continental strata. Volcanic ash beds, when present and recognizable, provide accurate depositional ages that can be used to assess the accuracy of detrital maximum depositional ages from adjacent units that potentially contain pyroclastic zircon. Paleosols are common in continental basins (Kraus, 1999) including the Ogallala Formation, where they are most often recognized as pedogenic calcretes formed as a result of the dry grassland climate of the Great Plains in the late Miocene (Wayne et al., 1991). Paleosols represent periods of landscape stability (Birkeland, 1999) and record a nearly uninterrupted record of atmospheric deposition (Sheldon and Tabor, 2009; Dunne, 2013). They are thus likely to capture and preserve the chemically resilient fraction of volcanic ash that includes zircon via bioturbation and piping through roots and desiccation cracks (Smith et al., 2014; Turner et al., 2015; Smith et al., 2016). These units could contain reliable temporal information that can be used to construct detailed depositional and landscape evolution histories for continental basins.

Sedimentary horizons from the Ogallala Formation were selected based on their ash-bearing potential and sampled from sites in Norton and Ellis counties in northwestern Kansas (Fig. 2). Sampled outcrops (Appendix A) include vitric ashes (Figs. 12, 13), calcretes (Figs. 7, 8, 9, 10, 14), and a bentonite (Fig. 11), all of which yield pyroclastic zircon. The Calvert volcanic ash mine of Norton County (Carey et al., 1952) exposes a bed of vitric ash that reaches ~8 m in thickness (Potter, 1991). Exposed in the active mine face is a meter-scale bed of pure ash (Fig. 13) that grades upwards into very fine sand and 5-10 m of marl, soil (Potter, 1991), and two rhizolith-bearing meter-scale bentonite lenses (Fig. 11), all of which is overlain by loess. A calcrete from Norton County (Fig. 14) was also sampled from a roadcut near the town of Almena. Ashes from the Calvert volcanic ash mine were sampled from an elevation of ~685 m, and the Norton County calcrete was sampled from an elevation of ~680 m. In both areas, the depth to pre-Cenozoic bedrock is ~35-45 m (Fig. 2). In Ellis County, three pedogenic calcrete sequences that were tentatively correlated to one another on the basis of plant fossils (Thomasson, 1979) contain abundant rounded quartz and lithic clasts (Figs. 7, 8, 9, 10) and were sampled from elevations of ~670-680 m, with depth to pre-Cenozoic bedrock ranging from ~5-15 m. Geochronology coupled with bedrock and outcrop elevation data provides three-dimensional architectural information that helps to illuminate the sequence and timing of aggradation at the formation scale.

Ogallala-High Plains Aquifer

The Ogallala Formation and hydrologically connected Quaternary units host the Ogallala-High Plains aquifer, one of the world's largest and most agriculturally important freshwater aquifers (Smith et al., 2014), and the primary domestic and irrigation water source for the High Plains (Frye and Leonard, 1949; Seni, 1980; Gutentag et al., 1984; Kreitzer, 2011; Harlow, 2013; Steward et al., 2013; Smith et al., 2014; Steward and Allen, 2016). Increasing withdrawals for irrigation and stress from climate change continue to diminish its water resources at an accelerating pace (Gutentag et al., 1984; Kustu et al., 2010). In many parts of the aquifer, irrigation withdrawals far exceed recharge, leading to drawdowns (Gutentag et al., 1984; McGuire, 2009) severe enough to warrant concerns about the long-term sustainability of High Plains agriculture (Dennehy et al., 2002; Macfarlane, 2009). The threat posed by the depletion of this critical resource necessitates development of groundwater management strategies and numerical models designed to predict aquifer response to those strategies (Harlow, 2013; Smith et al., 2014; Butler et al., 2016).

Groundwater recharge and flow modeling requires detailed information on aquifer thickness, porosity, grain size, sorting, and bedrock geology (Seni, 1980; Koltermann and Gorelick, 1996; Fogg et al., 1998). This information is even more critical within the highly heterogeneous Ogallala Formation, where hydraulic properties vary considerably over small lateral and vertical distances (Gutentag et al., 1984; Kreitzer, 2011). This aquifer heterogeneity would be better characterized by models that incorporate depositional mechanisms (Koltermann and Gorelick, 1996; Kreitzer, 2011), but due to incomplete knowledge of the depositional processes and timelines that governed development of the Ogallala Formation, neither depositional models nor vital hydrostratigraphic information are currently available on a broad scale (Kreitzer, 2011). Detailed stratigraphic and geochronologic information from numerous completed and planned boreholes in western Kansas is currently being applied to characterization of Ogallala Formation stratigraphy and hydraulic parameters (Zeigler et al., 2012; Smith et al., 2014). Interpretations based on high-precision radioisotopic dates for the Ogallala Formation presented here will thus eventually help to guide groundwater management initiatives in the High Plains.

METHODS

Zircon separation was achieved by a combination of chemical and physical disaggregation and separation techniques at the University of Kansas Isotope Geochemistry Laboratories (IGL). Calcretes were first disaggregated into a fine sand and carbonate powder using a jaw crusher and disc mill before partial dissolution in 1.5 N HCl to separate clasts from the carbonate matrix. Clay was then separated from heavier and larger mineral grains by turbulent flow in an ultrasonic bath using the method described by Hoke et al. (2014). Samples of vitric ash were bathed in cold 12 N HF in order to dissolve the matrix of fine-grained volcanic glass. A Frantz™ isodynamic magnetic separator and methylene iodide were then used to separate the heavy, non-magnetic mineral fraction. Dissolution of barite from a paleosol heavy mineral separate (HP14-06) was carried out following a method modified from Breit et al. (1985). Zircons were then hand-picked under a binocular microscope and mounted on double-sided tape, capturing a range of morphologies while selectively picking euhedral grains that are less likely to have undergone significant fluvial transport.

Zircon separates were analyzed by LA-ICP-MS at the University of Kansas using a Photon Machines Analyte.G2 193 nm ArF excimer laser ablation system feeding a Thermo Scientific Element2 ICP-MS (Appendix B). Circular 20 µm spots were ablated with the laser at 2.0 J/cm^2 fluency and 10 Hz repetition rate, and a He carrier gas carried ablated material to the ICP. Downhole elemental and isotopic fractionation and calibration drift during the analytical session were corrected by bracketing measurements of unknowns with the 600.4 ± 0.65 Ma GJ-1 zircon reference material (Jackson et al., 2004). Data were reduced using the VizualAge data reduction scheme (Petrus and Kamber, 2012) for the IOLITE software package (Paton et al., 2010; 2011).

Uncertainty (±2σ) in $^{206}Pb/^{238}U$ dates from single GJ-1 ablations is typically ~8 Ma. Secondary standards including Plešovice (Sláma et al., 2008; Horstwood et al., 2016), Peixe (G. Gehrels, unpublished data), and the Fish Canyon Tuff (Wotzlaw et al., 2013) yield dates that are in agreement with TIMS analyses (Appendix C). Concordia diagrams for all data were plotted using the ISOPLOT software (Ludwig, 2008). The results of the LA-ICP-MS U-Pb analyses of unknowns are reported in Appendix D.

Sub-Ogallala Formation bedrock elevations in Kansas (Fig. 2) were estimated from structure contours by Wilson et al. (2009), and regionally based on a map by Weeks and Gutentag (1981) converted to digital contours for use in geographic information system (GIS) software by Cederstrand and Becker (1998). Land surface elevations from sample sites were measured from field GPS measurements and cross-checked against a USGS DEM of the National Elevation Dataset.

RESULTS

Abundant zircons in calcretes, bentonites, and volcanic ashes yield the first high-precision (ca. 1-5%) radioisotopic dates measured from the Ogallala Formation. Mid-late Miocene zircons were measured in all samples, as well as older grains that range in age from early Miocene to Mesoarchean (Fig. 3). Calcretes from west-central Ellis County contain grains as young as 8.1-8.5 Ma (Figs. 4a, b), but also numerous Paleogene, Cretaceous, Jurassic, and Proterozoic (~1100, 1400, and 1700 Ma) grains. Northwestern Ellis County calcretes include grains as young as 9.1 Ma (Figs. 4c, d), as well as a similar suite of older grains. A Norton

County calcrete includes grains as young as 12.2 Ma (Fig. 4h), as well as a suite of older grains comparable to the age distribution derived from Ellis County samples.

A bentonite from the Calvert volcanic ash mine is dominated by middle Miocene zircons, but also includes a spectrum of older grains similar to those found in calcretes. Replicate samples from an underlying vitric ash also contain dominantly middle Miocene zircons, but with only limited inclusion of older grains. The middle Miocene zircons from the three Calvert mine samples (Figs. 4e, f, g) yield indistinguishable mean $^{206}Pb/^{238}U$ dates of ca. 11.7 Ma.

DISCUSSION

General Comments

The provenance of zircons is discussed, followed by the significance of zircon dates to two issues. Of the two, the depositional model and implications for High Plains stratigraphic architecture is discussed in detail. Potential applications of our data and interpretations to the development of numerical groundwater models is also presented.

It should be noted that detrital age spectra may not represent a random sample of their parent population due to the selective picking of euhedral grains that were unlikely to have undergone significant fluvial transport. Statistical likeness tests (e.g. the Kolmogorov–Smirnov test) therefore cannot be rigorously applied to these potentially biased detrital populations. However, the specifics of detrital age spectra have little bearing on the conclusions presented here, and the data are nevertheless consistent with potential source terranes.

Calvert Ash

A possible source of the vitric ash at the 11.7 Ma Calvert volcanic ash mine is one of approximately seven eruptions of the 10.5-12.7 Ma ignimbrite phase of the Bruneau-Jarbidge volcanic center, collectively known as the Cougar Point Tuff or CPT (Bonnichsen et al., 2008). The Bruneau-Jarbidge volcanic center is a product of the Yellowstone–Snake River Plain (YSRP) volcanic system, which initiated ca. 16 Ma near the Oregon-Idaho-Nevada border and migrated at ~4 cm/yr to its present location in northwestern Wyoming (Rodgers et al., 1990; Pierce and Morgan, 1992; Smith and Braille, 1993; Perkins et al., 1995). From 9.5-13.9 Ma, it produced frequent (~every 200 kyr) large silicic eruptions (Perkins et al., 1995), some of which have been recognized in the Great Plains (Perkins and Nash, 2002). Perkins (1998) tentatively correlated several ashes in northwestern Kansas to YSRP volcanic fields including Picabo, Twin Falls, and Bruneau-Jarbidge, consistent with geochronology presented here. All cited dates are based on $^{40}Ar/^{39}Ar$ analyses of proximal to medial ashes and rhyolites unless otherwise noted.

The most probable source of the Calvert ash is the voluminous (>1000 km^3) 11.81 ± 0.03 Ma CPT VII (Nash and Perkins, 2012), which is correlative with the 11.93 ± 0.03 Ma Ibex Hollow ash of Perkins et al. (1998). This eruption has been identified in Smith County, KS by chemical fingerprinting (Ludvigson et al., 2009), and is interpreted as the source of the Ashfall Fossil Beds in Nebraska and the Mission Pit locality of South Dakota (Famoso and Pagnac, 2011). Other potential sources include the 11.22 ± 0.07 Ma CPT XI (Bonnichsen et al., 2008), which has also been recognized in the Great Plains (Perkins and Nash, 2002), and the smaller 11.56 ± 0.07 Ma Cougar Point Tuff IX (Bonnichsen et al., 2008), which probably also reached the Great Plains (Perkins and Nash, 2002).

Volcanic ash can travel great distances from eruptive centers, likely due to the irregular surface geometry of glass shards (Rose et al., 2003), or by the dispersive expansion of umbrella clouds that can drive ash thousands of kilometers against prevailing winds (Mastin et al., 2014). Miocene and later ashes preserved in the Great Plains are commonly >1000 km from their source

(Rose et al., 2003), and the Calvert volcanic ash mine in particular is ~1350 km downwind from its presumptive source at the Bruneau-Jarbidge volcanic center. While heavy minerals like zircon have not previously been recognized in distal ashes of terrestrial sequences, given the remarkable potential for ash to travel great distances, it is perhaps unsurprising that dense minerals like zircon do not fully fractionate from glass particles. These previously unrecognized volcanogenic zircons provide the first reliable radioisotopic dates for the Neogene High Plains at ca. 1-5% precision. Our results imply that pyroclastic zircon might be present or even common in continental clastic sequences of the Great Plains and other basins that are far from active magmatic arcs.

Because the zircon content of vitric ashes (Figs. 4f, g) and paleosols derived from those ashes (Fig. 4e) are dominated by a pyroclastic component and contain only limited foreign epiclastic material, we interpret dates from such units as depositional ages. Given their unimodal date distribution, many such ashes might be dated quickly and relatively inexpensively as low *n* samples by LA-ICP-MS or as single grains via the CA-TIMS method without significant risk of omitting the youngest population.

Mean dates of ~11.7 Ma are reported without uncertainties for vitric ashes and bentonites derived from those ashes due to scatter somewhat in excess of uncertainty. Weighted mean $^{206}Pb/^{238}U$ dates for Calvert mine samples yield unacceptably high MSWDs (HP14-06 = 1.7 for n = 172; HP14-07 = 1.5 for n = 107) that might reflect a small underestimation of single-grain age uncertainties or inclusion in weighted mean calculations of zircons from geologically distinct populations. A replicate sample of the Calvert ash (HP14-05b) includes a small but consistent common Pb contamination that rendered ~1/2 of all grains discordant, potentially biasing any weighted mean age. We note that despite the potential for systematic error in weighted mean

$^{206}Pb/^{238}U$ dates calculated for HP14-05b, the data for single grains are indistinguishable from HP14-07 within uncertainty. Despite these complications, measured dates are internally consistent and likely accurate.

Norton County Calcrete

Pedogenic calcrete samples (HP14-02, -03, -08, -09b, -10b) contain rounded quartz and lithic fragments, as well as primarily detrital zircon grains with crystallization dates spanning from Archean to late Miocene time (Fig. 3). These units are interpreted as pedogenically altered fluvial deposits, and the youngest age populations are therefore interpreted as maximum depositional ages. In contrast to ash beds, whose zircon crystallization age was closely followed by deposition, the accuracy of maximum depositional ages is contingent on contribution of contemporaneous zircon from large eruptions.

The ~12.2 Ma maximum depositional age of a calcrete from Almena, Norton County (Fig. 4h) makes it possibly contemporaneous with the 12.7-15.2 Ma Owyhee-Humboldt volcanic field (Perkins and Nash, 2002), but more likely contemporaneous with the 10.5-12.7 Ma ignimbrite phase of the Bruneau-Jarbidge volcanic field (Bonnichsen et al., 2008). The most probable source of young zircons may be the 12.66 ± 0.02 Ma CPT III (Bonnichsen et al., 2008), which has previously been recognized in the Great Plains (Perkins and Nash, 2002).

Ellis County Calcretes

In contrast to the middle Miocene dates of Norton County, zircons from calcretes in Ellis County are late Miocene in age and yield ~8.1-9.1 Ma maximum depositional ages (Fig. 4a, b, c, d) contemporaneous with the 8.5-10.5 Ma Twin Falls volcanic field (Perkins and Nash, 2002) and the 6.7-10.4 Ma Picabo volcanic field (Anders et al., 2014). Eruptions contributing young zircon probably include the voluminous and widespread 10.79 ± 0.04 Ma CPT XIII (Bonnichsen et al., 2008) from the Bruneau-Jarbidge volcanic field and the widespread 10.13 ± 0.03 Ma Tuff of Wooden Shoe Butte from the Twin Falls volcanic field (Perkins and Nash, 2002). These eruptions are too old to account for the youngest detrital grains measured, but those grains are generally contemporaneous with dated ashfalls previously recognized in the Great Plains (Perkins and Nash, 2002), including the 8.94 ± 0.07 Ma Tuff of McMullen Creek (Nash et al., 2006), the 8.6 ± 0.1 Ma Inkom ash (Nash et al., 2006), and the 8.4 ± 0.2 Ma Rush Valley ash (Nash et al., 2006). Young zircons might also owe their provenance to the 9.8 ± 0.2 Ma Hazen ash, which was dated by interpolation of measured sections (Perkins et al., 1998) or the 9.4 ± 0.5 Ma Mink Creek ash (Nash et al., 2006). Neither of these ashes have been previously recognized in the Great Plains.

Ellis County zircon ages are consistent with the findings of Tallan (1978) and Zakrzewski (1990) who recognized early Hemphillian (4.9-10.3 Ma) land mammals and salamanders from an exposure coined the Bemis Local Fauna locality, located ~600 m to the southwest of a sampled outcrop (HP14-09b) at similar stratigraphic levels. These ages are younger than the probably inaccurate 18 ± 3.6 Ma volcanic glass K-Ar date reported from Ellis County, ~700 m southwest of HP14-09b (Thomasson, 1979).

Complications in Determining Provenance

Correlation of specific eruptive events, often dated using sanidine by the Ar-Ar system, to ashes recognized in the Great Plains, here dated using zircon and the U-Pb system, is made more difficult by a poorly quantified systematic bias between dates from the U-Pb and Ar-Ar isotopic systems. Potential uncertainties on the order of 1% for weighted mean $^{206}Pb/^{238}U$ zircon ages would likely allow unambiguous correlation between Ogallala Formation ashes and proximal YSRP tuffs and rhyolites if not for an imprecise and potentially inaccurate intercalibration of up to 2% between dates from the U-Pb and ^{40}Ar-^{39}Ar chronometers (Renne et al., 2010). Low *n* populations and uncertainty on the order of 5% for single-grain LA-ICP-MS dates precludes the correlation of individual zircons from detrital units to specific eruptions. However, temporal assignments of provenance in vitric ashes can be corroborated by petrographic arguments including shard morphology and index of refraction (e.g. Potter, 1991), or by trace element and isotopic fingerprinting of volcanic glass (e.g. Perkins, 1998; David, 2006). Further trace element characterizations of Miocene ashes in the High Plains would facilitate more precise correlations. Despite the uncertainties involved, new U-Pb dates and existing geologic information permit the robust correlation of volcanic ashes to specific volcanic fields and the tentative correlation of High Plains ashes to specific eruptive events.

Ash Depositional Environment

Most volcanic ashes in Kansas were originally interpreted as aeolian deposits that accumulated in hollows and on the leeward side of hills (Landes, 1928). More recent study has demonstrated that ashes in Kansas typically lack aeolian cross-bedding, and are often underlain by clay with interbedded gastropod and ostracod shells, indicating deposition in shallow ponded water (Carey et al., 1952; Swineford, 1963; Diffendal, 1982). Norton County ashes in particular are consistent with subaqueous deposition due to their dense packing and horizontal laminations (Landes, 1928). Standing water in the High Plains is currently restricted to small sandhills lakes (Gutentag et al., 1984), as well as ~22,000 extant playas in Kansas alone (Bowen et al., 2010). These playas are typically small, closed depressions that develop as aeolian scours and often persist in a given location as sediments aggrade around them (Holliday et al., 1996). They likely record sediment influx events in a reliable stratigraphic order as they concentrate local runoff and entrap sediments (Bowen et al., 2010) including volcanic ash (Cornwell, 1984). Playas are common both on the present surface of the High Plains, and within the Miocene Ogallala Formation (Holliday et al., 1996), and are thus the favored depositional environment for the Calvert ash. Remobilization of topography-mantling ashes and redeposition in playas accounts for the lenticular nature of ash deposits in Kansas (Carey et al., 1952), but makes them difficult to correlate over significant distances (Cornwell, 1984). Most of the recharge that enters the Ogallala-High Plains aquifer probably occurs as seepage from playas (Stone, 1990; Holliday et al., 1996), so understanding these features and their temporal evolution is critical to characterization of the High Plains water budget.

Depositional Model

Early workers assumed that the Ogallala Formation was deposited in an alluvial plain environment as a series of coalesced fans running the length of the Rocky Mountain front (Johnson, 1901; Smith, 1940; Frye and Leonard, 1964). The assumption that trunk streams sourced from ranges separated by hundreds of kilometers were synchronous may not be valid due to the potential for distinct uplift histories, asynchronous spillover from closed basins, and local differences in erosion (Ludvigson et al., 2009). More recent study of fluvial facies and lithological differences indicates that the Ogallala Formation may have been deposited as a series of temporally distinct, laterally discontinuous DFS lobes (Skinner and Johnson, 1984; Chapin, 2008; Galloway et al., 2011; Harlow, 2013). This model, proposed by Seni (1980) based on work in the Texas panhandle, and adopted by Skinner and Johnson (1984) for Nebraska and South Dakota involves the filling and overtopping of paleovalleys, followed by avulsion to lower topography. The dominantly aeolian facies recognized more recently in the southern High Plains (Gustavson and Winkler, 1988) undercuts the conclusions of Seni (1980) in that area, but the fluvial deposits that dominate north of the Canadian River (Holliday, 1991) remain consistent with diachronous aggradation of fluvial lobes. In particular, the recognition of diachronous paleodrainage systems in Nebraska and South Dakota by Skinner and Johnson (1984) remains a viable depositional model.

These competing hypotheses predict different spatial and temporal patterns of deposition: the alluvial plain model predicts nearly contemporaneous deposition of geographically extensive sequences and their correlatives over large areas along strike and down dip. In this model, deposition should proceed synchronously across the extent of the formation, with superposition dominating an orderly age progression occasionally disrupted by second-order scours and channel fills. In contrast to the alluvial plain model, the DFS model predicts lithologically similar but laterally diachronous eastward-prograding lobes that maintain internal superposition. These predictions can be evaluated by analyzing the three-dimensional distribution of depositional ages within the context of a basal unconformity that reveals Cenozoic topography. Though conclusions drawn from interpreted bedrock elevation data are probably useful and reasonably accurate, they should not be over-interpreted given the ~15 m uncertainty in these measurements (Wilson et al., 2009), which approaches the total land surface relief encountered in this study. Despite substantial evidence for Pliocene uplift of the High Plains, modern elevations are used as a proxy for paleoelevations due to the interpreted tilting gradient of ~0.001 (Heller et al., 2003). Tilting of this magnitude is unlikely to introduce measurable systematic error into elevation comparisons between samples in proximity to one another that sit along the strike of tilting.

Figure 5 illustrates that middle Miocene depositional ages were measured from Norton County outcrops at modern elevations ranging from 680-690 m. The sampled sequence is exposed in part by incision by the modern Prairie Dog Creek, which appears to coincide with a pre-Ogallala drainage incised into the Cretaceous Niobrara Chalk (Fig. 2). The maximum depositional age of a calcrete sampled near Almena (HP14-08) indicates that ca. 12.2 Ma or later, the Ogallala Formation had aggraded to ~40 m above the bedrock valley in that vicinity. At 11.7 Ma, the Calvert ash was then deposited ~10 m above and 6300 m upstream of the Almena calcrete along the paleovalley extending to the southwest, at ~30 m above the Cretaceous surface and far above the former confines of the pre-Ogallala valley. Thus by 11.7 Ma, the Ogallala Formation had filled and overtopped its confining bedrock valley in the vicinity of Prairie Dog Creek, aggrading to its modern elevation of ~690 m and reaching a thickness of ~30-40 m. Other mid-Miocene depositional ages have been applied to ashes from Kansas' northernmost counties: Landes (1928) correlated ashes from Rawlins County with the Calvert ash, and Ludvigson et al. (2009) correlated an ash from Smith County with the 11.93 Ma Ibex Peak Tuff.

Late Miocene maximum depositional ages were measured from Ellis County outcrops at modern elevations ranging from 670-680 m (Fig. 5). These units are partially exposed by the escarpment that separates the Ogallala-defined High Plains from the Plains Border region, placing them close to the pre-Ogallala basal unconformity. Maximum depositional ages of calcretes from northwestern Ellis County indicate that ca. 9.1 Ma or later, the Ogallala Formation had aggraded ~15 m above bedrock to an elevation of ~680 m. A calcrete from west-central Ellis County (HP14-09b) indicates that ca. 8.5 Ma or later, the Ogallala Formation had aggraded <5 m above bedrock to an elevation of ~670 m. A second calcrete from the same section (HP14-10b) indicates that ca. 8.1 Ma or later, aggradation had progressed by another 10 m to ~680 m. Aggradation in Ellis County therefore probably began shortly prior to ~9.1 Ma, and by ~8.1 Ma had likely progressed to a modern elevation comparable to or lower than had been achieved in Norton County by 11.7 Ma.

The proximity of Cretaceous bedrock to Ellis County calcretes implies that aggradation in this area likely began shortly prior to the measured maximum depositional ages. Deposition of the Ogallala Formation was thought to have initiated ca. 17 Ma in the northern High Plains and ca. 12 Ma in the southern High Plains (Roy et al., 2004). The inferred ~9-10 Ma deposition of basal Ogallala Formation in Ellis County might therefore indicate a younger and more diachronous depositional history than was previously suspected for parts of the formation.

The low relief surface of the modern High Plains means that surface outcrops in Norton and Ellis counties sit at nearly the same elevation, yet these beds differ in age by ~3 Myr over an along-strike distance of ~100 km. The inferred ~30-35 m depth to pre-Cenozoic bedrock beneath the Calvert ash indicates that aggradation in Norton County had reached an advanced stage by 11.7 Ma, in contrast to the basal units of Ellis County, which were likely not deposited until ca. 9-10 Ma. Ogallala deposits in Norton County must have therefore formed a topographic high relative to Ellis County before deposition in that area. These observations are inconsistent with predictions made by the alluvial plain model, which predicts that Norton and Ellis Counties would become alluviated at around the same time, given that they fall approximately along the strike of the Cretaceous bedrock surface and parallel to the Front Range.

The DFS lobe model provides a more satisfactory explanation. We propose that deposition of the Ogallala Formation in northern and central Kansas progressed as a series of at least two asynchronous DFS lobes, illustrated in Figure 6. The Norton lobe likely spread to the north of a central Kansas bedrock high ca. 12-13 Ma and aggraded in the vicinity of the Kansas-Nebraska border until sedimentation to levels above the former topographic barrier ca. 11.7 Ma caused avulsion into central Kansas ca. 9-10 Ma, forming the Ellis lobe. Further dating efforts concentrated in southwestern Kansas might help to better define an inferred Haskell lobe that potentially spans between the Ellis lobe and the aeolian sequence recognized in the southern High Plains.

This conjectured Haskell lobe may have already been identified: recent and in-progress U-Pb zircon geochronology and petrography from the HP1A core (Fig. 2) indicates that southwestern Kansas might host a White River Group equivalent that was previously unrecognized in Kansas (Smith et al., 2014; Turner et al., 2015; Smith et al., 2016). The ~29-37 Ma White River Group is a relatively homogenous, fine-grained, aeolian and volcaniclastic sequence that underlies the Arikaree Group in Nebraska (Swinehart et al., 1985). These Eocene-Oligocene deposits potentially constitute the southwestern Kansas Haskell lobe (Fig. 6) inferred between the Ellis lobe and the aeolian facies recognized in the southern High Plains. Age discrepancies larger than that inferred between the Norton and Ellis lobes might therefore exist within the Cenozoic terrestrial sequence of Kansas. Recognition of such lithologically disparate strata may inform the development of numerical groundwater models, which rely on sedimentological characteristics including grain size, porosity, and sorting for the selection of hydraulic parameters.

Significance of Results to the Ogallala-High Plains Aquifer

Fine-grained units typically have limited porosity and hydraulic conductivity, limiting their capacity to store and transmit water (Anderson and Woessner, 1992). The recent discovery based on age and sedimentological characteristics of a relatively fine-grained White River Group equivalent in southwestern Kansas in the vicinity of the HP1A core (Smith et al., 2014; Smith et al., 2016) occurs in a zone of relatively low hydraulic conductivity (Liu et al., 2010; Butler et al., 2016) that hosts the most severe aquifer drawdowns in Kansas (McGuire, 2009; Butler et al., 2016). Further delineation of this potential “Haskell lobe” and other low-hydraulic conductivity units will be critical to the understanding of spatial variations in groundwater resources.

Investigations into aquifer dynamics and development of numerical groundwater models might be best guided by the hypothesis that the aquifer is subdivided into eastward prograding DFS lobes. Such lobes may include zones of stacked, high-hydraulic conductivity channel deposits separated by interlobe zones of relatively low hydraulic conductivity (van Dijk et al., 2016). The aquifer therefore likely exhibits considerable anisotropy, with coarse-grained DFS channels forming east-trending high hydraulic conductivity pathways separated by low hydraulic conductivity interlobe zones. Hydraulic properties change significantly over small lateral distances, but such discontinuities can be better understood and predicted by a thorough understanding of age relationships. Knowledge of these differences will be critical to the future development of aquifer management strategies.

CONCLUSIONS

Miocene volcanic eruptions from the Yellowstone hotspot track in southern Idaho carried ash and volcanogenic zircon to the High Plains of western Kansas. The ash falls mantled topography before being remobilized and concentrated into playas eroded into the surface of the contemporaneous Ogallala Formation. These lenticular and small but numerous playa deposits contain dateable material that provides high precision (ca. 1-5% uncertainty) chronostratigraphic information for the Ogallala Formation. Refinement of LA-ICP-MS dates for previously dated young grains via the CA-TIMS method may be a fruitful avenue for further study, offering the potential to refine uncertainties to <1%. Depositional ages from ash beds are consistent with maximum depositional ages from fluvial sands and pedogenic calcretes, indicating that these units can be dated with some reliability due to the frequent contribution of pyroclastic zircons from magmatic centers in the western United States. The ash-bearing potential of volcanic arcs is widely appreciated, but perhaps underappreciated is the potential for large-volume eruptions to blanket large areas far from eruptive centers. These “supereruptions” might commonly enable high-precision U-Pb zircon dating of distal clastic basins worldwide.

Mid-late Miocene depositional timing of the Ogallala Formation in Kansas is consistent with previous studies, but high-precision geochronology reveals previously obscured spatial patterns that indicate a more diachronous depositional history than was formerly suspected. Middle Miocene deposition of a northern Kansas Norton lobe ca. 11-13 Ma preceded deposition of the late Miocene Ellis lobe over an area of Miocene high topography in central Kansas ca. 8-10 Ma. An inferred Haskell lobe and White River Group equivalent likely aggraded in late Eocene or early Oligocene time in southern Kansas (Smith et al., 2014; Turner et al., 2015; Smith et al., 2016). These DFS lobes potentially form the “missing link” between the paleodrainages recognized by Skinner and Johnson (1984) in Nebraska and the aeolian facies recognized in the southern High Plains by Gustavson and Winkler (1988).

Further dating of ashes and clastic units will help to refine understanding of the spatial relationships and stratigraphic architecture of the High Plains, and can inform other longstanding regional geologic problems. For instance, the interplays between Neogene climate change and Rocky Mountain uplift and tectonics are an area of active research. The data presented here do not unambiguously implicate either mechanism as the cause of Ogallala aggradation, but further dating efforts should help to pinpoint the onset of Ogallala deposition and any contemporaneous climatic or tectonic forcing mechanisms. Additionally, zircon dates derived from the Ogallala Formation in Kansas are broadly consistent with previously published biostratigraphic correlations. Absolute radioisotopic ages should help to date with previously unattainable precision Miocene floral zones and faunal assemblages from the Clarendonian and Hemphillian land mammal ages.

REFERENCES

Anders, M.H., Rodgers, D.W., Hemming, S.R., Saltzman, J., DiVenere, V.J., Hagstrum, J.T., Embree, G.F., and Walter, R.C., 2014, A fixed sublithospheric source for the late Neogene track of the Yellowstone hotspot: Implications of the Heise and Picabo volcanic fields: Journal of Geophysical Research: Solid Earth, v. 119, p. 2871-2906.

Anderson, M.P. and Woessner, W.W., 1992, Applied Groundwater Modeling: Simulation of Flow and Advective Transport: San Diego, California, Academic Press, 381 p.

Bartley, K.J., 2005, A taphonomic study of Clarendonian (Miocene) Teleoceras (Perissodactyla, Rhinocerotoidea) from the Ogallala Formation, northwestern Kansas [M.S. thesis]: Buffalo, NY, State University of New York at Buffalo, 122 p.

Bennett, D.K., 1983, Cenozoic rocks and faunas of north-central Kansas [Ph.D. dissertation]: Lawrence, KS, University of Kansas, 221 p.

Birkeland, P.W., 1999, Soils and Geomorphology: New York, New York, Oxford University Press, 430 p.

Boellstorff, J., 1976, The succession of late Cenozoic volcanic ashes of the Great Plains: a progress report, *in* Bayne, C.K., ed., Guidebook: 24th Annual Meeting, Midwestern Friends of the Pleistocene: Kansas Geological Survey Guidebook Series 1, p. 37-71.

Bonnichsen, B., Leeman, W.P., Honjo, N., McIntosh, W.C., and Godchaux, M.M., 2008, Miocene silicic volcanism in southwestern Idaho: geochronology, geochemistry, and evolution of the central Snake River Plain: Bulletin of Volcanology, v. 70, p. 315-342.

Bowen, M.W., Johnson, W.C., Egbert, S.L., and Klopfenstein, S.T., 2010, A GIS-based approach to identify and map playa wetlands on the High Plains, Kansas, USA: Wetlands, v. 30, p. 675-684.

Bowring, S.A. and Schmitz, M.D., 2003, High-precision U-Pb zircon geochronology and the stratigraphic record: Reviews in Mineralogy and Geochemistry, v. 53, p. 305-326.

Breit, G.N., Simmons, E.C., and Goldhaber, M.B., 1985, Dissolution of barite for the analysis of strontium isotopes and other chemical and isotopic variations using aqueous sodium carbonate: Chemical Geology: Isotope Geoscience section, v. 52, p. 333-336.

Burgess, S.D., Bowring, S., and Shen, S.Z., 2014, High-precision timeline for Earth's most severe extinction: Proceedings of the National Academy of Sciences, v. 111, p. 3316-3321.

Butler, J.J., Jr., Whittemore, D.O., Reboulet, E., Knobbe, S., Wilson, B.B., Stotler, R.L., and Bohling, G.C., 2016, High Plains aquifer index well program: 2015 annual report: Kansas Geological Survey, Open-File Report 2016-4, 179 p.

Carey, J.S., Frye, J.C., Plummer, N., and Swineford, A., 1952, Kansas volcanic ash resources: Kansas Geological Survey, Bulletin 96, pt. 1, p. 1-68.

Cederstrand, J.R. and Becker, M.F., 1998, Digital map of base of aquifer for High Plains Aquifer in parts of Colorado, Kansas, Nebraska, New Mexico, Oklahoma, South Dakota, Texas, and Wyoming: U.S. Geological Survey Open-File Report 98-393.

Cepeda, J.C. and Perkins, M.E., 2006, A 10 million year old ash deposit in the Ogallala Formation of the Texas Panhandle: Texas Journal of Science, v. 58, p. 3-12.

Chapin, C.E., 2008, Interplay of oceanographic and paleoclimate events with tectonism during middle to late Miocene sedimentation across the southwestern USA: Geosphere, v. 4, p. 976-991.

Cornwell, K.J., 1984, Evaluation of volcanic ash as a stratigraphic marker in playa basins, western Texas [M.S. thesis]: Lubbock, TX, Texas Tech University, 47 p.

Darton, N.H., 1903, Preliminary report on the geology and water resources of Nebraska west of the one hundred and third meridian: U.S. Geological Survey Professional Paper 17, 69 p.

David, B.T., 2006, "Chemical fingerprinting" of volcanic tephra found in Kansas using trace elements [M.S. thesis]: Manhattan, KS, Kansas State University, 115 p.

Dennehy, K.F., Litke, D.W., and McMahon, P.B., 2002, The High Plains aquifer, USA: groundwater development and sustainability, *in* Hiscock, K.M., Rivett, M.O., and Davidson, R.M., eds., Sustainable Groundwater Development: Geological Society of London Special Publication 193, p. 99-119.

Diffendal, R.F., 1982, Regional implications of the geology of the Ogallala Group (upper Tertiary) of southwestern Morrill County, Nebraska, and adjacent areas: Geological Society of America Bulletin, v. 93, p. 964–976.

Duller, R.A., Whittaker, A.C., Swinehart, J.B., Armitage, J.J., Sinclair, H.D., Bair, A., and Allen, P.A., 2012, Abrupt landscape change post–6 Ma on the central Great Plains, USA: Geology, v. 40, p. 871-874.

Dunne, G., 2013, A geological and sedimentological approach to infer paleoclimate from buried soils profiles within playa fills, southern High Plains, Texas [M.S. thesis]: Lubbock, TX, Texas Tech University, 185 p.

Eaton, G.P., 1987, Topography and origin of the southern Rocky Mountains and Alvarado Ridge, *in* Coward, M.P., Dewey, J.F., and Hancock, P.L., eds., Continental Extensional Tectonics: Geological Society of London Special Publication 28, p. 355-369.

Famoso, N.A. and Pagnac, D., 2011, A comparison of the Clarendonian equid assemblages from the Mission Pit, South Dakota and Ashfall Fossil Beds, Nebraska: Transactions of the Nebraska Academy of Sciences, v. 32, p. 98-107.

Fenneman, N.M., 1917, Physiographic Subdivision of the United States: Proceedings of the National Academy of Sciences, v. 3, p. 17–22.

Field, H.L., Ludvigson, G.A., Möller, A., Joeckel, R.M., and Stotler, R.L., 2015, Chronostratigraphic interpretations of Cenozoic paleosols in Nebraska using integrated U-Pb dating and carbon isotope chemostratigraphy: Geological Society of America Abstracts with Programs, v. 47, p. 595.

Fielding, C.R., LaGarry, H.E., LaGarry, L.A., Bailey, B.E., and Swinehart, J.B., 2007, Sedimentology of the Whiteclay Gravel Beds (Ogallala Group) in northwestern Nebraska, USA: Structurally controlled drainage promoted by Early Miocene uplift of the Black Hills Dome: Sedimentary Geology, v. 202, p. 58-71.

Fogg, G.E., Noyes, C.D., and Carle, S.F., 1998, Geologically based model of heterogeneous hydraulic conductivity in an alluvial setting: Hydrogeology Journal, v. 6, p.131-143.

Frye, J.C. and Leonard, A.B., 1949, Geology and ground-water resources of Norton County and northwestern Phillips County, Kansas: Kansas Geological Survey, Bulletin 81, 144 p.

Frye, J.C. and Leonard, A.B., 1964, Relation of Ogallala Formation to the southern High Plains in Texas: Texas Bureau of Economic Geology Report of Investigations 51, 25 p.

Frye, J.C., Leonard, A.B., and Swineford, A., 1956, Stratigraphy of the Ogallala Formation (Neogene) of northern Kansas: Kansas Geological Survey, Bulletin 118, 92 p.

Furin, S., Preto, N., Rigo, M., Roghi, G., Gianolla, P., Crowley, J.L., and Bowring, S.A., 2006, High-precision U-Pb zircon age from the Triassic of Italy: Implications for the Triassic time scale and the Carnian origin of calcareous nannoplankton and dinosaurs: Geology, v. 34, p. 1009-1012.

Galloway, W.E., Whiteaker, T.L., and Ganey-Curry, P., 2011, History of Cenozoic North American drainage basin evolution, sediment yield, and accumulation in the Gulf of Mexico basin: Geosphere, v. 7, p. 938-973.
Global Volcanism Program, 2013, Volcanoes of the World, v. 4.4.3, Venzke, E., ed., Smithsonian Institution: accessed 18 May 2016 <http://dx.doi.org/10.5479/si.GVP.VOTW4-2013>.
Goodwin, R.G. and Diffendal, R.F., Jr., 1987, Paleohydrology of some Ogallala (Neogene) streams in the southern panhandle of Nebraska, *in* Ethridge, F.G., Flores, R.M., and Harvey, M.D., eds., Recent Developments in Fluvial Sedimentology: SEPM Special Publication 39, p. 149-158.
Gustavson, T.C., and Winkler, D.A., 1988, Depositional facies of the Miocene-Pliocene Ogallala Formation, northwestern Texas and eastern New Mexico: Geology, v. 16, p. 203-206.
Gutentag, E.D., Heimes, F.J., Krothe, N.C., Luckey, R.R., and Weeks, J.B., 1984, Geohydrology of the High Plains aquifer in parts of Colorado, Kansas, Nebraska, New Mexico, Oklahoma, South Dakota, Texas, and Wyoming: U.S. Geological Survey Professional Paper 1400-B, 63 p.
Harlow, R.H., 2013, Depositional and paleoclimatic evolution of the Cenozoic High Plains Succession from core: Haskell Co., Kansas [M.S. thesis]: Lawrence, KS, University of Kansas, 124 p.
Hawley, J.W, Bachman, G.O., and Manley, K., 1976, Quaternary stratigraphy in the Basin and Range and Great Basin provinces, New Mexico and western Texas, *in* Mahaney, W.C., ed., Quaternary Stratigraphy of North America: Stroudsburg, PA, Dowden, Hutchinson, & Ross, p. 235-274.
Heller, P.L., Angevine, C.L., Winslow, N.S., and Paola, C., 1988, Two-phase stratigraphic model of foreland-basin sequences: Geology, v. 16, p. 501-504.
Heller, P.L., Dueker, K., and McMillan, M.E., 2003, Post-Paleozoic alluvial gravel transport as evidence of continental tilting in the US Cordillera: Geological Society of America Bulletin, v. 115, p.1122-1132.
Hoke, G.D., Schmitz, M.D., and Bowring, S.A., 2014, An ultrasonic method for isolating non-clay components from clay-rich material: Geochemistry, Geophysics, Geosystems, v. 15, p. 492-498.
Holliday, V.T., 1991, The geologic record of wind erosion, eolian deposition, and aridity on the Southern High Plains: Great Plains Research, v. 1, p. 6-25.
Holliday, V.T., Hovorka, S.D., and Gustavson, T.C., 1996, Lithostratigraphy and geochronology of fills in small playa basins on the Southern High Plains, United States: Geological Society of America Bulletin, v. 108, p. 953-965.
Horstwood, M.S.A., Košler, J., Gehrels, G., Jackson, S.E., McLean, N.M., Paton, C., Pearson, N.J., Sircombe, K., Sylvester, P., Vermeesch, P., Bowring, J.F., Condon, D.J., and Schoene, B., 2016, Community-derived standards for LA-ICP-MS U-(Th-)Pb geochronology – uncertainty propagation, age interpretation and data reporting: Geostandards and Geoanalytical Research, doi:10.1111/j.1751-908X.2016.00379.x, 22 p.
Izett, G.A. and Wilcox, R.E., 1982, Map showing localities and inferred distributions of the Huckleberry Ridge, Mesa Falls, and Lava Creek ash beds (Pearlette family ash beds) of Pliocene and Pleistocene age in the western United States and southern Canada: U.S. Geological Survey Miscellaneous Investigations Map I-1325, scale 1:400,000.

Jackson, S.E., Pearson, N.J., Griffin, W.L., and Belousova, E.A., 2004, The application of laser ablation-inductively coupled plasma-mass spectrometry to in situ U–Pb zircon geochronology: Chemical Geology, v. 211, p. 47-69.

Jochum, K.P., Weis, U., Stoll, B., Kuzmin, D., Yang, Q., Raczek, I., Jacob, D.E., Stracke, A., Birbaum, K., Frick, D.A., Günther, D., and Enzweiler, J., 2011, Determination of reference values for NIST SRM 610–617 glasses following ISO guidelines: Geostandards and Geoanalytical Research, v. 35, p. 397-429.

Johnson, W.D., 1901, The High Plains and their utilization: Report of the U.S. Geological Survey, v. 21, p. 609-741 and v. 22, p. 640-669.

Kansas Geological Survey, 2008, Surficial geology of Kansas: Kansas Geological Survey, Map M-118, scale 1:500,000.

Koltermann, C.E. and Gorelick, S.M., 1996, Heterogeneity in sedimentary deposits: A review of structure-imitating, process imitating, and descriptive approaches: Water Resources Research, v. 32, p. 2617–2658.

Kraus, M.J., 1999, Paleosols in clastic sedimentary rocks: their geologic applications: Earth-Science Reviews, v. 47, p. 41-70.

Kreitzer, S.R., 2011, An evaluation of hydrostratigraphic characterization methods based on well logs for groundwater modeling of the High Plains aquifer in southwest Kansas [M.S. thesis]: Lawrence, KS, University of Kansas, 100 p.

Kustu, M.D., Fan, Y., and Robock, A., 2010, Large-scale water cycle perturbation due to irrigation pumping in the US High Plains: A synthesis of observed streamflow changes: Journal of Hydrology, v. 390, p. 222-244.

Landes, K.K., 1928, Volcanic ash resources of Kansas: Kansas Geological Survey, Bulletin 14, 58 p.

Leonard, E.M., 2002, Geomorphic and tectonic forcing of late Cenozoic warping of the Colorado piedmont: Geology, v. 30, p. 595-598.

Liu, G., Wilson, B., Whittemore, D., Jin, W., and Butler, J., Jr., 2010, Ground-water model for Southwest Kansas Groundwater Management District No. 3: Kansas Geological Survey, Open-File Report 2010-18, 109 p.

Ludvigson, G.A., Sawin, R.S., Franseen, E.K., Watney, W.L., West, R.R., and Smith, J.J., 2009, A review of the stratigraphy of the Ogallala Formation and revision of Neogene ("Tertiary") nomenclature in Kansas: Kansas Geological Survey, Bulletin 256, pt. 2, 9 p.

Ludwig, K.R., 2008, User's Manual for Isoplot 3.70: a geochronological toolkit for Microsoft Excel: Berkeley Geochronology Center Special Publication 4, 76 p.

Macfarlane, P.A., 2009, New insights into the hydrostratigraphy of the High Plains aquifer from three-dimensional visualizations based on well records: Geosphere, v. 5, p. 51-58.

Mastin, L.G., Guffanti, M., Servranckx, R., Webley, P., Barsotti, S., Dean, K., Durant, A., Ewert, J.W., Neri, A., Rose, W.I., Schneider, D., Siebert, L., Stunder, B., Swanson, G., Tupper, A., Volentik, A., and Waythomas, C.F., 2009a, A multidisciplinary effort to assign realistic source parameters to models of volcanic ash-cloud transport and dispersion during eruptions: Journal of Volcanology and Geothermal Research, v. 186, p. 10-21.

Mastin, L.G., Guffanti, M., Ewert, J.E., and Spiegel, J., 2009b, Preliminary spreadsheet of eruption source parameters for volcanoes of the world: U.S. Geological Survey Open-File Report 09-1133, v. 1.2, 25 p.

Mastin, L.G., Van Eaton, A.R., and Lowenstern, J.B., 2014, Modeling ash fall distribution from a Yellowstone supereruption: Geochemistry, Geophysics, Geosystems, v. 15, p. 3459-3475.

McGuire, V.L., 2009, Water-level changes in the High Plains aquifer, predevelopment to 2007, 2005-06, and 2006-07: U.S. Geological Survey Scientific Investigations Report 2009-5019, 9 p.

McMillan, M.E., Angevine, C.L., and Heller, P.L., 2002, Postdepositional tilt of the Miocene-Pliocene Ogallala Group on the western Great Plains: Evidence of late Cenozoic uplift of the Rocky Mountains: Geology, v. 30, p. 63–66.

McMillan, M.E., Heller, P.L., and Wing, S.L., 2006, History and causes of post-Laramide relief in the Rocky Mountain orogenic plateau: Geological Society of America Bulletin, v. 118, p. 393-405.

Molnar, P., 2004, Late Cenozoic increase in accumulation rates of terrestrial sediment: how might climate change have affected erosion rates? Annual Review of Earth and Planetary Sciences, v. 32, p. 67-89.

Molnar, P. and England, P., 1990, Late Cenozoic uplift of mountain ranges and global climate change: chicken or egg? Nature, v. 346, p. 29-34.

Moore, R.C., Frye, J.C., Jewett, J.M., Lee, W., and O'Connor, H.G., 1951, The Kansas Rock Column: Kansas Geological Survey, Bulletin 89, 132 p.

Mundil, R., Ludwig, K.R., Metcalfe, I., and Renne, P.R., 2004, Age and timing of the Permian mass extinctions: U/Pb dating of closed-system zircons: Science, v. 305, p. 1760-1763.

Naeser, C.W., Izett, G.A., and Obradovich, J.D., 1980, Fission-track and K-Ar ages of natural glasses: U.S. Geological Survey Bulletin 1489, 31 p.

Nash, B.P. and Perkins, M.E., 2012, Neogene fallout tuffs from the Yellowstone hotspot in the Columbia plateau region, Oregon, Washington and Idaho, USA: PLoS One, v. 7, 13 p.

Nash, B.P., Perkins, M.E., Christensen, J.N., Lee, D.C., and Halliday, A.N., 2006, The Yellowstone hotspot in space and time: Nd and Hf isotopes in silicic magmas: Earth and Planetary Science Letters, v. 247, p. 143-156.

Neuhauser, K.R. and Pool, J.C., 1988, Geologic map, Ellis County, Kansas: Kansas Geological Survey, Map M-19, scale 1:53,870, 48 x 39 inches.

Newell, A.J., 2001, Bounding surfaces in a mixed aeolian–fluvial system (Rotliegend, Wessex Basin, SW UK): Marine and Petroleum Geology, v. 18, p. 339-347.

North, C.P. and Prosser, D.J., 1993, Characterization of fluvial and aeolian reservoirs: problems and approaches, *in* North, C.P. and Prosser, D.J., eds., Characterization of Fluvial and Aeolian Reservoirs: Geological Society of London Special Publication 73, p. 1-6.

Oskin, M. and Stock, J., 2003, Marine incursion synchronous with plate-boundary localization in the Gulf of California: Geology, v. 31, p. 23–26.

Paton, C., Hellstrom, J., Paul, B., Woodhead, J., and Hergt, J., 2011, Iolite: Freeware for the visualisation and processing of mass spectrometric data: Journal of Analytical Atomic Spectrometry, v. 26, p. 2508-2518.

Paton, C., Woodhead, J.D., Hellstrom, J.C., Hergt, J.M., Greig, A., and Maas, R., 2010, Improved laser ablation U-Pb zircon geochronology through robust downhole fractionation correction: Geochemistry, Geophysics, Geosystems, v. 11, 36 p.

Perkins, M.E., 1998, Tephrochronologic and volcanologic studies of silicic fallout tuffs in Miocene basins of the northern Basin and Range Province, U.S.A. [Ph.D. dissertation]: Salt Lake City, UT, University of Utah, 206 p.

Perkins, M.E., Brown, F.H., Nash, W.P., McIntosh, W., and Williams, S.K., 1998, Sequence, age, and source of silicic fallout tuffs in middle to late Miocene basins of the northern Basin and Range province: Geological Society of America Bulletin, v. 110, p. 344-360.

Perkins, M. and Nash, B., 2002, Explosive silicic volcanism of the Yellowstone hotspot: the ash fall tuff record: Geological Society of America Bulletin, v. 114, p. 367–381.

Perkins, M.E., Nash, W.P., Brown, F.H., and Fleck, R.J., 1995, Fallout tuffs of Trapper Creek, Idaho—a record of Miocene explosive volcanism in the Snake River Plain volcanic province: Geological Society of America Bulletin, v. 107, p. 1484-1506.

Petrus, J.A. and Kamber, B.S., 2012, VizualAge: A novel approach to laser ablation ICP-MS U-Pb geochronology data reduction: Geostandards and Geoanalytical Research, v. 36, p. 247-270.

Pierce, K.L. and Morgan, L.A., 1992, The track of the Yellowstone hot spot: volcanism, faulting, and uplift, *in* Link, P.K., Kuntz, M.A., and Platt, L.B., eds., Regional Geology of Eastern Idaho and Western Wyoming: Geological Society of America Memoir 179, 53 p.

Potter, S.L., 1991, Geologic characteristics of the Calvert ash bed, Ogallala Group (Miocene), western Kansas [M.S. thesis]: Hays, KS, Fort Hays State University, 86 p.

Qi, S.L., 2010, Digital map of the aquifer boundary of the High Plains aquifer in parts of Colorado, Kansas, Nebraska, New Mexico, Oklahoma, South Dakota, Texas, and Wyoming: U.S. Geological Survey Data Series 543.

Rasmussen, B. and Fletcher, I.R., 2010, Dating sedimentary rocks using in situ U-Pb geochronology of syneruptive zircon in ash-fall tuffs < 1 mm thick: Geology, v. 38, p. 299-302.

Renne, P.R., Mundil, R., Balco, G., Min, K., and Ludwig, K.R., 2010, Joint determination of ^{40}K decay constants and $^{40}Ar^{*}/^{40}K$ for the Fish Canyon sanidine standard, and improved accuracy for $^{40}Ar/^{39}Ar$ geochronology: Geochimica et Cosmochimica Acta, v. 74, p. 5349-5367.

Riihimaki, C.A., Anderson, R.S., and Safran, E.B., 2007, Impact of rock uplift on rates of late Cenozoic Rocky Mountain river incision: Journal of Geophysical Research: Earth Surface, v. 112, 15 p.

Rodgers, D.W., Hackett, W.R., and Ore, H.T., 1990, Extension of the Yellowstone Plateau, eastern Snake River Plain, Owyhee Plateau: Geology, v. 18, p. 1138-1141.

Rose, W.I., Riley, C.M. and Dartevelle, S., 2003, Sizes and shapes of 10-Ma distal fall pyroclasts in the Ogallala Group, Nebraska: The Journal of geology, v. 111, p. 115-124.

Roy, M., Kelley, S., Pazzaglia, F., Cather, S., and House, M., 2004, Middle Tertiary buoyancy modification and its relationship to rock exhumation, cooling, and subsequent extension at the eastern margin of the Colorado Plateau: Geology, v. 32, p. 925-928.

Santos, R.V., Souza, P.A., de Alvarenga, C.J.S., Dantas, E.L., Pimentel, M.M., de Oliveira, C.G. and de Araújo, L.M., 2006, Shrimp U–Pb zircon dating and palynology of bentonitic layers from the Permian Irati Formation, Paraná Basin, Brazil: Gondwana Research, v. 9, p. 456-463.

Seni, S.J., 1980, Sand-body geometry and depositional systems, Ogallala Formation, Texas: Texas Bureau of Economic Geology Report of Investigations 105, 36 p.

Sheldon, N.D. and Tabor, N.J., 2009, Quantitative paleoenvironmental and paleoclimatic reconstruction using paleosols: Earth-Science Reviews, v. 95, p. 1–52.

Skinner, M.F. and Johnson, F.W., 1984, Tertiary stratigraphy and the Frick Collection of fossil vertebrates from north-central Nebraska: Bulletin of the American Museum of Natural History, v. 178, p. 215-368.

Sláma, J., Košler, J., Condon, D.J., Crowley, J.L., Gerdes, A., Hanchar, J.M., Horstwood, M.S.A., Morris, G.A., Nasdala, L., Norberg, N., Schaltegger, U., Schoene, B., Tubrett, M.N., and

Whitehouse, M.J., 2008, Plešovice zircon—a new natural reference material for U–Pb and Hf isotopic microanalysis: Chemical Geology, v. 249, p. 1-35.

Smith, H.T.U., 1940, Geological studies in southwestern Kansas: Kansas Geological Survey, Bulletin 34, p. 1-212.

Smith, J.J., Layzell, A.L., Lukens, W.E., Morgan, M.L., Keller, S.M., Martin, R.A., and Fox, D.L., 2016, Getting to the bottom of the High Plains aquifer: new insights into the depositional history, stratigraphy, and paleoecology of the Cenozoic High Plains, *in* Morgan, M.L. and Keller, S.M., eds., Geological Society of America Field Guides (in press).

Smith, J. and Ludvigson, G., 2011, A Report to the Calvert Corporation on a Geologic Inspection of the Calvert Volcanic Ash Mine: Kansas Geological Survey, Open-File Report 2014-3, 5 p.

Smith, J., Ludvigson, G.A., Harlow, H., and Platt, B., 2014, Ogallala-High Plains aquifer special study phase III: Lithologic calibration of practical saturated thickness in the Ogallala-High Plains aquifer: Kansas Geological Survey, Open-File Report 2014-2, 9 p.

Smith, R.B. and Braile, L.W., 1993, Topographic signature, space-time evolution, and physical properties of the Yellowstone-Snake River Plain volcanic system: the Yellowstone hotspot, *in* Snoke, A.W., Steidtmann, J.R., and Roberts, S.M., eds., Geological Survey of Wyoming Memoir 5, p. 694-754.

Soller, D.R. and Reheis, M.C., 2004, Surficial materials in the conterminous United States: U.S. Geological Survey Open-File Report 03-275, scale 1:5,000,000.

Steward, D.R. and Allen, A.J., 2016, Peak groundwater depletion in the High Plains Aquifer, projections from 1930 to 2110: Agricultural Water Management, v. 170, p. 36-48.

Steward, D.R., Bruss, P.J., Yang, X., Staggenborg, S.A., Welch, S.M., and Apley, M.D., 2013, Tapping unsustainable groundwater stores for agricultural production in the High Plains Aquifer of Kansas, projections to 2110: Proceedings of the National Academy of Sciences, v. 110, p. E3477-E3486.

Stone, W.J., 1990, Natural recharge of the Ogallala aquifer through playas and other non-stream-channel settings, eastern New Mexico, *in* Gustavson, T.C., ed., Geologic Framework and Regional Hydrology: Upper Cenozoic Blackwater Draw and Ogallala Formations, Great Plains: Texas Bureau of Economic Geology Symposium Publication 6, p. 180-192.

Sweet, M.L., 1999, Interaction between aeolian, fluvial and playa environments in the Permian Upper Rotliegend Group, UK southern North Sea: Sedimentology, v. 46, p. 171-188.

Swineford, A, 1963, The Pearlette ash as a stratigraphic marker: Transactions of the Kansas Academy of Science, v. 66, p. 359-362.

Swineford, A., Frye, J.C., and Leonard, A.B., 1955, Petrography of the late Tertiary volcanic ash falls in the central Great Plains: Journal of Sedimentary Petrology, v. 25, p. 243-261.

Swineford, A., Leonard, A.B., and Frye, J.C., 1958, Petrology of the pisolitic limestone in the Great Plains: Kansas Geological Survey, Bulletin 130, pt. 2, p. 97-116.

Swinehart, J.B., 1974, Ogallala stratigraphy of southwest Nebraska: a proposal: Nebraska Academy of Science Program, p. 36-37.

Swinehart, J.B., Souders, V.L., DeGraw, H.M., and Diffendal R.F., Jr., 1985, Cenozoic paleogeography of western Nebraska, *in* Flores, R.M. and Kaplan, S.S., eds., Cenozoic Paleogeography of West-Central United States: Rocky Mountain Paleogeography Symposium, v.3, p. 209–229.

Tallan, M.E., 1978, Systematics and biostratigraphy of the early Hemphillian Bemis local fauna, Ellis County, Kansas [M.S. thesis]: Hays, KS, Fort Hays State University, 36 p.

Thomasson, J.R., 1979, Late Cenozoic grasses and other angiosperms from Kansas, Nebraska, and Colorado: Biostratigraphy and relationships to living taxa: Kansas Geological Survey, Bulletin 218, 68 p.

Thomasson, J.R., 1990, Fossil plants from the late Miocene Ogallala Formation of central North America: possible paleoenvironmental and biostratigraphic significance, *in* Gustavson, T.C., ed., Geologic Framework and Regional Hydrology: Upper Cenozoic Blackwater Draw and Ogallala Formations, Great Plains: Texas Bureau of Economic Geology Symposium Publication 6, p. 99-114.

Trimble, D.E., 1980, Cenozoic tectonic history of the Great Plains contrasted with that of the Southern Rocky Mountains: a synthesis: The Mountain Geologist, v. 17, p. 59-69.

Turner, E., Smith, J.J., Ludvigson, G.A., Layzell, A.L., and Möller, A., 2015, Maximum depositional age constraints from U-Pb dating of zircons in Cenozoic deposits of the High Plains Aquifer, southwestern Kansas: Geological Society of America Abstracts with Programs, v. 47, p. 801.

van Dijk, W.M., Densmore, A.L., Singh, A., Gupta, S., Sinha, R., Mason, P.J., Joshi, S.K., Nayak, N., Kumar, M., Shekhar, S., Kumar, D., and Rai, S.P., 2016, Linking the morphology of fluvial fan systems to aquifer stratigraphy in the Sutlej-Yamuna plain of northwest India: Journal of Geophysical Research: Earth Surface, v. 121, p. 201-222.

Vermeesch, P., 2012, On the visualisation of detrital age distributions: Chemical Geology, v. 312-313, p. 190-194.

Wayne, W.J., Aber, J.S., Agard, S.S., Bergantino, R.N., Bluemle, J.P., Coates, D.A., Cooley, M.E., Madole, R.F., Martin, J.E., Mears, B., Jr., Morrison, R.B., and Sutherland, W.M., 1991, Quaternary geology of the Northern Great Plains, *in* Morrison, R.B., ed., The Geology of North America, v. K-2: Quaternary Nonglacial Geology: Conterminous U.S., p. 441-476.

Weeks, J.B. and Gutentag, E.D., 1981, Bedrock geology, altitude of base, and 1980 saturated thickness of the high plains aquifer in parts of Colorado, Kansas, Nebraska, New Mexico, Oklahoma, South Dakota, Texas, and Wyoming: U.S. Geological Survey Hydrologic Investigations Atlas HA-648, scale 1:2,500,000, 2 sheets.

Weissmann, G.S., Hartley, A.J., Nichols, G.J., Scuderi, L.A., Olson, M., Buehler, H., and Banteah, R., 2010, Fluvial form in modern continental sedimentary basins: Distributive fluvial systems: Geology, v. 38, p. 39-42.

Wilson, B., MacFarlane, P.A., Young, D.P., and Sleezer, R., 2009, High Plains aquifer bedrock isolines: accessed 24 May 2016 <http://www.kansasgis.org/catalog/index.cfm>.

Wobus, C.W., Tucker, G.E., and Anderson, R.S., 2010, Does climate change create distinctive patterns of landscape incision? Journal of Geophysical Research: Earth Surface, v. 115, 12 p.

Wotzlaw, J.F., Schaltegger, U., Frick, D.A., Dungan, M.A., Gerdes, A., and Günther, D., 2013, Tracking the evolution of large-volume silicic magma reservoirs from assembly to supereruption: Geology, v. 41, p. 867-870.

Zakrzewski, R.J., 1990, Biostratigraphy of fossil mammals from the Ogallala (Miocene) of north-central Kansas, *in* Gustavson, T.C., ed., Geologic Framework and Regional Hydrology: Upper Cenozoic Blackwater Draw and Ogallala Formations, Great Plains: Texas Bureau of Economic Geology Symposium Publication 6, p. 98.

Zeigler, K.E., Petronis, M.S., Smith, J.J., Ludvigson, G.A., and Doveton, J., 2012, The Neogene Ogallala Formation in southwestern Kansas and northeastern New Mexico: Preliminary magnetostratigraphic analyses for the High Plains-Ogallala Drilling Program: AGU Fall Meeting Abstracts, v. 1, p. 1032.

Zeller, D.E., ed., 1968, The stratigraphic succession in Kansas: Kansas Geological Survey, Bulletin 189, 81 p.

FIGURES

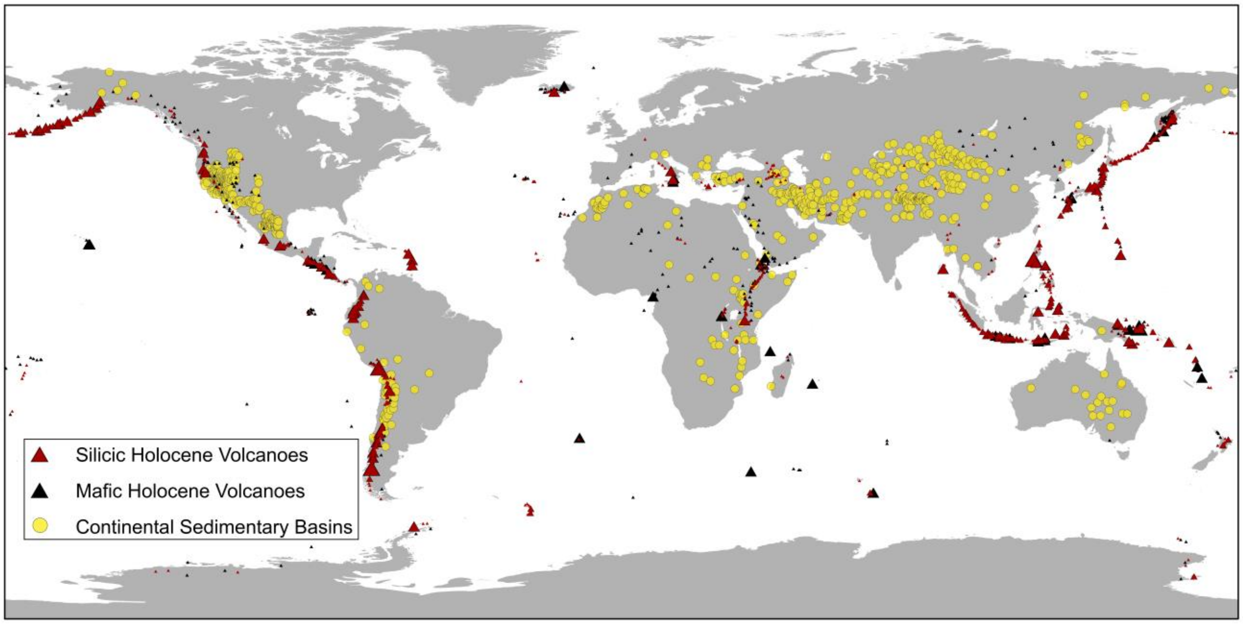

Figure 1. Spatial distribution of modern non-marine continental sedimentary basins (Weissmann et al., 2010) compared to Holocene subaerial volcanoes (Global Volcanism Program, 2013) scaled by size according to their ash-bearing potential using the model of Mastin et al. (2009a,b). Many continental clastic basins, for instance in North America, are hundreds to thousands of kilometers from active volcanic arcs, rifts, and hot spots. These basins potentially preserve volcanogenic zircon from volcanic ash distributed in large eruptions. When recognized, zircon-bearing volcanic ash can provide valuable age information in strata that are poor in other common chronological and correlative means, such as marine fossils.

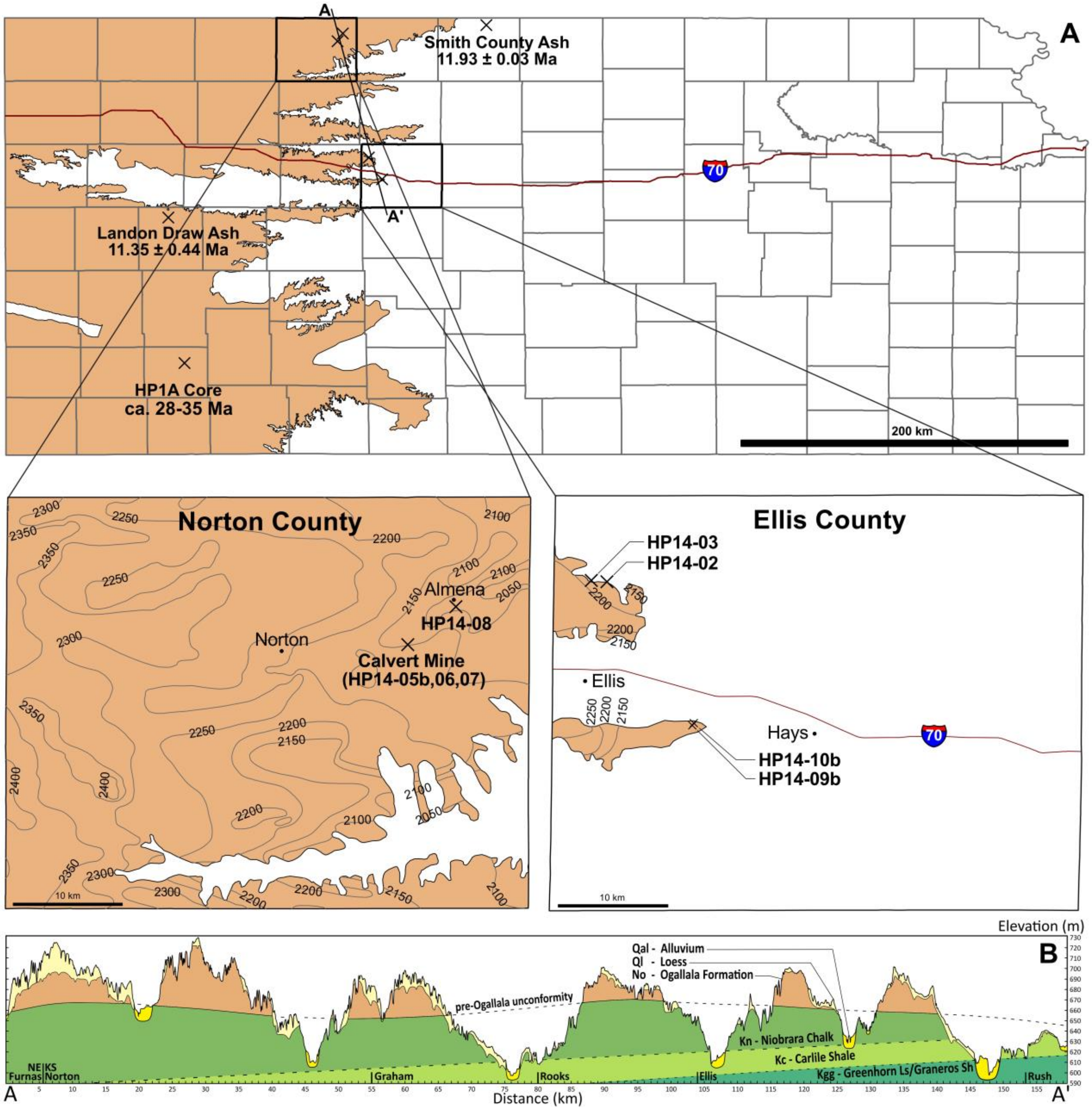

Figure 2. (A) The Ogallala Formation and associated Ogallala-High Plains aquifer serve as the primary water source for irrigation and domestic water consumption in the High Plains of the central United States. The subsurface and exposed extent of the Ogallala Formation in western Kansas is modified from Qi (2010) in order to exclude hydrologically connected Quaternary units of the Ogallala-High Plains aquifer using maps by Moore et al. (1951) and Zeller (1968). Pre-Ogallala topography is revealed by structure contours (ft) of the base of the Ogallala Formation

(Wilson et al., 2009). Existing absolute dates are sparse: chemical fingerprinting of an ash from Smith County most closely matches the 11.93 ± 0.03 Ma Ibex Hollow ash (Ludvigson et al., 2009). This ash plots outside of the currently mapped extent of the Ogallala Formation, indicating that revisions to lithologic mapping criteria are needed (Ludvigson et al., 2009). A single zircon from an ash at Landon Draw yields an LA-ICP-MS date of 11.35 ± 0.44 Ma (personal communication from analyst Brian Sitek, 2014). Sedimentological characteristics and U-Pb zircon data from the HP1A core indicates that parts of southwestern Kansas mapped as Ogallala Formation may be a previously unrecognized equivalent of the Paleogene White River Group (Smith et al., 2014; Turner et al., 2015; Smith et al., 2016). **(B)** Cross section showing depositional and cross-cutting relations between units exposed in western Kansas inferred from existing maps (Frye and Leonard, 1949; Neuhauser and Pool, 1988). Location and dip of the Niobrara-Carlile and Carlile-Greenhorn contact is approximate and inferred from map M-118 by the Kansas Geological Survey (2008). The Ogallala basal unconformity is modified from smoothed regional-scale structure contours by Weeks and Gutentag (1981) and Cederstrand and Becker (1998). All contacts except Carlile-Greenhorn are unconformable. Vertical exaggeration is ~150.

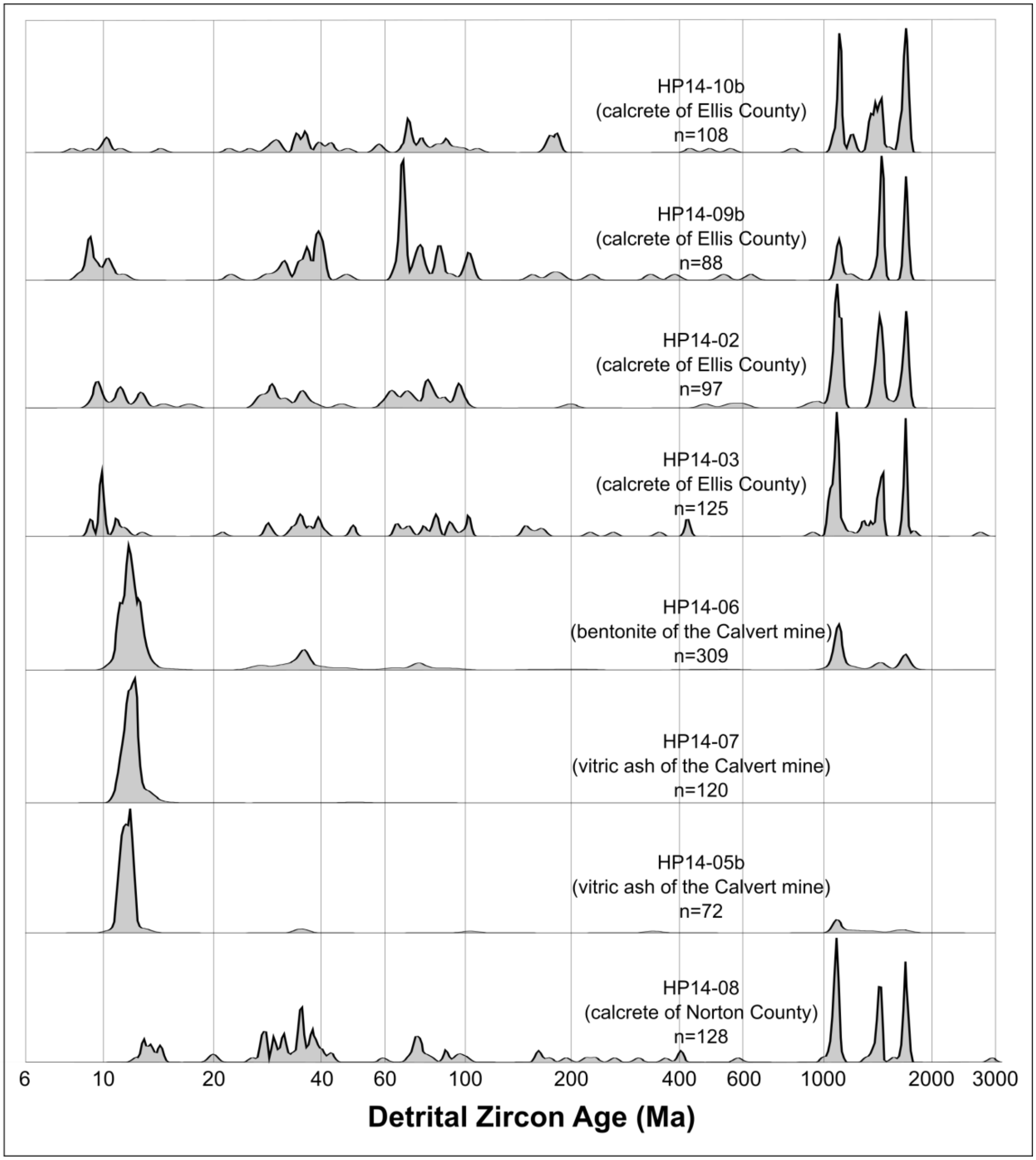

Figure 3. Kernel density plots based on $^{206}Pb/^{238}U$ ages (<850 Ma) and $^{207}Pb/^{206}Pb$ ages (≥850 Ma) constructed with DensityPlotter (Vermeesch, 2012). Calcretes contain abundant volcanogenic zircons, as well as Miocene to Archean detrital grains. Norton County vitric ashes and bentonites derived from those ashes are dominated by volcanogenic middle Miocene grains. Analyses with normalized discordance ($^{207}Pb/^{235}U_{age}$ - $^{206}Pb/^{238}U_{age}$)/($^{207}Pb/^{235}U_{2\sigma\ age\ uncertainty}$) >5 were omitted.

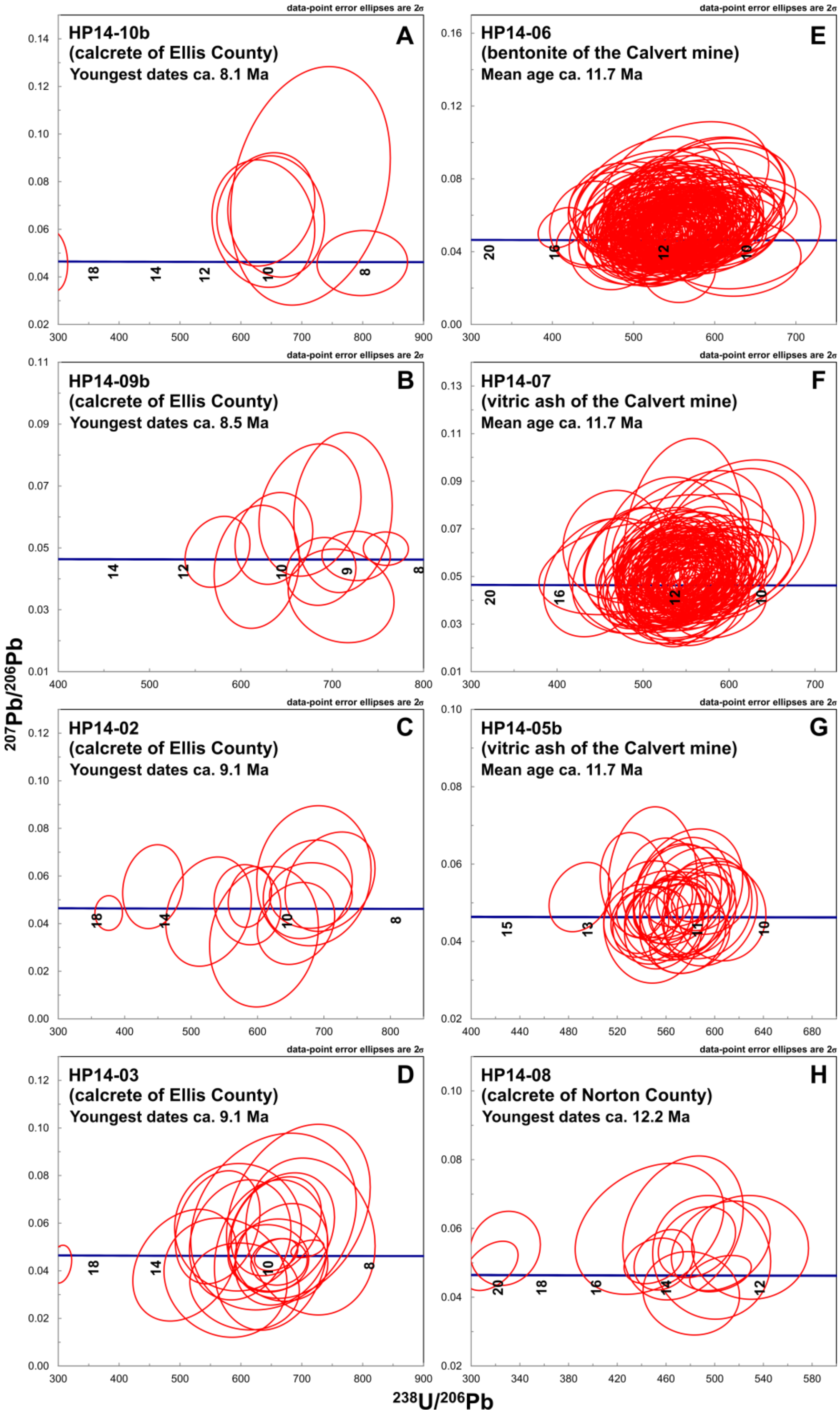
HP14-10b
(calcrete of Ellis County)
Youngest dates ca. 8.1 Ma
A
HP14-06
(bentonite of the Calvert mine)
Mean age ca. 11.7 Ma
E
HP14-09b
(calcrete of Ellis County)
Youngest dates ca. 8.5 Ma
B
HP14-07
(vitric ash of the Calvert mine)
Mean age ca. 11.7 Ma
F
HP14-02
(calcrete of Ellis County)
Youngest dates ca. 9.1 Ma
C
HP14-05b
(vitric ash of the Calvert mine)
Mean age ca. 11.7 Ma
G
HP14-03
(calcrete of Ellis County)
Youngest dates ca. 9.1 Ma
D
HP14-08
(calcrete of Norton County)
Youngest dates ca. 12.2 Ma
H
data-point error ellipses are 2σ
207Pb/206Pb
238U/206Pb

Figure 4. U-Pb concordia diagrams depicting the youngest concordant dates from each dated sample. Ellis County calcretes include grains as young as ~8.1-9.1 Ma, Norton County ashes and bentonites are each dominated by an ~11.7 Ma population, and a Norton County calcrete includes grains as young as ~12.2 Ma. Full detrital age spectra are presented in Figure 3. Analyses with normalized discordance ($^{207}Pb/^{235}U_{age}$ - $^{206}Pb/^{238}U_{age}$)/($^{207}Pb/^{235}U_{2\sigma\ age\ uncertainty}$) >1.2 were omitted for clarity.

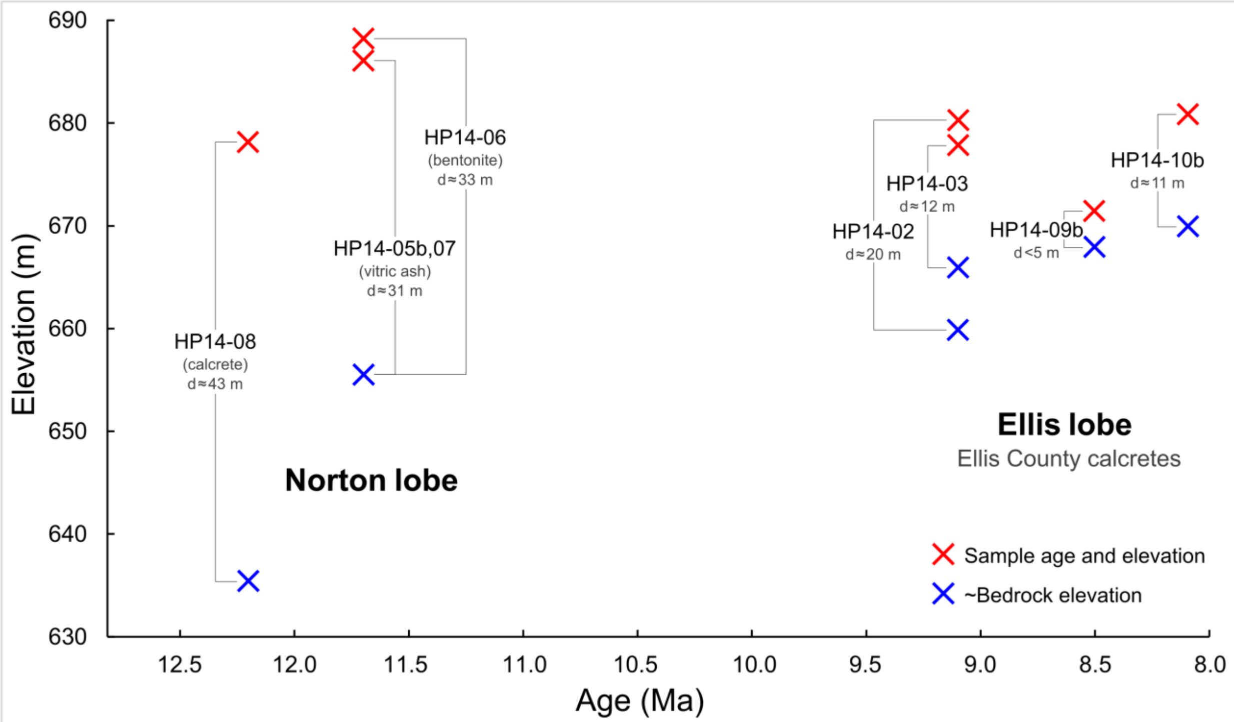

Figure 5. Bedrock topography (adapted from Wilson et al., 2009) governed the timing of Ogallala Formation deposition in northwestern Kansas and locally within Norton and Ellis counties. Deposition in the vicinity of Norton County began prior to 12.2 Ma and aggraded to ~690 m in elevation by ca. 11.7 Ma. Aggradation in the vicinity of Ellis County began shortly before 9 Ma and aggraded to ~680 m in elevation ca. 8.1 Ma or later.

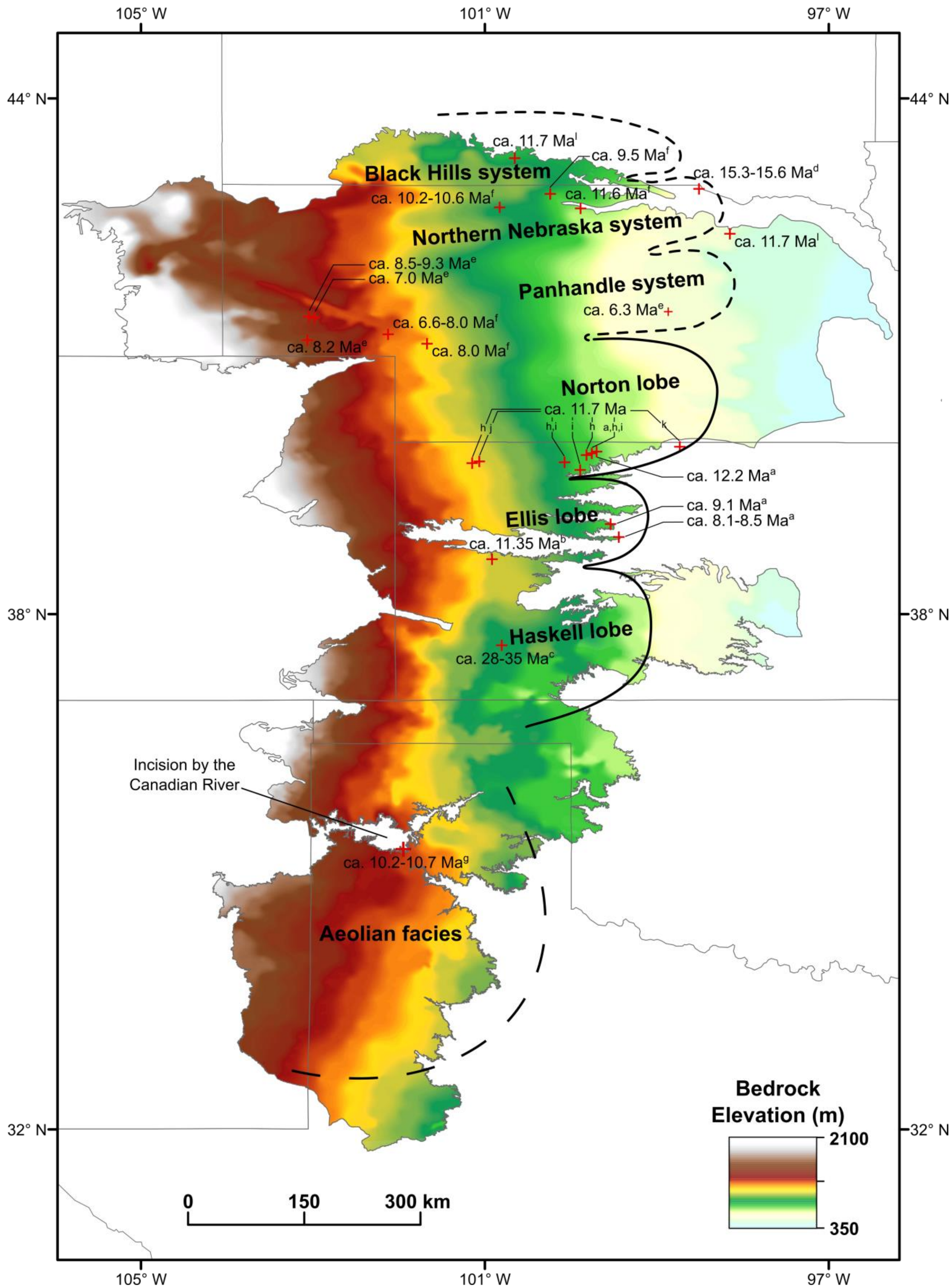
105° W
101° W
97° W
44° N
38° N
32° N
ca. 11.7 Ma[l]
ca. 9.5 Ma[f]
Black Hills system
ca. 15.3-15.6 Ma[d]
ca. 10.2-10.6 Ma[f]
ca. 11.6 Ma[f]
Northern Nebraska system
ca. 11.7 Ma[l]
ca. 8.5-9.3 Ma[e]
ca. 7.0 Ma[e]
Panhandle system
ca. 6.3 Ma[e]
ca. 6.6-8.0 Ma[f]
ca. 8.2 Ma[e]
ca. 8.0 Ma[f]
Norton lobe
ca. 11.7 Ma
ca. 12.2 Ma[a]
Ellis lobe
ca. 9.1 Ma[a]
ca. 8.1-8.5 Ma[a]
ca. 11.35 Ma[b]
Haskell lobe
ca. 28-35 Ma[c]
Incision by the Canadian River
ca. 10.2-10.7 Ma[g]
Aeolian facies
Bedrock Elevation (m)
2100
350
0
150
300 km

Figure 6. The spatial and temporal architecture of the Ogallala Formation, with bedrock elevations illustrated over its regional extent and inferred depositional ages marked in red, is consistent with its aggradation as a series of diachronous fluvial lobes. The middle Miocene Norton lobe aggraded on the northern flank of a central Kansas bedrock ridge ca. 11-13 Ma, followed by the late Miocene Ellis lobe over the inverted topography of the central Kansas ridge ca. 8-10 Ma. Eocene-Oligocene deposits of southwestern Kansas (Smith et al., 2014; Turner et al., 2015; Smith et al., 2016) potentially constitute an inferred Haskell lobe. Kansas lobe geometry is based on bedrock topography and geochronology presented here. To the north of Kansas, three Nebraska paleodrainage systems inferred by Skinner and Johnson (1984) are plotted as fluvial lobes (small dashes). The Ogallala Formation south of the Canadian River consists of a sheet of aeolian deposits (dashed) overlying fluvial channel fills and bedrock interfluves (Gustavson and Winkler, 1988; Holliday, 1991).

Bedrock topography is revealed by a DEM modified from the bedrock structure contours of Weeks and Gutentag (1981) and Cederstrand and Becker (1998). This late Cenozoic surface controlled deposition of the Ogallala Formation and associated units both locally (Fig. 5) and regionally. Geographic extent of the Cenozoic continental clastic units associated with the Ogallala-High Plains aquifer is given by the boundary of Qi (2010).

Plotted ages for the undated Ashfall Fossil Beds, Mission Pit (Famoso and Pagnac, 2011), and Smith County ashes (Ludvigson et al., 2009) are revised to ca. 11.7 Ma because of their shared correlation with the Ibex Hollow ash and by extension, the Calvert ash dated as part of this study. Dates are sourced from: a, this study; b, personal communication from analyst Brian Sitek, 2014 (zircon LA-ICP-MS); c, Turner et al., 2015; Smith et al., 2016 (zircon LA-ICP-MS); d, Field et al., 2015 (zircon LA-ICP-MS); e, Boellstorff, 1976 (glass fission-track); f, Skinner and Johnson, 1984 (glass fission-track); g, Cepeda and Perkins, 2006 (glass K-Ar). Plotted yet undated ashes are correlated to dated beds by ash petrography unless otherwise specified: h, Potter, 1991; i, Carey et al., 1952; j, Swineford et al., 1955; k, Ludvigson et al., 2009 (chemical fingerprinting); l, Famoso and Pagnac, 2011.

APPENDICES

Appendix A: Annotated Outcrop Photographs

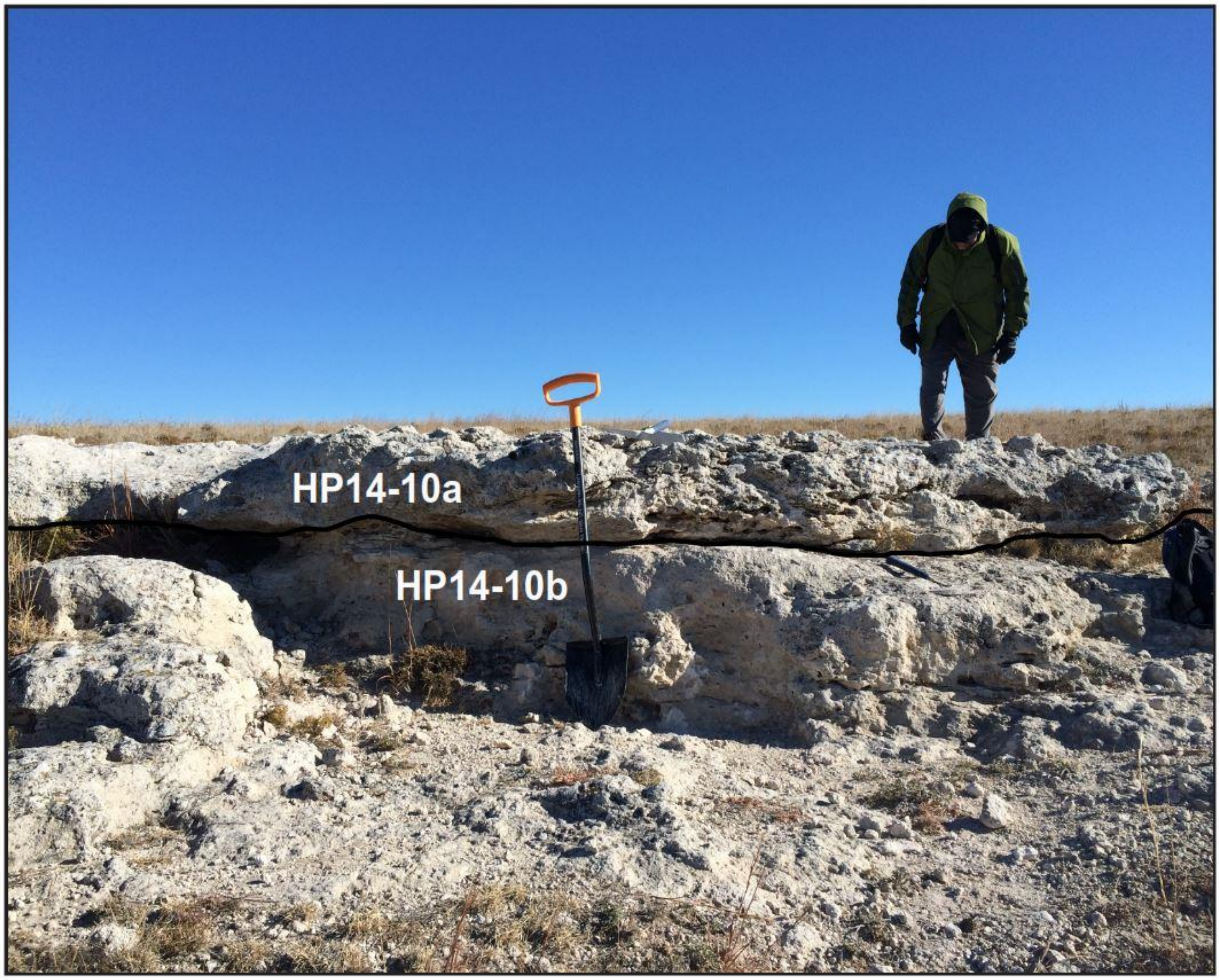

Figure 7. Calcrete near the Bemis Local Fauna locality of Tallan (1978) in west-central Ellis County. Both HP14-10b and HP14-10a (not dated) include sand and pebbles.

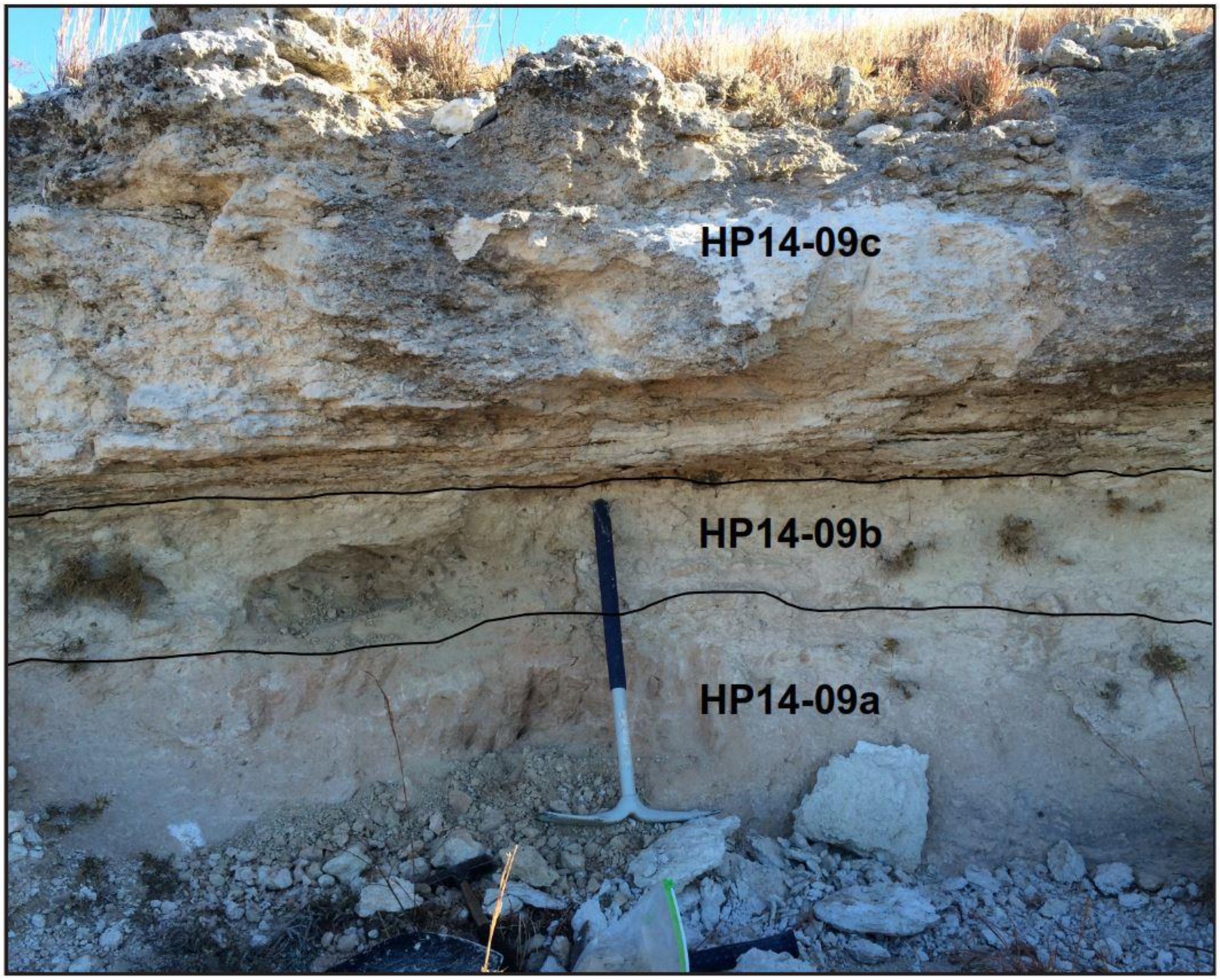

Figure 8. Calcrete near the Bemis Local Fauna locality (Tallan, 1978; Thomasson, 1979) in west-central Ellis County. Units are distinguished primarily by color and weathering profile.

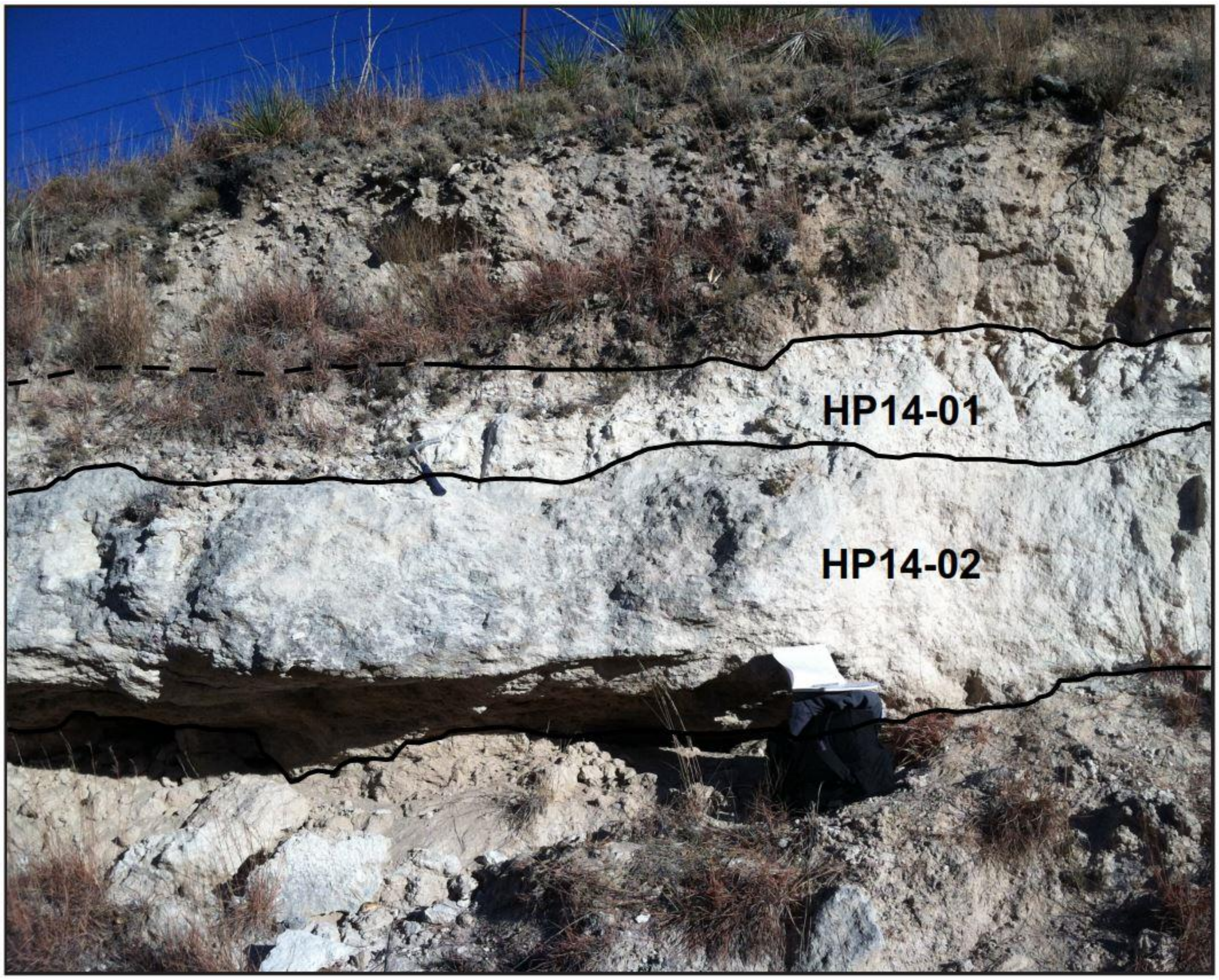

Figure 9. Calcrete in a roadcut along 130th Ave previously described by Thomasson (1979). The upper unit (HP14-01; not dated) contains gastropod casts and a finer-grained clastic assemblage than the lower unit (HP14-02).

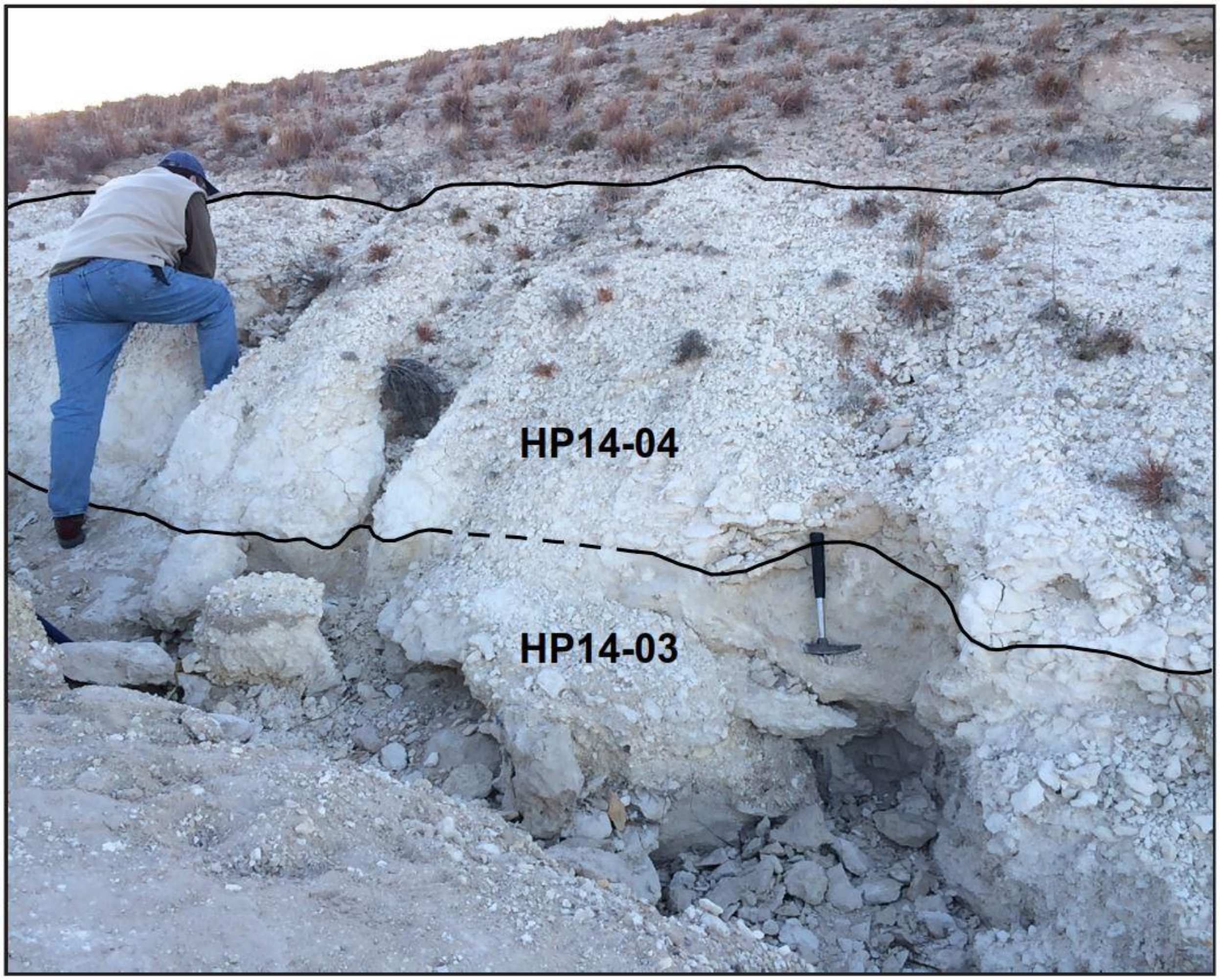

Figure 10. Calcrete in a roadcut along 120th Ave. The lower unit (HP14-03) includes a larger, coarser-grained assemblage of sand and pebbles than the upper unit (HP14-04; not dated).

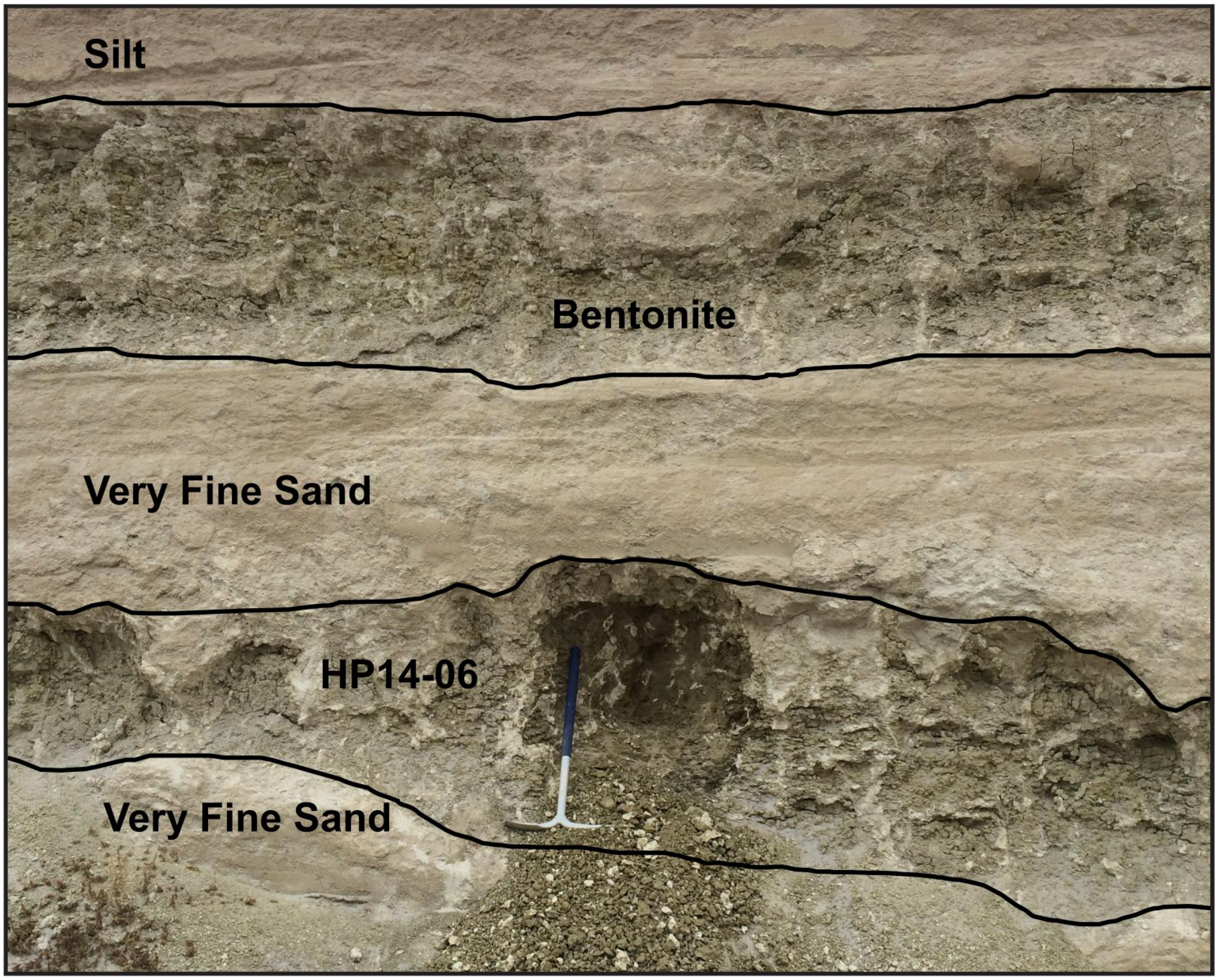

Figure 11. Bentonite paleosols (HP14-06) exposed at the Calvert volcanic ash mine are composed of green montmorillonite (Carey et al., 1952; Frye et al., 1956) and contain abundant rhizoliths.

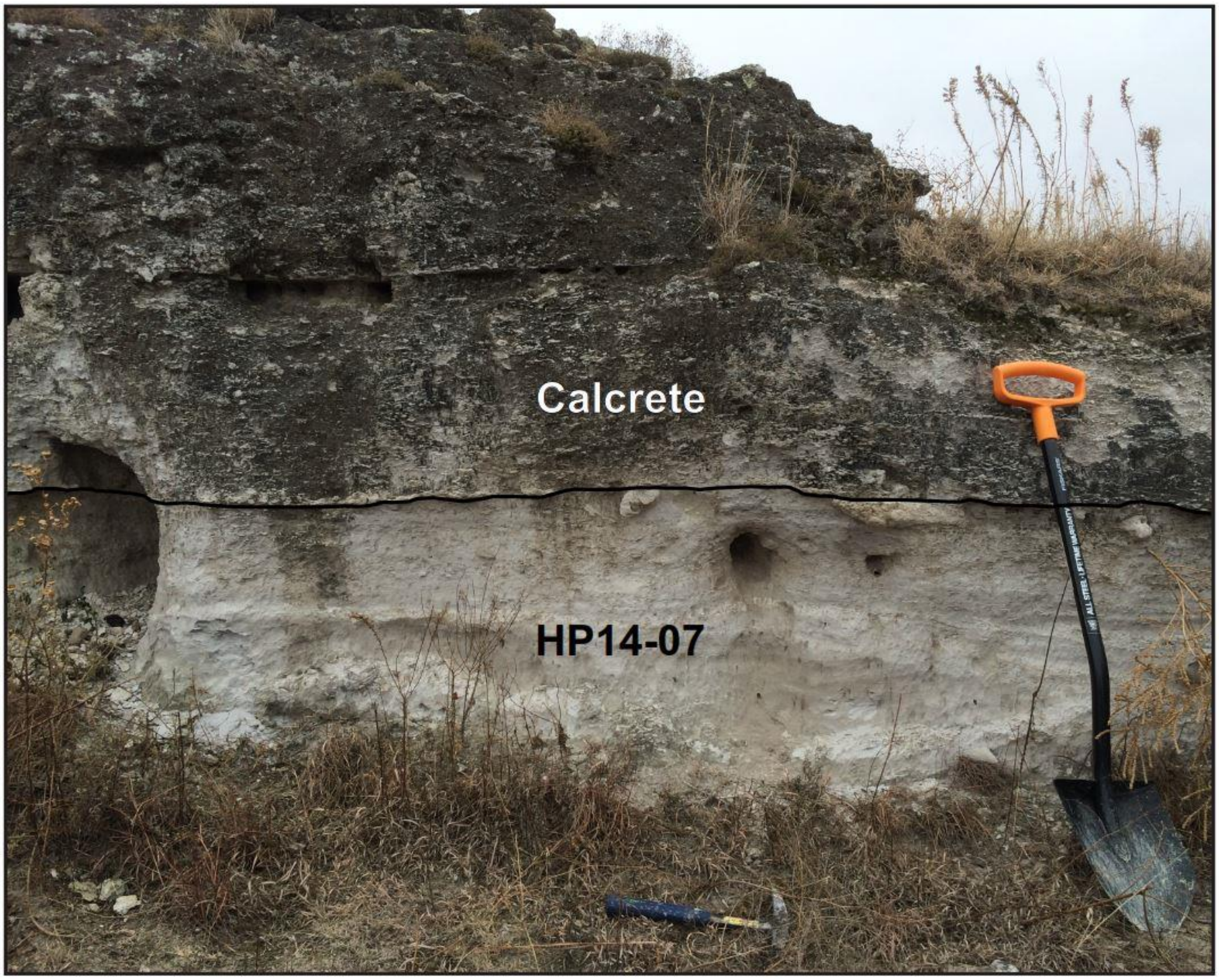

Figure 12. Fine-grained vitric ash from an abandoned face of the Calvert volcanic ash mine.

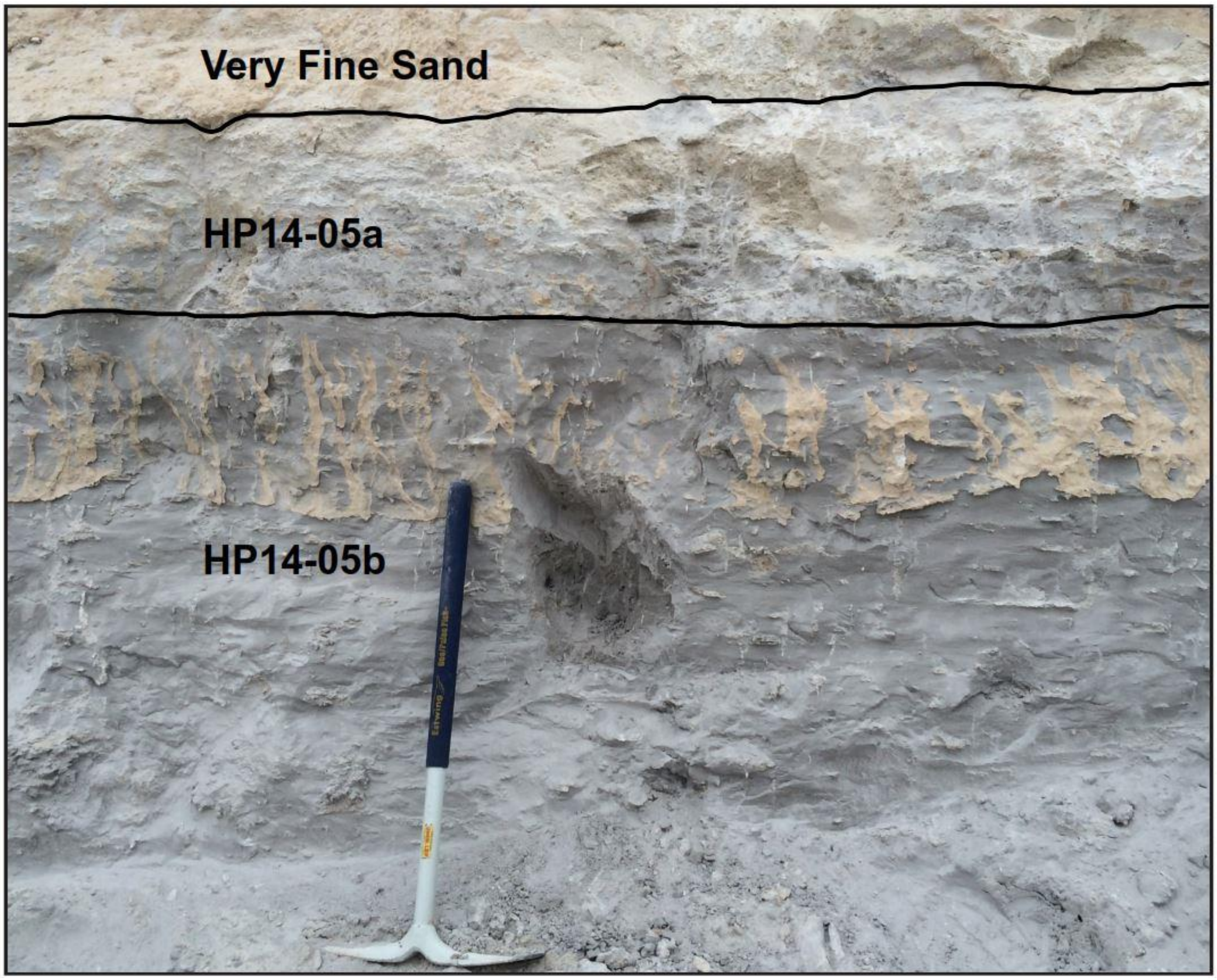

Figure 13. Fine-grained vitric ash from the Calvert volcanic ash mine. HP14-05b is a massively bedded and clean vitric ash. HP14-05a (not dated) is a finely laminated vitric ash that contains calcrete nodules and poorly sorted sand.

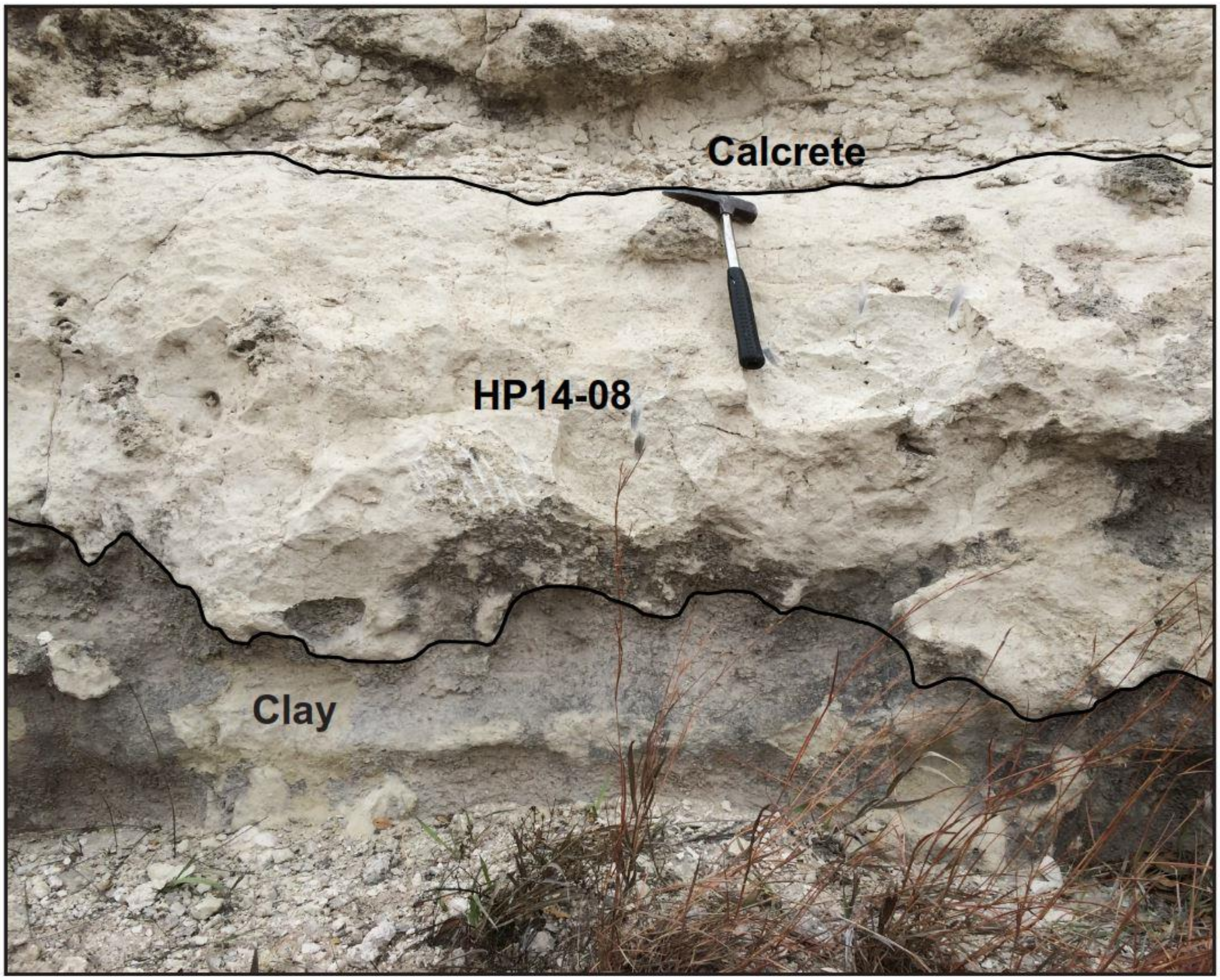

Figure 14. Calcrete in a roadcut along US Route 383 near the town of Almena that contains abundant rhizoliths. The upper calcrete is defined by its thin bedding planes and reduced resistance to weathering.

Appendix B: LA-ICP-MS Metadata

Laboratory & Sample Preparation	
Laboratory name	KU Geology Isotope Geochemistry Laboratories
Sample type/mineral	Zircon
Sample preparation	Conventional mineral separation, tape mount
Laser Ablation System	
Make, Model & type	ArF excimer 193 nm, Photon Machines Analyte G2, ATLEX 300
Ablation cell & volume	Helex 2, two-volume cell
Laser wavelength (nm)	193
Pulse width	5 ns
Fluence	2 J/cm^2
Repetition rate	10 Hz
Spot diameter (nominal/actual)	20/20 μm
Sampling mode/pattern	Single spot
Carrier gas (l/min)	He, 1.01; Ar, 1.1
Ablation duration (secs)	15 (short method); 26 (long method)[a]
Cell carrier gas flow	1.1 l/min
ICP-MS Instrument	
Make, Model & type	Thermo Element2 magnetic sector field ICP-MS
Sample introduction	Ablation aerosol
RF power	1100 W
Make-up gas flow	Ar, 1.1 l/min
Sampling depth	~15 μm
Detection system	Single detector, counting & analog
Masses measured	^{206}Pb, ^{207}Pb, ^{208}Pb, ^{232}Th, ^{238}U
Integration time per peak (ms)	1-6 (short); 1-5 (long)
Total integration time per reading (secs)	7-13 (short); 8-23 (long)
Total method time	23 (short); 42 (long)
Sensitivity/Efficiency	~0.1% U, GJ-1
IC Dead time (ns)	4
UO+/U+ (%)	<0.2
$^{238}U+/^{232}Th+$	0.70

Data Processing	
Gas blank (s)	9 (short); 21 (long)
Calibration strategy	GJ-1 used as primary reference material, Plešovice, Peixe, and Fish Canyon Tuff used as secondary/validation materials
Reference Material info	NIST 612 (Jochum et al., 2011) GJ-1 (Jackson et al., 2004) Plešovice (Horstwood et al., 2016) Peixe (G. Gehrels, unpublished data) Fish Canyon Tuff (Wotzlaw et al., 2013)
Data processing package used/Correction for LIEF	IGOR PRO, Iolite 2.5. LIEF correction assumes reference material and samples behave identically
Mass discrimination	IGOR PRO, Iolite 2.5. Correction assumes reference material and samples behave identically
Common-Pb correction, composition and uncertainty	No common-Pb correction applied to the data.
Uncertainty level & propagation	Age uncertainties are reported at ±2s absolute, propagation is by quadratic addition, following Paton et al. (2010)
Reproducibility	~0.7% and 1.8% in replicate measurements of the Fish Canyon Tuff and Plešovice, respectively
Quality control/Validation	Peixe, Plešovice, and Fish Canyon Tuff (see Table C2 for details)

[a]An initial ICP-MS method file used to analyze four samples (HP14-02, -05b, -09b, -10b) was shortened for the remaining four samples (HP14-03, -06, -07, -08) to improve accuracy and precision, primarily on ^{207}Pb measurements. Parameters that varied by method are specified as either short (method) or long (method).

Appendix C: LA-ICP-MS Quality Control and Validation

Sample	Secondary Standard		
	Peixe	**Plešovice**	**Fish Canyon Tuff**
HP14-05, -09b	561 ± 12 Ma (n=23, MSWD=0.79)	348.6 ± 8.5 Ma (n=21, MSWD=1.8)	N/A
HP14-02, -10b	N/A	342.6 ± 7.9 Ma (n=27, MSWD=1.3)	28.7 ± 1.3 Ma (n=25, MSWD=1.8)
HP14-03, -08	N/A	N/A	28.6 ± 1.7 Ma (n=25, MSWD=2.1)
HP14-06	N/A	N/A	28.62 ± 0.91 Ma (n=24, MSWD=0.51)
HP14-07	N/A	N/A	28.5 ± 1.0 Ma (n=17, MSWD=1.6)
Accepted Age	**564 ± 4 Ma[a]**	**337.2 ± 0.13 Ma[b]**	**ca. 28.642 ± 0.025 Ma to 28.196 ± 0.038 Ma[c]**

Weighted average $^{206}Pb/^{238}U$ ages ± 2s: [a]G. Gehrels, unpublished data; [b]Horstwood et al., 2016; [c]Wotzlaw et al., 2013.

Appendix D: LA-ICP-MS U-Pb Zircon Data

Table D-1: Zircon LA-ICP-MS U-Pb Isotopic Data and Ages: HP14-10b (IGSN: IEKHP10b0[a]): Calcrete of west-central Ellis County (461256, 4304829)[b]

Grain #[c]	U[d] [ppm]	Th[d] [ppm]	Th/U	eU[e] [ppm]	Corrected Isotopic Ratios $^{207}Pb/^{235}U$[f]	±2s[g]	$^{206}Pb/^{238}U$[f]	±2s[g]	Rho[h]	$^{207}Pb/^{206}Pb$[i]	±2s[g]	Ages (Ma)[j] $^{207}Pb/^{235}U$	±2s	$^{206}Pb/^{238}U$	±2s	$^{207}Pb/^{206}Pb$	±2s	Disc. %[k]	Wtd. Disc.[l]
1	130	90	0.68	151	2.523	0.067	0.2069	0.0029	0.41	0.088	0.002	1280	20	1212	15	1394	44	5.3	12.1
2	116	103	0.90	140	0.022	0.005	0.0034	0.0002	-0.02	0.049	0.012	21.8	5.2	22.1	1.5	-10	350	-1.4	-0.1
3	262	127	0.49	292	2.044	0.049	0.1911	0.0030	0.47	0.077	0.002	1129	16	1128	16	1116	40	0.1	-0.8
4	69	73	1.11	87	0.258	0.025	0.0120	0.0005	0.27	0.157	0.015	228	20	77.1	3.3	2360	180	66.2	7.5
5	420	127	0.30	450	0.077	0.004	0.0117	0.0002	0.08	0.047	0.003	75.4	3.8	75.2	1.5	110	110	0.3	0.1
6	86	42	0.49	96	2.854	0.072	0.2382	0.0043	0.51	0.087	0.002	1371	19	1379	22	1360	44	-0.6	-0.9
7	**167**	**94**	**0.55**	**189**	**0.014**	**0.005**	**0.0015**	**0.0002**	**-0.19**	**0.074**	**0.027**	**13.6**	**4.7**	**9.79**	**0.97**	**440**	**570**	**28.0**	**0.8**
8	447	195	0.41	493	0.041	0.003	0.0047	0.0002	0.41	0.063	0.004	40.9	3.1	30.0	1.1	690	140	26.7	3.5
9	284	175	0.62	325	0.375	0.031	0.0079	0.0004	0.41	0.352	0.030	320	22	50.4	2.4	3650	110	84.3	12.3
10	401	105	0.27	426	4.470	0.140	0.3055	0.0084	0.88	0.107	0.002	1720	25	1715	41	1742	35	0.3	0.7
11	127	66	0.51	143	1.997	0.053	0.1897	0.0029	0.32	0.077	0.002	1113	18	1120	16	1104	51	-0.6	-1.0
12	509	487	0.82	623	0.039	0.003	0.0056	0.0001	0.09	0.050	0.004	38.3	2.8	35.87	0.75	210	140	6.3	0.9
13	563	155	0.28	599	2.365	0.056	0.2114	0.0028	0.55	0.081	0.002	1231	17	1236	15	1209	38	-0.4	-1.8
14	493	347	0.65	575	0.035	0.003	0.0053	0.0001	0.06	0.047	0.004	34.5	2.5	34.16	0.81	80	140	1.0	0.1
15	591	356	0.59	675	0.061	0.003	0.0053	0.0001	0.20	0.085	0.005	60.3	3.3	33.88	0.83	1340	110	43.8	8.0
16	405	258	0.63	466	0.606	0.017	0.0774	0.0012	0.39	0.057	0.001	480	11	481.5	7.6	479	54	-0.2	-0.1
17	283	166	0.59	322	0.558	0.020	0.0682	0.0014	0.47	0.059	0.002	451	13	424.9	8.6	551	69	5.8	2.0
18	103	46	0.46	114	4.389	0.110	0.2993	0.0050	0.32	0.104	0.003	1707	21	1689	24	1709	43	1.1	0.8
19	140	56	0.41	153	2.456	0.085	0.1893	0.0055	0.67	0.093	0.002	1259	25	1116	30	1472	51	11.4	11.9
20	316	34	0.11	324	3.204	0.070	0.2549	0.0034	0.39	0.091	0.002	1458	17	1465	17	1441	36	-0.5	-1.4
21	333	95	0.29	355	0.104	0.005	0.0155	0.0003	0.05	0.048	0.003	99.7	4.8	98.8	1.9	140	100	0.9	0.2
22	474	153	0.31	510	3.820	0.100	0.2646	0.0059	0.75	0.104	0.002	1597	22	1512	30	1707	35	5.3	6.5
23	78	57	0.73	91	0.066	0.010	0.0062	0.0004	0.07	0.077	0.012	63.7	9.2	39.7	2.3	960	300	37.7	2.6
24	165	61	0.38	179	0.366	0.021	0.0137	0.0004	0.41	0.194	0.010	314	16	87.4	2.7	2746	89	72.2	14.2
25	238	55	0.20	251	3.208	0.076	0.2535	0.0039	0.51	0.092	0.002	1459	18	1456	20	1451	39	0.2	-0.3
26	97	43	0.45	107	2.042	0.057	0.1921	0.0033	0.28	0.078	0.002	1130	19	1132	18	1128	56	-0.2	-0.2
27	116	74	0.59	133	1.942	0.059	0.1853	0.0027	0.35	0.077	0.002	1092	20	1095	15	1111	53	-0.3	1.1
28	260	21	0.09	265	0.065	0.005	0.0091	0.0003	0.19	0.050	0.004	63.5	4.8	58.6	1.6	190	140	7.7	1.0
29	142	89	0.53	163	0.072	0.006	0.0110	0.0004	-0.12	0.047	0.005	71.0	5.8	70.5	2.4	90	160	0.7	0.1
30	91	49	0.55	102	1.950	0.055	0.1841	0.0030	0.37	0.077	0.002	1101	19	1089	16	1103	53	1.1	0.9
31	73	50	0.65	85	1.969	0.061	0.1816	0.0036	0.30	0.079	0.002	1107	20	1075	19	1188	58	2.9	5.9
32	143	47	0.28	154	2.794	0.080	0.2340	0.0038	0.32	0.087	0.002	1354	22	1355	20	1339	50	-0.1	-0.8
33	104	88	0.82	124	2.343	0.071	0.2088	0.0038	0.46	0.081	0.002	1225	22	1224	21	1208	56	0.1	-0.8
34	30	29	0.96	37	2.885	0.110	0.2402	0.0058	0.24	0.088	0.003	1379	29	1386	30	1399	72	-0.5	0.4

Table D-1: Zircon LA-ICP-MS U-Pb Isotopic Data and Ages: HP14-10b (IGSN: IEKHP10b0[a]): Calcrete of west-central Ellis County (461256, 4304829)[b]

					Corrected Isotopic Ratios							Ages (Ma)[j]							
Grain #[c]	U[d] [ppm]	Th[d] [ppm]	Th/U	eU[e] [ppm]	$^{207}Pb/^{235}U$[f]	±2s[g]	$^{206}Pb/^{238}U$[f]	±2s[g]	Rho[h]	$^{207}Pb/^{206}Pb$[i]	±2s[g]	$^{207}Pb/^{235}U$	±2s	$^{206}Pb/^{238}U$	±2s	$^{207}Pb/^{206}Pb$	±2s	Disc. %[k]	Wtd. Disc.[l]
35	73	80	1.09	92	0.069	0.008	0.0105	0.0004	-0.09	0.050	0.007	67.3	7.2	67.1	2.8	100	210	0.3	0.0
36	276	112	0.41	302	1.962	0.048	0.1880	0.0027	0.42	0.076	0.002	1101	16	1110	15	1100	42	-0.8	-0.7
37	265	115	0.41	292	4.650	0.170	0.3202	0.0100	0.84	0.105	0.003	1753	31	1793	49	1708	43	-2.3	-1.7
38	44	55	1.30	57	3.110	0.130	0.2555	0.0057	0.52	0.089	0.003	1439	32	1466	29	1397	71	-1.9	-2.4
39	89	49	0.56	100	1.992	0.069	0.1892	0.0035	0.45	0.077	0.002	1107	24	1116	19	1120	58	-0.8	0.2
40	370	74	0.20	387	0.187	0.008	0.0272	0.0005	0.38	0.050	0.002	173.8	6.4	172.8	3.4	180	74	0.6	0.2
41	38	20	0.56	43	4.180	0.140	0.2894	0.0065	0.45	0.106	0.003	1667	28	1637	33	1729	58	1.8	2.8
42	456	177	0.38	498	0.088	0.004	0.0118	0.0002	0.13	0.052	0.002	85.5	3.4	75.6	1.5	249	88	11.6	2.9
43	463	305	0.60	535	0.085	0.007	0.0129	0.0004	-0.03	0.049	0.004	83.6	6.0	82.4	2.3	120	140	1.4	0.2
44	393	217	0.52	444	0.310	0.033	0.0289	0.0006	0.46	0.081	0.008	268	24	184	4	1030	180	31.4	3.5
45	297	209	0.70	346	0.102	0.012	0.0061	0.0002	0.51	0.119	0.012	99	11	39.5	1.5	1860	200	60.1	5.4
46	116	141	1.18	149	0.077	0.008	0.0109	0.0005	0.10	0.052	0.006	75.1	7.6	69.7	2.8	210	200	7.2	0.7
47	50	26	0.53	56	3.970	0.130	0.2787	0.0065	0.44	0.104	0.003	1622	26	1583	33	1678	54	2.4	2.9
48	391	78	0.14	409	3.690	0.160	0.2804	0.0077	0.79	0.095	0.003	1560	35	1591	38	1528	51	-2.0	-1.7
49	115	33	0.29	123	1.986	0.073	0.1914	0.0039	0.44	0.075	0.002	1113	25	1128	21	1058	62	-1.3	-3.3
50	222	92	0.43	244	2.067	0.069	0.1931	0.0043	0.56	0.077	0.002	1135	23	1137	23	1109	56	-0.2	-1.2
51	191	49	0.26	202	4.570	0.140	0.3158	0.0062	0.58	0.105	0.003	1741	26	1768	30	1706	46	-1.6	-2.1
52	235	414	1.78	332	0.075	0.007	0.0109	0.0005	0.14	0.052	0.005	73.0	6.9	69.5	3.0	250	200	4.8	0.5
54	820	368	0.42	906	0.241	0.032	0.0170	0.0004	0.51	0.101	0.012	213	24	108.5	2.6	1460	190	49.1	4.4
55	123	84	0.68	142	0.073	0.006	0.0108	0.0004	0.14	0.050	0.005	72.0	6.1	69.5	2.8	180	170	3.5	0.4
56	169	67	0.40	185	3.981	0.110	0.2879	0.0044	0.43	0.100	0.002	1628	23	1630	22	1624	45	-0.1	-0.3
57	**131**	**72**	**0.55**	**148**	**0.015**	**0.004**	**0.0016**	**0.0002**	**0.19**	**0.067**	**0.022**	**14.7**	**4.2**	**10.1**	**1.0**	**550**	**540**	**31.3**	**1.1**
58	360	55	0.15	373	3.160	0.073	0.2520	0.0043	0.48	0.090	0.002	1447	18	1453	22	1441	41	-0.4	-0.5
59	120	41	0.32	130	1.999	0.052	0.1897	0.0035	0.24	0.077	0.002	1114	18	1121	19	1107	54	-0.6	-0.7
60	89	40	0.46	98	2.888	0.075	0.2399	0.0044	0.38	0.087	0.002	1380	19	1386	23	1357	50	-0.4	-1.3
61	1192	445	0.38	1297	0.595	0.026	0.0448	0.0017	0.72	0.095	0.003	472	16	283	10	1537	59	40.0	11.8
62	241	142	0.59	275	0.075	0.011	0.0039	0.0002	0.27	0.141	0.020	73	10	25.2	1.2	1930	300	65.5	4.8
63	116	79	0.69	134	3.297	0.087	0.2625	0.0041	0.40	0.090	0.002	1479	20	1504	21	1430	42	-1.7	-3.5
64	63	29	0.46	70	0.249	0.024	0.0037	0.0003	0.35	0.589	0.074	224	20	23.7	2.1	4270	220	89.4	10.0
65	**94**	**38**	**0.41**	**103**	**0.014**	**0.005**	**0.0016**	**0.0002**	**-0.04**	**0.087**	**0.044**	**13.3**	**5.1**	**10.1**	**1.1**	**-600**	**1000**	**24.1**	**0.6**
66	**591**	**76**	**0.13**	**609**	**0.008**	**0.002**	**0.0013**	**0.0001**	**0.27**	**0.050**	**0.012**	**8**	**2**	**8.06**	**0.61**	**130**	**400**	**-0.8**	**0.0**
67	380	378	1.15	469	0.100	0.005	0.0146	0.0003	0.09	0.050	0.003	96.4	4.7	93.5	1.9	210	110	3.0	0.6
68	235	107	0.48	260	0.106	0.008	0.0133	0.0003	0.37	0.057	0.004	103.1	7.4	85.0	2.2	530	140	17.6	2.4
69	211	201	0.70	258	0.081	0.006	0.0112	0.0004	0.08	0.052	0.005	78.4	5.9	71.8	2.3	280	160	8.4	1.1

Table D-1: Zircon LA-ICP-MS U-Pb Isotopic Data and Ages: HP14-10b (IGSN: IEKHP10b0[a]): Calcrete of west-central Ellis County (461256, 4304829)[b]

					Corrected Isotopic Ratios							Ages (Ma)[j]							
Grain #[c]	U[d] [ppm]	Th[d] [ppm]	Th/U	eU[e] [ppm]	$^{207}Pb/^{235}U$[f]	±2s[g]	$^{206}Pb/^{238}U$[f]	±2s[g]	Rho[h]	$^{207}Pb/^{206}Pb$[i]	±2s[g]	$^{207}Pb/^{235}U$	±2s	$^{206}Pb/^{238}U$	±2s	$^{207}Pb/^{206}Pb$	±2s	Disc. %[k]	Wtd. Disc.[l]
70	108	34	0.31	116	4.590	0.120	0.3294	0.0075	0.60	0.102	0.002	1747	23	1833	37	1665	43	-4.9	-4.5
71	611	241	0.34	668	0.044	0.003	0.0065	0.0002	0.11	0.048	0.003	44.0	2.8	41.88	0.99	120	120	4.8	0.8
72	68	30	0.44	75	0.731	0.038	0.0892	0.0024	0.24	0.061	0.003	557	22	551	14	610	100	1.1	0.3
73	124	58	0.47	137	1.847	0.064	0.1462	0.0044	0.17	0.092	0.003	1063	24	879	24	1483	61	17.3	25.2
74	224	85	0.38	244	1.960	0.043	0.1872	0.0025	0.45	0.076	0.001	1101	15	1106	13	1091	36	-0.5	-1.2
75	125	30	0.20	131	4.172	0.110	0.2986	0.0049	0.59	0.101	0.002	1667	22	1683	24	1647	41	-1.0	-1.5
76	792	459	0.54	900	0.031	0.002	0.0045	0.0001	0.14	0.050	0.004	31.4	2.2	29.21	0.63	190	130	7.0	1.0
77	142	75	0.53	160	0.032	0.008	0.0017	0.0002	0.15	0.142	0.033	31.7	7.3	11.0	1.0	1650	510	65.3	2.8
78	377	34	0.09	385	0.042	0.003	0.0061	0.0002	0.21	0.051	0.004	41.8	3.0	39.0	1.2	200	140	6.7	0.9
79	177	23	0.13	182	0.134	0.011	0.0102	0.0005	-0.11	0.096	0.009	127.2	9.5	65.6	2.9	1500	190	48.4	6.5
80	123	200	1.47	170	2.895	0.074	0.2391	0.0041	0.42	0.088	0.002	1380	20	1381	21	1375	44	-0.1	-0.3
81	**80**	**46**	**0.58**	**90**	**0.015**	**0.008**	**0.0014**	**0.0002**	**0.06**	**0.120**	**0.091**	**15.7**	**7.8**	**9.0**	**1.3**	**-600**	**1100**	**42.7**	**0.9**
82	89	33	0.39	97	1.986	0.069	0.1913	0.0041	0.38	0.076	0.002	1114	24	1128	22	1111	60	-1.3	-0.8
83	218	74	0.33	235	0.091	0.009	0.0022	0.0001	0.48	0.339	0.041	87.9	8.3	14.23	0.91	3340	220	83.8	8.9
84	85	28	0.29	91	0.092	0.011	0.0122	0.0005	0.20	0.053	0.007	90	10	77.9	3.2	310	220	13.4	1.2
85	542	61	0.11	556	3.590	0.140	0.2486	0.0091	0.95	0.104	0.002	1543	30	1428	46	1688	31	7.5	5.7
86	197	46	0.23	208	4.436	0.097	0.3081	0.0044	0.33	0.104	0.002	1720	19	1733	21	1688	37	-0.8	-2.1
87	815	328	0.37	892	4.450	0.140	0.3101	0.0085	0.89	0.104	0.002	1722	26	1738	41	1688	32	-0.9	-1.2
88	849	733	0.85	1021	0.198	0.007	0.0285	0.0009	0.48	0.050	0.002	184.1	6.2	181.4	5.8	191	80	1.5	0.4
89	157	107	0.69	182	2.006	0.050	0.1868	0.0031	0.44	0.077	0.002	1116	17	1104	17	1134	44	1.1	1.8
90	1286	820	0.48	1479	0.038	0.002	0.0056	0.0001	0.13	0.049	0.003	37.6	1.9	35.81	0.78	120	100	4.8	0.9
91	102	75	0.71	120	1.969	0.054	0.1886	0.0026	0.32	0.076	0.002	1105	18	1114	14	1088	50	-0.8	-1.9
92	354	203	0.57	402	0.189	0.007	0.0274	0.0006	0.29	0.049	0.002	176.1	5.9	174.2	3.6	172	70	1.1	0.3
93	703	645	0.89	855	0.042	0.003	0.0067	0.0002	0.09	0.046	0.003	42.0	2.7	42.8	1.2	40	130	-1.9	-0.3
94	80	42	0.52	90	3.268	0.091	0.2610	0.0052	0.53	0.091	0.002	1472	22	1494	27	1446	49	-1.5	-1.8
95	293	75	0.25	311	4.706	0.110	0.3261	0.0056	0.71	0.105	0.002	1768	20	1822	28	1712	32	-3.1	-3.9
96	200	73	0.36	217	4.493	0.110	0.3044	0.0057	0.73	0.106	0.002	1730	19	1712	28	1728	32	1.0	0.6
97	284	57	0.20	297	4.465	0.100	0.3078	0.0052	0.65	0.105	0.002	1722	19	1729	26	1709	34	-0.4	-0.8
98	83	41	0.49	92	2.794	0.075	0.2326	0.0041	0.52	0.086	0.002	1352	21	1349	22	1341	45	0.2	-0.4
99	159	107	0.63	184	0.120	0.009	0.0139	0.0004	0.03	0.065	0.005	114	8	89.1	2.6	670	170	21.8	3.1
100	115	89	0.77	135	1.977	0.056	0.1897	0.0032	0.10	0.075	0.002	1107	19	1123	17	1071	58	-1.4	-3.1
101	421	320	0.75	496	0.186	0.007	0.0265	0.0005	0.13	0.051	0.002	172.7	6.1	168.8	2.9	225	78	2.3	0.6
102	242	160	0.64	279	0.042	0.005	0.0074	0.0003	0.11	0.043	0.005	41.7	4.6	47.2	1.9	-50	200	-13.2	-1.2
103	460	155	0.33	496	0.034	0.003	0.0048	0.0002	0.17	0.052	0.005	34.2	2.8	30.6	1.2	290	180	10.5	1.3

Table D-1: Zircon LA-ICP-MS U-Pb Isotopic Data and Ages: HP14-10b (IGSN: IEKHP10b0[a]): Calcrete of west-central Ellis County (461256, 4304829)[b]

					Corrected Isotopic Ratios							Ages (Ma)[j]							
Grain #[c]	U[d] [ppm]	Th[d] [ppm]	Th/U	eU[e] [ppm]	$^{207}Pb/^{235}U$[f]	±2s[g]	$^{206}Pb/^{238}U$[f]	±2s[g]	Rho[h]	$^{207}Pb/^{206}Pb$[i]	±2s[g]	$^{207}Pb/^{235}U$	±2s	$^{206}Pb/^{238}U$	±2s	$^{207}Pb/^{206}Pb$	±2s	Disc. %[k]	Wtd. Disc.[l]
104	226	97	0.48	249	4.299	0.120	0.3027	0.0064	0.74	0.103	0.002	1689	22	1703	32	1674	38	-0.8	-0.9
105	1414	319	0.22	1489	0.197	0.006	0.0283	0.0005	0.63	0.050	0.001	182	5	179.7	3.2	195	52	1.3	0.5
106	235	181	0.76	278	0.063	0.005	0.0089	0.0003	0.15	0.051	0.004	62.5	4.9	56.9	1.6	290	170	9.0	1.1
107	463	221	0.48	515	4.344	0.099	0.3057	0.0048	0.60	0.104	0.002	1700	19	1718	24	1685	34	-1.1	-1.4
108	152	81	0.53	171	3.059	0.082	0.2465	0.0038	0.46	0.089	0.002	1419	21	1420	20	1409	45	-0.1	-0.6
109	58	18	0.29	62	1.560	0.084	0.1349	0.0052	0.60	0.085	0.004	951	34	819	29	1292	83	13.9	3.9
110	348	91	0.25	369	3.441	0.100	0.2376	0.0058	0.79	0.105	0.002	1514	25	1373	30	1719	39	9.3	11.5
111	848	504	0.61	966	0.033	0.002	0.0044	0.0001	0.13	0.054	0.004	32.5	2.4	28.18	0.74	390	150	13.3	1.8
112	332	96	0.28	355	0.047	0.004	0.0053	0.0002	0.12	0.062	0.005	46.1	3.7	33.7	1.2	630	170	26.9	3.4
113	80	33	0.41	88	3.139	0.086	0.2486	0.0044	0.51	0.092	0.002	1441	21	1430	23	1466	44	0.8	1.6
114	336	136	0.34	368	5.220	0.360	0.3520	0.0200	0.99	0.107	0.002	1818	39	1903	73	1742	33	-4.7	-2.2
115	145	124	0.81	174	0.068	0.008	0.0057	0.0003	0.14	0.090	0.010	66.6	7.2	36.3	1.8	1310	230	45.5	4.2
116	122	85	0.72	142	1.970	0.060	0.1859	0.0034	0.25	0.077	0.002	1102	21	1098	19	1114	56	0.4	0.8
117	102	45	0.40	113	4.353	0.120	0.3061	0.0054	0.60	0.103	0.002	1699	23	1720	27	1669	39	-1.2	-1.9
118	473	49	0.11	484	1.371	0.055	0.1102	0.0051	0.86	0.089	0.003	874	23	673	30	1385	57	23.0	8.7
119	165	161	0.88	203	0.097	0.008	0.0139	0.0005	-0.11	0.053	0.005	93.3	7.4	88.8	2.8	290	190	4.8	0.6
120	105	75	0.74	122	0.040	0.007	0.0054	0.0003	0.00	0.055	0.011	39.1	6.8	34.4	1.8	390	310	12.0	0.7
121	230	38	0.17	239	4.160	0.120	0.2963	0.0051	0.62	0.100	0.002	1667	24	1675	26	1633	44	-0.5	-1.6

[a]International Geo Sample Number (IGSN) registered in the SESAR database
[b]All locations reported as UTM coordinates using Zone 14 NAD 27
[c]Emboldened rows indicate the youngest measured concordant grains
[d]U and Th concentrations and Th/U ratios calculated relative to the GJ-1 zircon standard ID-TIMS values using 287 ± 76 ppm for U and 8.4 ± 2.6 ppm for Th (Jackson et al., 2004)
[e]Equivalent U defined by the equation: eU = U ppm + 0.235*Th ppm
[f]Corrected for U-Pb fractionation and background and normalized to the GJ-1 zircon standard ID-TIMS values: $^{207}Pb/^{235}U = 0.8093 \pm 0.0009$ and $^{206}Pb/^{238}U = 0.09761 \pm 0.00011$ (Jackson et al., 2004)
[g]Propagated uncertainty of internal uncertainties (2 SE) and within run reproducibility of GJ-1 (2 SE)
[h]Uncertainty correlation between $^{206}Pb/^{238}U$ and $^{207}Pb/^{235}U$ uncertainties
[i]Corrected for background and Pb isotopic fractionation using the GJ-1 zircon standard ID-TIMS value: $^{207}Pb/^{206}Pb = 0.06014 \pm 0.00001$ (Jackson et al., 2004)
[j]U-Pb ages calculated relative to the GJ-1 zircon standard
[k]Discordance defined as $[(^{207}Pb/^{235}U_{age} - {}^{206}Pb/^{238}U_{age})/(^{207}Pb/^{235}U_{age})]*100$
[l]Uncertainty weighted age difference defined as $(^{207}Pb/^{235}U_{age} - {}^{206}Pb/^{238}U_{age})/(^{207}Pb/^{235}U_{age\ uncertainty})$ for grains with $^{206}Pb/^{238}U$ ages <850 Ma and $(^{207}Pb/^{206}Pb_{age} - {}^{206}Pb/^{238}U_{age})/(^{206}Pb/^{238}U_{age\ uncertainty})$ for grains with $^{206}Pb/^{238}U$ ages ≥850 Ma

Table D-2: Zircon LA-ICP-MS U-Pb Isotopic Data and Ages: HP14-09b (IGSN: IEKHP09b0[a]): Calcrete of west-central Ellis County (461110, 4304567)[b]

					Corrected Isotopic Ratios							Ages (Ma)[j]							
Grain #[c]	U[d] [ppm]	Th[d] [ppm]	Th/U	eU[e] [ppm]	$^{207}Pb/^{235}U$[f]	±2s[g]	$^{206}Pb/^{238}U$[f]	±2s[g]	Rho[h]	$^{207}Pb/^{206}Pb$[i]	±2s[g]	$^{207}Pb/^{235}U$	±2s	$^{206}Pb/^{238}U$	±2s	$^{207}Pb/^{206}Pb$	±2s	Disc. %[k]	Wtd. Disc.[l]
1	98	73	0.75	115	1.934	0.037	0.1852	0.0022	0.40	0.076	0.001	1093	13	1095	12	1090	38	-0.2	-0.4
2	**121**	**73**	**0.60**	**138**	**0.012**	**0.004**	**0.0014**	**0.0001**	**0.10**	**0.056**	**0.022**	**11.9**	**4.1**	**9.05**	**0.56**	**350**	**560**	**23.9**	**0.7**
3	381	202	0.53	428	0.095	0.003	0.0143	0.0002	0.25	0.048	0.001	91.6	2.6	91.5	1.4	119	58	0.1	0.0
4	404	259	0.64	465	0.087	0.003	0.0131	0.0002	0.04	0.049	0.002	84.8	2.8	83.9	1.2	128	73	1.1	0.3
5	195	44	0.23	205	0.068	0.006	0.0103	0.0003	0.24	0.047	0.004	66.3	5.9	66.1	1.7	60	160	0.3	0.0
6	168	81	0.49	187	0.034	0.003	0.0049	0.0001	-0.03	0.050	0.004	33.6	2.6	31.48	0.89	180	160	6.3	0.8
7	90	52	0.58	102	0.410	0.021	0.0526	0.0016	0.34	0.056	0.003	350	15	331	10	450	110	5.5	1.3
8	313	29	0.09	320	0.068	0.003	0.0106	0.0002	-0.02	0.047	0.002	66.2	2.5	67.8	1.2	71	85	-2.4	-0.6
9	185	198	1.07	232	0.073	0.004	0.0105	0.0002	0.14	0.050	0.003	71.2	4.2	67.1	1.3	200	120	5.8	1.0
10	499	132	0.26	530	0.113	0.003	0.0165	0.0002	0.28	0.050	0.001	108.3	2.7	105.4	1.4	196	60	2.7	1.1
11	145	108	0.74	170	0.175	0.006	0.0243	0.0004	0.17	0.052	0.002	163	5	154.9	2.8	296	72	5.0	1.7
12	160	75	0.47	177	0.458	0.012	0.0616	0.0010	0.37	0.055	0.001	382.2	8.6	385.4	5.8	386	60	-0.8	-0.4
13	785	23	0.03	790	3.184	0.055	0.2537	0.0036	0.79	0.091	0.001	1453	13	1459	18	1458	26	-0.4	-0.1
14	57	30	0.52	64	1.919	0.046	0.1826	0.0027	0.41	0.077	0.002	1089	16	1081	15	1107	48	0.7	1.7
15	1080	1380	1.28	1404	0.038	0.001	0.0060	0.0001	0.28	0.046	0.002	37.4	1.3	38.27	0.72	12	66	-2.3	-0.7
16	284	214	0.75	334	0.250	0.008	0.0356	0.0007	0.50	0.051	0.001	226.3	6.2	225.7	4.2	254	60	0.3	0.1
17	170	238	1.40	226	0.042	0.003	0.0062	0.0002	0.21	0.048	0.004	41.1	3.3	40.0	1.2	110	150	2.7	0.3
18	48	27	0.55	55	0.067	0.009	0.0105	0.0003	-0.01	0.047	0.006	65.2	8.2	67.1	2.0	70	230	-2.9	-0.2
19	792	554	0.70	922	0.029	0.001	0.0044	0.0001	0.08	0.049	0.002	29.4	1.1	28.08	0.47	158	80	4.5	1.2
20	123	79	0.64	141	3.150	0.054	0.2523	0.0041	0.67	0.091	0.002	1446	14	1449	21	1447	31	-0.2	-0.1
21	221	151	0.68	256	0.013	0.002	0.0016	0.0001	0.00	0.062	0.011	12.7	1.8	10.04	0.46	460	250	20.9	1.5
22	196	98	0.50	219	0.037	0.003	0.0056	0.0002	0.22	0.050	0.004	37.0	2.7	36.2	1.2	180	150	2.2	0.3
23	507	308	0.61	579	0.183	0.004	0.0275	0.0004	0.43	0.049	0.001	170.1	3.3	174.6	2.5	149	45	-2.6	-1.4
24	201	34	0.17	209	0.037	0.003	0.0057	0.0001	0.04	0.046	0.003	36.3	2.4	36.78	0.87	20	130	-1.3	-0.2
25	**279**	**71**	**0.25**	**296**	**0.009**	**0.001**	**0.0014**	**0.0001**	**0.31**	**0.047**	**0.007**	**9.0**	**1.3**	**8.87**	**0.37**	**10**	**260**	**1.4**	**0.1**
26	278	27	0.10	284	0.082	0.003	0.0122	0.0002	0.16	0.048	0.002	80	3	78.4	1.5	136	77	2.0	0.5
27	50	36	0.72	59	0.075	0.013	0.0112	0.0004	0.04	0.049	0.009	73	12	71.8	2.5	190	310	1.6	0.1
28	115	59	0.51	129	0.070	0.005	0.0103	0.0003	0.01	0.049	0.004	68.1	4.8	66.2	1.8	150	150	2.8	0.4
29	114	47	0.41	125	0.070	0.006	0.0104	0.0003	0.00	0.049	0.005	68.1	6.0	66.4	1.9	130	170	2.5	0.3
30	700	406	0.58	795	0.033	0.001	0.0049	0.0001	0.19	0.047	0.002	32.6	1.3	31.58	0.63	69	80	3.1	0.8
31	102	63	0.62	116	0.073	0.009	0.0054	0.0003	0.16	0.102	0.012	70.7	8.2	34.8	1.7	1560	230	50.8	4.4
32	115	24	0.21	120	0.077	0.004	0.0119	0.0003	0.12	0.047	0.003	75.0	3.7	76.2	1.8	60	100	-1.6	-0.3
33	387	68	0.18	403	4.500	0.078	0.3166	0.0051	0.79	0.103	0.002	1729	14	1772	25	1676	26	-2.5	-3.8
34	285	254	0.89	345	0.037	0.002	0.0061	0.0001	0.01	0.044	0.003	37.1	2.2	39.12	0.79	-30	110	-5.4	-0.9

Table D-2: Zircon LA-ICP-MS U-Pb Isotopic Data and Ages: HP14-09b (IGSN: IEKHP09b0[a]): Calcrete of west-central Ellis County (461110, 4304567)[b]

Grain #[c]	U[d] [ppm]	Th[d] [ppm]	Th/U	eU[e] [ppm]	Corrected Isotopic Ratios $^{207}Pb/^{235}U$[f]	±2s[g]	$^{206}Pb/^{238}U$[f]	±2s[g]	Rho[h]	$^{207}Pb/^{206}Pb$[i]	±2s[g]	Ages (Ma)[j] $^{207}Pb/^{235}U$	±2s	$^{206}Pb/^{238}U$	±2s	$^{207}Pb/^{206}Pb$	±2s	Disc. %[k]	Wtd. Disc.[l]
35	299	63	0.21	314	0.078	0.004	0.0116	0.0004	0.42	0.049	0.002	76.3	3.7	74.3	2.4	132	94	2.6	0.5
36	140	39	0.28	149	4.756	0.087	0.3364	0.0053	0.73	0.104	0.002	1778	15	1868	26	1696	29	-5.1	-6.6
37	94	54	0.57	107	0.013	0.004	0.0015	0.0001	0.05	0.061	0.020	12.7	3.5	9.55	0.67	220	490	24.8	0.9
38	129	125	0.97	159	0.079	0.004	0.0106	0.0003	0.15	0.055	0.003	77.2	4.1	68.2	1.7	400	120	11.7	2.2
39	78	56	0.71	91	3.168	0.060	0.2500	0.0043	0.55	0.092	0.002	1452	15	1440	22	1468	34	0.8	1.3
40	178	80	0.45	196	2.084	0.048	0.1918	0.0039	0.60	0.080	0.002	1144	16	1132	22	1192	42	1.0	2.7
41	230	37	0.16	239	0.101	0.004	0.0157	0.0003	0.42	0.047	0.002	97.6	3.6	100.1	1.8	77	72	-2.6	-0.7
42	235	36	0.15	243	0.070	0.003	0.0102	0.0003	0.28	0.051	0.002	69.5	3.1	65.3	1.7	227	96	6.0	1.4
43	172	92	0.54	193	0.066	0.004	0.0106	0.0004	0.32	0.046	0.003	65.0	3.8	67.8	2.3	10	110	-4.3	-0.7
44	312	240	0.77	368	0.038	0.003	0.0060	0.0002	0.09	0.046	0.004	38.0	2.7	38.66	0.97	20	130	-1.7	-0.2
45	135	64	0.48	150	0.012	0.003	0.0016	0.0001	0.08	0.053	0.014	11.5	2.6	10.12	0.55	150	360	12.0	0.5
46	233	140	0.60	266	0.009	0.002	0.0015	0.0001	0.12	0.049	0.010	8.6	1.8	9.37	0.42	10	320	-9.0	-0.4
47	68	33	0.48	76	3.100	0.083	0.2488	0.0058	0.76	0.093	0.002	1431	21	1435	29	1472	38	-0.3	1.3
48	85	66	0.78	101	4.564	0.100	0.3210	0.0061	0.78	0.104	0.002	1739	18	1793	30	1699	29	-3.1	-3.1
49	129	127	0.98	159	3.162	0.064	0.2589	0.0042	0.67	0.089	0.002	1448	16	1484	22	1399	32	-2.5	-3.9
50	279	115	0.41	306	3.256	0.046	0.2592	0.0030	0.77	0.091	0.001	1472	11	1486	15	1458	25	-1.0	-1.9
51	120	94	0.78	143	3.127	0.052	0.2481	0.0030	0.53	0.091	0.002	1438	13	1429	15	1438	32	0.6	0.6
52	121	66	0.54	137	0.010	0.004	0.0016	0.0001	0.04	0.043	0.016	9.8	3.6	10.43	0.65	-110	510	-6.4	-0.2
53	234	52	0.22	246	3.092	0.054	0.2471	0.0031	0.67	0.092	0.001	1429	13	1423	16	1461	28	0.4	2.4
54	**117**	**77**	**0.66**	**135**	**0.007**	**0.003**	**0.0014**	**0.0001**	**-0.01**	**0.042**	**0.015**	**6.7**	**2.5**	**9.08**	**0.60**	**-150**	**460**	**-35.5**	**-1.0**
55	290	378	1.30	379	4.244	0.060	0.2960	0.0033	0.63	0.104	0.002	1684	12	1673	17	1694	26	0.6	1.2
56	205	98	0.48	228	0.067	0.004	0.0107	0.0002	0.26	0.046	0.003	65.3	3.6	68.6	1.3	30	100	-5.1	-0.9
57	**604**	**273**	**0.45**	**668**	**0.009**	**0.001**	**0.0013**	**0.0000**	**-0.07**	**0.051**	**0.005**	**9.13**	**0.85**	**8.49**	**0.23**	**220**	**170**	**7.0**	**0.8**
58	401	251	0.63	460	0.096	0.003	0.0134	0.0003	0.30	0.052	0.002	92.5	2.9	85.7	2.0	284	70	7.4	2.3
59	272	253	0.93	332	0.048	0.003	0.0073	0.0002	0.23	0.047	0.003	47.4	3.0	46.9	1.2	80	110	1.1	0.2
60	338	55	0.16	351	0.843	0.016	0.1022	0.0015	0.75	0.060	0.001	620	9	627.9	8.7	616	34	-1.2	-0.8
61	289	29	0.10	296	0.066	0.003	0.0105	0.0002	-0.19	0.046	0.002	65.1	2.4	67.2	1.2	33	82	-3.2	-0.9
62	103	43	0.42	113	1.190	0.210	0.0880	0.0150	0.99	0.092	0.006	660	100	527	88	1430	130	20.2	1.3
63	20	29	1.49	26	0.071	0.016	0.0115	0.0006	0.07	0.047	0.011	67	15	73.6	3.7	50	330	-9.9	-0.4
64	125	83	0.67	144	0.041	0.004	0.0063	0.0002	-0.01	0.049	0.005	40.4	3.6	40.3	1.3	110	170	0.2	0.0
65	86	59	0.69	100	1.943	0.037	0.1868	0.0024	0.36	0.076	0.002	1097	13	1104	13	1098	40	-0.6	-0.5
66	75	50	0.66	87	3.220	0.068	0.2571	0.0044	0.63	0.091	0.002	1466	17	1474	22	1452	33	-0.5	-1.0
67	138	131	0.95	168	0.192	0.007	0.0291	0.0006	0.16	0.049	0.002	179.5	6.0	184.8	3.5	161	83	-3.0	-0.9
68	214	57	0.26	227	3.829	0.087	0.2648	0.0063	0.85	0.104	0.002	1598	18	1512	32	1701	30	5.4	5.9

Table D-2: Zircon LA-ICP-MS U-Pb Isotopic Data and Ages: HP14-09b (IGSN: IEKHP09b0[a]): Calcrete of west-central Ellis County (461110, 4304567)[b]

Grain #[c]	U[d] [ppm]	Th[d] [ppm]	Th/U	eU[e] [ppm]	Corrected Isotopic Ratios $^{207}Pb/^{235}U$[f]	±2s[g]	$^{206}Pb/^{238}U$[f]	±2s[g]	Rho[h]	$^{207}Pb/^{206}Pb$[i]	±2s[g]	Ages (Ma)[j] $^{207}Pb/^{235}U$	±2s	$^{206}Pb/^{238}U$	±2s	$^{207}Pb/^{206}Pb$	±2s	Disc. %[k]	Wtd. Disc.[l]
69	294	293	1.00	363	0.022	0.002	0.0035	0.0001	0.18	0.047	0.004	22.2	1.9	22.38	0.55	50	160	-0.8	-0.1
70	1006	940	0.93	1227	0.040	0.001	0.0063	0.0001	0.20	0.046	0.002	39.7	1.4	40.65	0.67	23	67	-2.4	-0.7
71	94	61	0.65	108	0.080	0.006	0.0118	0.0003	0.07	0.048	0.004	78.8	5.8	75.8	1.9	150	150	3.8	0.5
72	364	260	0.71	425	4.343	0.071	0.3040	0.0038	0.68	0.105	0.002	1703	13	1711	19	1704	27	-0.5	-0.4
73	189	150	0.80	224	3.210	0.080	0.2568	0.0057	0.79	0.091	0.002	1460	19	1473	29	1437	34	-0.9	-1.2
74	382	102	0.27	406	4.239	0.074	0.2980	0.0040	0.64	0.104	0.002	1683	14	1681	20	1692	29	0.1	0.6
75	35	53	1.51	47	0.100	0.016	0.0107	0.0005	0.08	0.069	0.012	94	15	68.5	3.1	680	300	27.1	1.7
76	62	39	0.64	71	0.071	0.008	0.0099	0.0004	0.15	0.053	0.006	69.3	7.5	63.8	2.8	220	200	7.9	0.7
77	386	166	0.43	425	0.102	0.004	0.0160	0.0003	0.32	0.047	0.002	98.8	3.3	102.1	1.9	78	74	-3.3	-1.0
78	70	57	0.81	83	0.038	0.006	0.0054	0.0002	0.18	0.051	0.008	37.8	5.8	34.5	1.3	160	270	8.7	0.6
79	107	118	1.10	135	0.035	0.004	0.0061	0.0002	0.14	0.044	0.005	34.3	3.8	39.2	1.3	-60	180	-14.3	-1.3
80	360	212	0.59	410	0.118	0.005	0.0162	0.0004	0.25	0.054	0.002	112.7	4.2	103.8	2.5	337	85	7.9	2.1
81	115	59	0.51	129	1.938	0.037	0.1827	0.0025	0.56	0.077	0.001	1095	12	1081	13	1115	36	1.3	2.6
82	126	64	0.51	141	0.089	0.008	0.0131	0.0004	-0.18	0.049	0.005	87.4	6.8	84.1	2.5	230	160	3.8	0.5
83	137	75	0.55	154	4.390	0.130	0.3013	0.0074	0.65	0.106	0.003	1704	25	1704	37	1724	47	0.0	0.5
84	89	25	0.28	94	6.570	0.140	0.2892	0.0049	0.67	0.157	0.003	2053	19	1637	25	2425	31	20.3	31.5
85	372	158	0.43	409	4.496	0.089	0.3121	0.0058	0.71	0.106	0.002	1729	17	1750	28	1718	33	-1.2	-1.1
86	155	140	0.90	188	0.033	0.004	0.0047	0.0002	0.14	0.051	0.006	32.8	3.7	30.1	1.1	190	200	8.2	0.7
87	496	122	0.25	525	0.036	0.002	0.0056	0.0001	0.29	0.047	0.002	36.0	1.6	36.35	0.88	66	82	-1.0	-0.2
88	112	53	0.48	124	0.019	0.003	0.0014	0.0001	-0.14	0.097	0.019	19.1	3.0	8.97	0.56	1350	370	53.0	3.4
89	149	78	0.52	168	0.012	0.002	0.0017	0.0001	0.05	0.048	0.009	11.7	2.2	11.22	0.57	180	300	4.1	0.2
90	485	94	0.19	507	0.089	0.003	0.0135	0.0002	0.29	0.047	0.002	86.8	2.4	86.3	1.5	80	64	0.6	0.2

[a]International Geo Sample Number (IGSN) registered in the SESAR database
[b]All locations reported as UTM coordinates using Zone 14 NAD 27
[c]Emboldened rows indicate the youngest measured concordant grains
[d]U and Th concentrations and Th/U ratios calculated relative to the GJ-1 zircon standard ID-TIMS values using 287 ± 76 ppm for U and 8.4 ± 2.6 ppm for Th (Jackson et al., 2004)
[e]Equivalent U defined by the equation: eU = U ppm + 0.235*Th ppm
[f]Corrected for U-Pb fractionation and background and normalized to the GJ-1 zircon standard ID-TIMS values: $^{207}Pb/^{235}U = 0.8093 \pm 0.0009$ and $^{206}Pb/^{238}U = 0.09761 \pm 0.00011$ (Jackson et al., 2004)
[g]Propagated uncertainty of internal uncertainties (2 SE) and within run reproducibility of GJ-1 (2 SE)
[h]Uncertainty correlation between $^{206}Pb/^{238}U$ and $^{207}Pb/^{235}U$ uncertainties
[i]Corrected for background and Pb isotopic fractionation using the GJ-1 zircon standard ID-TIMS value: $^{207}Pb/^{206}Pb = 0.06014 \pm 0.00001$ (Jackson et al., 2004)
[j]U-Pb ages calculated relative to the GJ-1 zircon standard
[k]Discordance defined as $[(^{207}Pb/^{235}U_{age} - ^{206}Pb/^{238}U_{age})/(^{207}Pb/^{235}U_{age})]*100$
[l]Uncertainty weighted age difference defined as $(^{207}Pb/^{235}U_{age} - ^{206}Pb/^{238}U_{age})/(^{207}Pb/^{235}U_{age\ uncertainty})$ for grains with $^{206}Pb/^{238}U$ ages <850 Ma and $(^{207}Pb/^{206}Pb_{age} - ^{206}Pb/^{238}U_{age})/(^{206}Pb/^{238}U_{age\ uncertainty})$ for grains with $^{206}Pb/^{238}U$ ages ≥850 Ma

Table D-3: Zircon LA-ICP-MS U-Pb Isotopic Data and Ages: HP14-02 (IGSN: IEKHP0200[a]): Calcrete of northwestern Ellis County (453422, 4321341)[b]

					Corrected Isotopic Ratios							Ages (Ma)[j]							
Grain #[c]	U[d] [ppm]	Th[d] [ppm]	Th/U	eU[e] [ppm]	$^{207}Pb/^{235}U$[f]	±2s[g]	$^{206}Pb/^{238}U$[f]	±2s[g]	Rho[h]	$^{207}Pb/^{206}Pb$[i]	±2s[g]	$^{207}Pb/^{235}U$	±2s	$^{206}Pb/^{238}U$	±2s	$^{207}Pb/^{206}Pb$	±2s	Disc. %[k]	Wtd. Disc.[l]
1	459	67	0.14	475	0.079	0.005	0.0123	0.0003	-0.15	0.047	0.004	77.7	5.3	78.7	1.8	80	150	-1.3	-0.2
2	433	67	0.15	449	3.060	0.110	0.2205	0.0073	0.88	0.100	0.002	1418	28	1283	39	1617	36	9.5	8.6
3	46	47	1.04	57	1.951	0.075	0.1887	0.0032	0.09	0.076	0.003	1103	26	1116	17	1059	81	-1.2	-3.4
4	277	119	0.42	305	0.032	0.004	0.0045	0.0002	0.07	0.051	0.006	32.2	3.6	29.1	1.2	200	200	9.6	0.9
5	144	77	0.52	162	2.885	0.073	0.2409	0.0035	0.40	0.087	0.002	1375	19	1391	18	1370	44	-1.2	-1.2
6	413	304	0.73	484	0.016	0.002	0.0027	0.0001	-0.05	0.049	0.008	16.4	2.3	17.11	0.75	40	230	-4.3	-0.3
7	257	68	0.27	273	4.450	0.110	0.3108	0.0043	0.58	0.104	0.002	1720	20	1746	21	1701	35	-1.5	-2.1
8	**177**	**82**	**0.46**	**196**	**0.011**	**0.003**	**0.0014**	**0.0001**	**0.00**	**0.061**	**0.019**	**11.2**	**3.2**	**9.11**	**0.72**	**290**	**460**	**18.7**	**0.7**
9	118	79	0.65	137	1.965	0.056	0.1897	0.0035	0.47	0.075	0.002	1106	19	1121	19	1086	48	-1.4	-1.8
10	**80**	**32**	**0.40**	**87**	**0.008**	**0.005**	**0.0016**	**0.0002**	**0.02**	**0.044**	**0.027**	**7.6**	**5.4**	**10.5**	**1.2**	**-740**	**740**	**-38.2**	**-0.5**
11	139	64	0.40	154	4.479	0.110	0.3128	0.0053	0.54	0.105	0.002	1728	21	1754	26	1707	39	-1.5	-1.8
12	187	59	0.32	200	4.130	0.160	0.2877	0.0094	0.64	0.104	0.003	1671	32	1637	49	1691	58	2.0	1.1
13	133	223	1.75	185	0.017	0.005	0.0023	0.0002	0.17	0.060	0.016	17.2	4.5	14.5	1.2	310	430	15.7	0.6
14	266	192	0.73	311	0.039	0.005	0.0055	0.0002	0.13	0.052	0.006	38.9	4.6	35.1	1.1	230	220	9.8	0.8
15	166	74	0.45	183	0.011	0.003	0.0017	0.0001	-0.11	0.050	0.015	11.3	3.4	10.99	0.77	-60	460	2.7	0.1
16	136	51	0.38	148	1.997	0.059	0.1873	0.0035	0.35	0.078	0.002	1113	20	1108	19	1136	54	0.4	1.5
17	189	81	0.43	208	0.016	0.004	0.0017	0.0001	-0.15	0.065	0.019	15.4	3.3	11.2	0.8	280	460	27.3	1.3
18	46	25	0.54	52	0.055	0.014	0.0020	0.0004	0.12	0.272	0.099	53	14	12.6	2.2	1300	1200	76.2	2.9
19	356	115	0.33	383	0.029	0.003	0.0044	0.0001	0.27	0.047	0.005	28.4	2.8	28.02	0.85	130	180	1.3	0.1
20	106	78	0.73	124	1.614	0.062	0.1604	0.0035	0.43	0.072	0.002	970	24	959	20	977	73	1.1	0.9
21	473	237	0.51	529	0.037	0.003	0.0059	0.0002	0.03	0.045	0.004	36.5	3.0	38.1	1.1	0	150	-4.4	-0.5
22	359	239	0.65	415	0.033	0.004	0.0048	0.0002	-0.14	0.049	0.006	32.7	3.4	31.12	0.98	160	200	4.8	0.5
23	191	51	0.27	203	0.101	0.007	0.0157	0.0004	0.08	0.046	0.003	98.2	5.9	100.4	2.4	0	120	-2.2	-0.4
24	102	56	0.53	115	2.039	0.070	0.1967	0.0047	0.43	0.076	0.002	1129	24	1157	25	1089	58	-2.5	-2.7
25	**347**	**242**	**0.55**	**404**	**0.011**	**0.003**	**0.0015**	**0.0001**	**0.08**	**0.058**	**0.021**	**11.1**	**3.4**	**9.56**	**0.76**	**50**	**530**	**13.9**	**0.5**
26	431	126	0.30	461	0.029	0.003	0.0045	0.0002	0.09	0.050	0.005	28.9	2.5	29	1	180	170	-0.3	0.0
27	**207**	**70**	**0.34**	**223**	**0.008**	**0.003**	**0.0015**	**0.0001**	**0.02**	**0.037**	**0.014**	**8.4**	**2.9**	**9.82**	**0.68**	**-350**	**450**	**-16.9**	**-0.5**
28	249	168	0.66	288	0.039	0.004	0.0054	0.0002	-0.05	0.054	0.005	38.8	3.4	34.8	1.4	280	180	10.3	1.2
29	183	113	0.62	210	0.061	0.006	0.0093	0.0003	0.20	0.052	0.005	60.1	5.5	59.6	1.9	260	170	0.8	0.1
30	79	39	0.49	88	0.065	0.011	0.0101	0.0006	-0.14	0.056	0.011	63	10	64.6	3.6	170	290	-2.5	-0.2

Table D-3: Zircon LA-ICP-MS U-Pb Isotopic Data and Ages: HP14-02 (IGSN: IEKHP0200[a]): Calcrete of northwestern Ellis County (453422, 4321341)[b]

Grain #[c]	U[d] [ppm]	Th[d] [ppm]	Th/U	eU[e] [ppm]	Corrected Isotopic Ratios							Ages (Ma)[j]						Disc. %[k]	Wtd. Disc.[l]
					^{207}Pb/^{235}U[f]	±2s[g]	^{206}Pb/^{238}U[f]	±2s[g]	Rho[h]	^{207}Pb/^{206}Pb[i]	±2s[g]	^{207}Pb/^{235}U	±2s	^{206}Pb/^{238}U	±2s	^{207}Pb/^{206}Pb	±2s		
31	438	38	0.09	447	3.042	0.097	0.2445	0.0058	0.76	0.091	0.002	1421	24	1409	30	1436	43	0.8	0.9
32	216	82	0.41	235	1.931	0.061	0.1839	0.0034	0.49	0.075	0.002	1088	21	1088	18	1085	51	0.0	-0.2
33	271	66	0.25	287	4.466	0.100	0.3068	0.0049	0.62	0.106	0.002	1723	19	1724	24	1728	34	-0.1	0.2
34	90	46	0.50	100	1.987	0.067	0.1911	0.0039	0.36	0.076	0.002	1109	23	1127	21	1089	63	-1.6	-1.8
35	**106**	**47**	**0.44**	**117**	**0.012**	**0.005**	**0.0015**	**0.0002**	**0.17**	**0.058**	**0.028**	**11.9**	**4.9**	**9.4**	**0.9**	**-110**	**650**	**21.0**	**0.5**
36	253	209	0.86	302	0.035	0.003	0.0042	0.0002	0.19	0.058	0.006	34.4	3.4	27.1	1.4	610	210	21.2	2.1
37	58	47	0.80	69	1.974	0.084	0.1851	0.0043	0.22	0.077	0.003	1106	28	1097	23	1120	84	0.8	1.0
38	297	47	0.17	308	3.176	0.089	0.2510	0.0037	0.49	0.091	0.002	1450	21	1445	19	1445	45	0.3	0.0
39	157	89	0.58	178	1.925	0.067	0.1809	0.0042	0.49	0.077	0.002	1087	24	1074	22	1120	59	1.2	2.1
40	519	98	0.19	542	0.047	0.003	0.0071	0.0002	0.09	0.048	0.003	46.8	2.9	45.4	1.2	110	120	3.0	0.5
41	86	71	0.83	103	1.897	0.068	0.1820	0.0035	0.31	0.076	0.003	1082	24	1077	19	1099	67	0.5	1.2
42	57	39	0.68	66	1.927	0.063	0.1868	0.0041	0.32	0.074	0.003	1086	22	1104	22	1041	73	-1.7	-2.9
43	425	167	0.41	464	0.594	0.019	0.0754	0.0014	0.52	0.057	0.002	472	12	468.5	8.1	466	57	0.7	0.3
44	492	367	0.76	578	3.117	0.100	0.2485	0.0049	0.62	0.090	0.002	1433	26	1432	25	1421	47	0.1	-0.4
45	276	89	0.32	297	1.947	0.053	0.1872	0.0034	0.48	0.075	0.002	1095	18	1106	18	1071	47	-1.0	-1.9
46	356	151	0.42	391	0.012	0.002	0.0017	0.0001	0.03	0.055	0.011	12.1	2.4	10.94	0.5	80	320	9.6	0.5
47	342	102	0.26	366	0.074	0.005	0.0108	0.0003	0.22	0.050	0.004	73.2	5.0	69	2	220	140	5.7	0.8
48	136	73	0.53	153	2.043	0.064	0.1926	0.0037	0.42	0.077	0.002	1130	21	1135	20	1110	53	-0.4	-1.3
49	738	180	0.24	780	0.036	0.003	0.0046	0.0001	0.28	0.056	0.004	36.0	2.9	29.5	0.8	410	150	18.1	2.2
50	113	105	0.93	137	0.074	0.008	0.0106	0.0004	0.01	0.052	0.006	72.2	7.5	67.7	2.3	230	200	6.2	0.6
51	**244**	**145**	**0.58**	**278**	**0.011**	**0.002**	**0.0015**	**0.0001**	**-0.12**	**0.058**	**0.014**	**10.5**	**2.4**	**9.47**	**0.72**	**230**	**390**	**9.8**	**0.4**
52	369	109	0.23	395	3.199	0.097	0.2510	0.0068	0.83	0.092	0.002	1457	23	1446	36	1464	35	0.8	0.5
53	475	144	0.31	509	0.103	0.006	0.0150	0.0004	0.22	0.050	0.003	100.2	5.3	96.2	2.8	210	110	4.0	0.8
54	389	212	0.55	439	3.121	0.099	0.2481	0.0057	0.54	0.090	0.002	1438	24	1430	30	1427	49	0.6	-0.1
55	41	27	0.64	47	1.946	0.076	0.1857	0.0042	0.24	0.076	0.003	1096	26	1099	23	1058	77	-0.3	-1.8
56	69	29	0.43	75	1.896	0.067	0.1804	0.0034	0.31	0.076	0.003	1075	24	1069	19	1085	67	0.6	0.8
57	217	69	0.30	233	4.441	0.100	0.3098	0.0052	0.63	0.104	0.002	1722	20	1739	26	1703	34	-1.0	-1.4
58	204	99	0.48	228	0.062	0.006	0.0050	0.0002	0.03	0.088	0.009	60.4	5.3	32.1	1.3	1250	200	46.9	5.3
59	148	60	0.39	162	3.564	0.084	0.2700	0.0046	0.52	0.095	0.002	1539	19	1540	24	1532	39	-0.1	-0.3
60	99	46	0.47	110	3.293	0.100	0.2658	0.0076	0.71	0.091	0.003	1480	23	1518	38	1433	55	-2.6	-2.2

Table D-3: Zircon LA-ICP-MS U-Pb Isotopic Data and Ages: HP14-02 (IGSN: IEKHP0200[a]): Calcrete of northwestern Ellis County (453422, 4321341)[b]

					Corrected Isotopic Ratios							Ages (Ma)[j]							
Grain #[c]	U[d] [ppm]	Th[d] [ppm]	Th/U	eU[e] [ppm]	$^{207}Pb/^{235}U$[f]	±2s[g]	$^{206}Pb/^{238}U$[f]	±2s[g]	Rho[h]	$^{207}Pb/^{206}Pb$[i]	±2s[g]	$^{207}Pb/^{235}U$	±2s	$^{206}Pb/^{238}U$	±2s	$^{207}Pb/^{206}Pb$	±2s	Disc. %[k]	Wtd. Disc.[l]
61	434	102	0.23	458	0.066	0.004	0.0097	0.0003	0.23	0.050	0.003	65.6	3.9	61.9	1.6	190	110	5.6	0.9
62	36	40	1.13	45	0.085	0.020	0.0110	0.0009	0.06	0.058	0.015	82	19	70.7	5.4	110	440	13.8	0.6
63	69	30	0.43	76	1.974	0.057	0.1863	0.0035	0.43	0.077	0.002	1106	20	1101	19	1124	52	0.5	1.2
64	163	56	0.34	176	0.100	0.008	0.0135	0.0005	-0.16	0.056	0.005	97.3	8.0	86.6	2.9	420	190	11.0	1.3
65	111	52	0.41	124	0.012	0.005	0.0019	0.0002	0.03	0.079	0.040	11.6	4.9	12.2	1.2	-200	580	-5.2	-0.1
66	67	44	0.65	77	2.001	0.070	0.1833	0.0035	0.19	0.079	0.003	1111	24	1084	19	1130	69	2.4	2.4
67	275	264	0.98	337	4.216	0.088	0.2950	0.0043	0.52	0.103	0.002	1677	18	1668	22	1680	34	0.5	0.5
68	110	66	0.57	125	1.430	0.055	0.1043	0.0032	0.29	0.101	0.004	905	22	639	19	1623	76	29.4	12.1
69	168	61	0.38	182	0.039	0.005	0.0056	0.0003	0.21	0.049	0.006	38.3	5.2	36.0	1.6	230	230	6.0	0.4
70	443	87	0.19	464	4.660	0.180	0.3222	0.0100	0.72	0.106	0.003	1777	31	1797	49	1730	54	-1.1	-1.4
71	220	208	1.00	269	3.244	0.085	0.2653	0.0052	0.65	0.088	0.002	1465	20	1516	26	1398	42	-3.5	-4.5
72	169	37	0.22	178	4.691	0.110	0.3263	0.0058	0.60	0.105	0.002	1763	20	1819	28	1704	35	-3.2	-4.1
73	88	44	0.50	98	0.027	0.006	0.0020	0.0002	-0.02	0.149	0.039	26.8	6.0	12.7	1.3	1270	530	52.6	2.4
74	322	144	0.44	356	0.085	0.005	0.0127	0.0003	0.03	0.048	0.003	82.2	4.6	81.0	1.9	120	110	1.5	0.3
75	110	54	0.50	123	1.952	0.051	0.1872	0.0031	0.34	0.075	0.002	1099	18	1107	16	1080	50	-0.7	-1.7
76	133	115	0.86	160	0.089	0.008	0.0127	0.0005	0.00	0.052	0.005	86.0	7.7	82	3	250	190	4.7	0.5
77	194	69	0.38	210	3.309	0.079	0.2572	0.0041	0.56	0.092	0.002	1484	18	1475	21	1469	37	0.6	-0.3
78	619	43	0.07	629	3.751	0.098	0.2663	0.0048	0.66	0.102	0.002	1588	21	1521	24	1660	39	4.2	5.8
79	198	96	0.49	221	1.930	0.049	0.1834	0.0029	0.44	0.076	0.002	1091	17	1085	16	1082	48	0.5	-0.2
80	302	142	0.27	335	0.083	0.005	0.0123	0.0003	0.23	0.049	0.003	81.6	4.7	78.5	2.1	110	120	3.8	0.7
81	99	50	0.51	111	0.034	0.007	0.0041	0.0003	0.14	0.057	0.013	33.7	7.1	26.5	1.6	260	390	21.4	1.0
82	185	128	0.66	215	1.883	0.053	0.1798	0.0029	0.40	0.077	0.002	1076	18	1066	16	1114	50	0.9	3.0
83	159	107	0.68	184	3.006	0.081	0.2449	0.0044	0.68	0.088	0.002	1406	20	1412	23	1387	41	-0.4	-1.1
86	324	12	0.02	327	3.150	0.120	0.2497	0.0078	0.60	0.091	0.003	1443	30	1436	40	1440	58	0.5	0.1
87	262	53	0.16	274	0.090	0.007	0.0122	0.0004	0.15	0.052	0.004	87.4	6.1	78.0	2.6	310	150	10.8	1.5
88	154	101	0.65	178	3.311	0.090	0.2618	0.0048	0.63	0.092	0.002	1482	21	1498	24	1465	41	-1.1	-1.4
89	72	38	0.51	81	0.756	0.041	0.0889	0.0025	0.45	0.061	0.003	569	24	548	15	620	110	3.7	0.9
90	158	74	0.49	175	3.068	0.079	0.2503	0.0039	0.43	0.089	0.002	1428	20	1440	20	1411	46	-0.8	-1.5
91	56	42	0.75	66	0.078	0.013	0.0113	0.0006	0.07	0.055	0.011	74	13	73.1	3.7	140	300	1.2	0.1
92	381	305	0.78	453	1.485	0.063	0.1307	0.0041	0.69	0.082	0.002	921	26	791	23	1255	57	14.1	5.0

Table D-3: Zircon LA-ICP-MS U-Pb Isotopic Data and Ages: HP14-02 (IGSN: IEKHP0200[a]): Calcrete of northwestern Ellis County (453422, 4321341)[b]

					Corrected Isotopic Ratios							Ages (Ma)[j]							
Grain #[c]	U[d] [ppm]	Th[d] [ppm]	Th/U	eU[e] [ppm]	$^{207}Pb/^{235}U$[f]	±2s[g]	$^{206}Pb/^{238}U$[f]	±2s[g]	Rho[h]	$^{207}Pb/^{206}Pb$[i]	±2s[g]	$^{207}Pb/^{235}U$	±2s	$^{206}Pb/^{238}U$	±2s	$^{207}Pb/^{206}Pb$	±2s	Disc. %[k]	Wtd. Disc.[l]
93	517	177	0.34	559	0.101	0.004	0.0150	0.0003	0.05	0.048	0.002	97.7	3.9	96	2	146	91	1.5	0.4
94	313	109	0.35	338	0.101	0.005	0.0150	0.0005	0.44	0.049	0.003	97.0	4.7	96.0	3.1	170	100	1.0	0.2
95	286	35	0.12	294	7.880	0.300	0.3170	0.0100	0.82	0.179	0.004	2213	35	1771	51	2643	38	20.0	17.1
96	228	107	0.47	253	0.089	0.006	0.0138	0.0004	0.13	0.047	0.003	87.1	5.3	88.5	2.4	70	120	-1.6	-0.3
97	193	40	0.21	202	1.432	0.060	0.1497	0.0046	0.75	0.070	0.002	904	25	898	26	920	56	0.7	0.8
98	1150	367	0.31	1236	2.360	0.120	0.0781	0.0029	0.66	0.217	0.009	1225	37	485	18	2953	68	60.4	20.0
99	291	148	0.48	326	0.817	0.029	0.0970	0.0023	0.59	0.061	0.002	604	16	597	14	629	64	1.2	0.4
100	147	31	0.22	154	0.218	0.013	0.0309	0.0008	0.32	0.051	0.003	200	11	197	5	220	110	1.5	0.3
101	185	70	0.39	201	0.065	0.006	0.0098	0.0003	0.00	0.048	0.004	63.8	5.3	62.8	2.0	100	150	1.6	0.2
102	262	57	0.22	275	4.640	0.180	0.3211	0.0085	0.55	0.105	0.003	1752	32	1794	42	1704	58	-2.4	-2.1

[a]International Geo Sample Number (IGSN) registered in the SESAR database
[b]All locations reported as UTM coordinates using Zone 14 NAD 27
[c]Emboldened rows indicate the youngest measured concordant grains
[d]U and Th concentrations and Th/U ratios calculated relative to the GJ-1 zircon standard ID-TIMS values using 287 ± 76 ppm for U and 8.4 ± 2.6 ppm for Th (Jackson et al., 2004)
[e]Equivalent U defined by the equation: eU = U ppm + 0.235*Th ppm
[f]Corrected for U-Pb fractionation and background and normalized to the GJ-1 zircon standard ID-TIMS values: $^{207}Pb/^{235}U = 0.8093 \pm 0.0009$ and $^{206}Pb/^{238}U = 0.09761 \pm 0.00011$ (Jackson et al., 2004)
[g]Propagated uncertainty of internal uncertainties (2 SE) and within run reproducibility of GJ-1 (2 SE)
[h]Uncertainty correlation between $^{206}Pb/^{238}U$ and $^{207}Pb/^{235}U$ uncertainties
[i]Corrected for background and Pb isotopic fractionation using the GJ-1 zircon standard ID-TIMS value: $^{207}Pb/^{206}Pb = 0.06014 \pm 0.00001$ (Jackson et al., 2004)
[j]U-Pb ages calculated relative to the GJ-1 zircon standard
[k]Discordance defined as $[(^{207}Pb/^{235}U_{age} - ^{206}Pb/^{238}U_{age})/(^{207}Pb/^{235}U_{age})]*100$
[l]Uncertainty weighted age difference defined as $(^{207}Pb/^{235}U_{age} - ^{206}Pb/^{238}U_{age})/(^{207}Pb/^{235}U_{age\ uncertainty})$ for grains with $^{206}Pb/^{238}U$ ages <850 Ma and $(^{207}Pb/^{206}Pb_{age} - ^{206}Pb/^{238}U_{age})/(^{206}Pb/^{238}U_{age\ uncertainty})$ for grains with $^{206}Pb/^{238}U$ ages ≥850 Ma

Table D-4: Zircon LA-ICP-MS U-Pb Isotopic Data and Ages: HP14-03 (IGSN: IEKHP0300[a]): Calcrete of northwestern Ellis County (452005, 4321496)[b]

					Corrected Isotopic Ratios							Ages (Ma)[j]							
Grain #[c]	U[d] [ppm]	Th[d] [ppm]	Th/U	eU[e] [ppm]	$^{207}Pb/^{235}U$[f]	±2s[g]	$^{206}Pb/^{238}U$[f]	±2s[g]	Rho[h]	$^{207}Pb/^{206}Pb$[i]	±2s[g]	$^{207}Pb/^{235}U$	±2s	$^{206}Pb/^{238}U$	±2s	$^{207}Pb/^{206}Pb$	±2s	Disc. %[k]	Wtd. Disc.[l]
1	69	28	0.40	76	0.014	0.005	0.0017	0.0002	-0.12	0.073	0.056	13.4	5.4	10.8	1.5	-800	1200	19.4	0.5
2	126	65	0.52	141	1.856	0.056	0.1803	0.0044	0.59	0.074	0.002	1063	20	1068	24	1048	54	-0.5	-0.8
3	87	42	0.50	97	1.918	0.057	0.1819	0.0042	0.44	0.077	0.002	1092	20	1077	23	1104	58	1.4	1.2
4	**82**	**37**	**0.45**	**91**	**0.010**	**0.005**	**0.0015**	**0.0002**	**0.04**	**0.059**	**0.037**	**9.7**	**5.4**	**9.9**	**1.2**	**-470**	**950**	**-2.1**	**0.0**
5	42	19	0.46	46	2.268	0.082	0.2042	0.0053	0.36	0.080	0.003	1204	25	1200	28	1195	67	0.3	-0.2
6	**130**	**71**	**0.55**	**147**	**0.012**	**0.003**	**0.0015**	**0.0001**	**0.02**	**0.061**	**0.020**	**12.4**	**3.4**	**9.81**	**0.93**	**390**	**530**	**20.9**	**0.8**
7	147	71	0.48	164	1.893	0.054	0.1802	0.0041	0.46	0.075	0.002	1077	19	1067	22	1069	52	0.9	0.1
8	202	52	0.13	214	4.418	0.110	0.3037	0.0068	0.69	0.105	0.002	1718	20	1708	33	1708	38	0.6	0.0
9	223	209	0.94	272	0.034	0.003	0.0057	0.0002	0.18	0.043	0.005	34.2	3.4	36.7	1.4	-90	170	-7.3	-0.7
10	263	96	0.39	285	1.921	0.049	0.1833	0.0039	0.65	0.075	0.002	1087	17	1084	21	1081	44	0.3	-0.1
11	223	143	0.64	257	0.520	0.017	0.0674	0.0020	0.46	0.055	0.002	424	12	421	12	437	78	0.7	0.3
12	262	192	0.75	307	0.041	0.004	0.0061	0.0002	0.04	0.048	0.005	41.1	4.2	38.9	1.5	80	190	5.4	0.5
13	100	27	0.28	106	0.009	0.005	0.0017	0.0003	-0.14	0.045	0.033	8.8	5.2	11.2	1.6	-20	780	-27.3	-0.5
14	137	140	1.04	170	14.340	0.420	0.5450	0.0150	0.79	0.190	0.004	2771	29	2816	66	2745	36	-1.6	-1.1
15	204	170	0.82	243	0.073	0.007	0.0104	0.0004	0.03	0.050	0.005	71.5	6.8	67.1	2.7	150	180	6.2	0.6
16	81	37	0.45	90	1.878	0.062	0.1816	0.0047	0.40	0.075	0.002	1075	21	1075	26	1050	66	0.0	-1.0
17	161	85	0.52	181	2.854	0.070	0.2365	0.0041	0.56	0.087	0.002	1370	18	1368	22	1358	42	0.1	-0.5
18	278	61	0.22	292	0.300	0.011	0.0412	0.0010	0.34	0.051	0.002	265.7	8.7	260	6	247	76	2.2	0.7
19	248	110	0.45	274	1.806	0.053	0.1765	0.0039	0.72	0.074	0.002	1048	20	1048	22	1040	48	0.0	-0.4
20	111	75	0.66	128	2.752	0.079	0.2281	0.0046	0.52	0.087	0.002	1342	22	1330	22	1366	50	0.9	1.6
21	148	95	0.62	170	1.915	0.056	0.1795	0.0039	0.54	0.076	0.002	1084	19	1064	21	1088	53	1.8	1.1
22	280	53	0.16	292	4.560	0.130	0.3128	0.0085	0.76	0.105	0.002	1741	24	1752	42	1708	40	-0.6	-1.0
23	43	27	0.63	50	0.095	0.026	0.0109	0.0011	0.17	0.058	0.016	90	23	69.6	6.8	450	500	22.7	0.9
24	68	105	1.54	92	0.105	0.015	0.0132	0.0009	0.12	0.054	0.008	103	13	84.2	6.0	420	280	18.3	1.4
25	444	103	0.23	468	3.143	0.070	0.2509	0.0050	0.64	0.090	0.002	1444	17	1443	26	1428	38	0.1	-0.6
26	221	138	0.62	253	0.036	0.004	0.0052	0.0003	-0.07	0.051	0.006	35.7	3.9	33.5	1.6	170	210	6.2	0.6
27	308	352	1.14	391	0.038	0.003	0.0055	0.0002	0.28	0.049	0.004	37.9	2.9	35.3	1.3	140	150	6.9	0.9
28	139	151	1.09	174	0.164	0.010	0.0243	0.0008	0.03	0.049	0.003	154.5	8.4	155	5	180	130	-0.2	0.0
29	565	131	0.23	596	0.048	0.002	0.0077	0.0003	0.21	0.046	0.003	47.9	2.3	49.2	1.6	30	110	-2.7	-0.6
30	114	87	0.74	134	0.044	0.006	0.0061	0.0004	0.35	0.053	0.007	43.2	5.8	39.2	2.2	350	260	9.3	0.7

Table D-4: Zircon LA-ICP-MS U-Pb Isotopic Data and Ages: HP14-03 (IGSN: IEKHP0300[a]): Calcrete of northwestern Ellis County (452005, 4321496)[b]

					Corrected Isotopic Ratios							Ages (Ma)[j]							
Grain #[c]	U[d] [ppm]	Th[d] [ppm]	Th/U	eU[e] [ppm]	$^{207}Pb/^{235}U$[f]	±2s[g]	$^{206}Pb/^{238}U$[f]	±2s[g]	Rho[h]	$^{207}Pb/^{206}Pb$[i]	±2s[g]	$^{207}Pb/^{235}U$	±2s	$^{206}Pb/^{238}U$	±2s	$^{207}Pb/^{206}Pb$	±2s	Disc. %[k]	Wtd. Disc.[l]
31	**741**	**365**	**0.50**	**827**	**0.010**	**0.001**	**0.0015**	**0.0001**	**0.06**	**0.050**	**0.006**	**9.9**	**1.1**	**9.79**	**0.43**	**120**	**210**	**1.1**	**0.1**
32	138	51	0.37	150	3.218	0.086	0.2536	0.0061	0.61	0.092	0.002	1461	21	1456	31	1455	42	0.3	0.0
33	275	85	0.33	295	0.093	0.006	0.0131	0.0004	-0.03	0.051	0.004	90.6	5.2	84.1	2.4	220	140	7.2	1.3
34	52	32	0.62	59	1.881	0.072	0.1792	0.0047	0.45	0.077	0.003	1073	25	1062	26	1147	71	1.0	3.3
35	219	224	0.97	272	0.167	0.008	0.0255	0.0006	0.28	0.048	0.002	156.1	7.2	162	4	94	95	-3.9	-0.8
36	150	65	0.43	165	0.096	0.007	0.0147	0.0006	0.10	0.049	0.004	93.7	6.8	93.8	3.6	140	150	-0.1	0.0
37	194	98	0.58	217	1.855	0.049	0.1766	0.0041	0.60	0.076	0.002	1068	17	1048	23	1105	48	1.9	2.5
38	114	65	0.55	129	2.891	0.077	0.2367	0.0057	0.60	0.089	0.002	1384	21	1369	30	1413	46	1.1	1.5
39	244	183	0.70	287	0.183	0.009	0.0262	0.0007	0.21	0.051	0.002	170.5	7.4	166.9	4.1	230	85	2.1	0.5
40	552	612	1.11	696	0.037	0.003	0.0055	0.0002	-0.01	0.048	0.005	37.2	2.9	35.4	1.4	100	180	4.8	0.6
41	78	51	0.65	90	1.910	0.063	0.1821	0.0041	0.59	0.077	0.002	1081	22	1078	22	1130	55	0.3	2.4
42	246	63	0.25	261	4.235	0.089	0.2965	0.0049	0.66	0.104	0.002	1680	17	1673	25	1693	33	0.4	0.8
43	191	86	0.45	211	1.823	0.045	0.1795	0.0034	0.59	0.075	0.002	1052	16	1064	19	1058	45	-1.1	-0.3
44	100	64	0.66	116	3.153	0.110	0.2464	0.0059	0.61	0.092	0.002	1443	26	1419	30	1469	46	1.7	1.7
45	154	103	0.68	178	2.873	0.093	0.2354	0.0058	0.54	0.090	0.002	1381	22	1362	30	1409	51	1.4	1.6
46	438	253	0.58	497	0.029	0.003	0.0045	0.0001	0.08	0.047	0.005	29.0	2.8	29.1	0.9	50	170	-0.2	0.0
47	591	80	0.13	610	0.411	0.012	0.0557	0.0013	0.47	0.055	0.002	349.3	8.9	349	8	392	64	0.0	0.0
48	**166**	**83**	**0.47**	**186**	**0.010**	**0.003**	**0.0016**	**0.0001**	**-0.22**	**0.055**	**0.016**	**9.8**	**2.6**	**9.98**	**0.83**	**-30**	**430**	**-1.8**	**-0.1**
49	630	316	0.52	704	0.107	0.005	0.0162	0.0004	0.30	0.049	0.002	103.3	4.2	103.6	2.4	142	83	-0.3	-0.1
50	166	71	0.42	183	0.244	0.012	0.0354	0.0008	0.18	0.050	0.003	221	10	224.3	5.3	210	110	-1.5	-0.3
51	715	453	0.60	821	2.950	0.130	0.2400	0.0130	0.86	0.092	0.003	1397	31	1385	68	1454	55	0.9	1.0
52	**67**	**32**	**0.48**	**75**	**0.013**	**0.006**	**0.0014**	**0.0002**	**0.03**	**0.077**	**0.038**	**12.8**	**5.7**	**9.2**	**1.3**	**320**	**780**	**28.1**	**0.6**
53	165	118	0.72	193	4.729	0.120	0.3154	0.0071	0.62	0.110	0.002	1774	22	1766	35	1795	39	0.5	0.8
54	195	122	0.63	224	3.071	0.077	0.2467	0.0045	0.61	0.090	0.002	1426	20	1421	23	1428	39	0.4	0.3
55	298	128	0.43	328	3.131	0.084	0.2538	0.0059	0.79	0.090	0.002	1438	21	1457	30	1429	38	-1.3	-0.9
56	238	156	0.67	275	0.029	0.004	0.0044	0.0002	-0.09	0.049	0.007	29.0	3.8	28.0	1.3	170	250	3.4	0.3
57	36	16	0.44	39	1.575	0.066	0.1629	0.0039	0.13	0.070	0.003	959	27	972	21	935	90	-1.4	-1.8
58	185	56	0.30	198	1.841	0.046	0.1815	0.0033	0.47	0.075	0.002	1061	16	1075	18	1064	48	-1.3	-0.6
59	89	60	0.68	103	1.885	0.061	0.1798	0.0041	0.44	0.076	0.002	1076	21	1065	23	1106	60	1.0	1.8
60	227	57	0.25	240	4.341	0.110	0.3070	0.0056	0.71	0.104	0.002	1699	21	1725	28	1696	36	-1.5	-1.0

Table D-4: Zircon LA-ICP-MS U-Pb Isotopic Data and Ages: HP14-03 (IGSN: IEKHP0300[a]): Calcrete of northwestern Ellis County (452005, 4321496)[b]

					Corrected Isotopic Ratios							Ages (Ma)[j]							
Grain #[c]	U[d] [ppm]	Th[d] [ppm]	Th/U	eU[e] [ppm]	$^{207}Pb/^{235}U$[f]	±2s[g]	$^{206}Pb/^{238}U$[f]	±2s[g]	Rho[h]	$^{207}Pb/^{206}Pb$[i]	±2s[g]	$^{207}Pb/^{235}U$	±2s	$^{206}Pb/^{238}U$	±2s	$^{207}Pb/^{206}Pb$	±2s	Disc. %[k]	Wtd. Disc.[l]
61	250	102	0.40	274	0.100	0.007	0.0143	0.0005	-0.16	0.051	0.004	97	6	91.4	2.8	230	160	5.3	0.8
62	135	57	0.42	149	1.852	0.060	0.1783	0.0055	0.57	0.076	0.002	1065	22	1057	30	1090	58	0.8	1.1
63	502	168	0.34	542	0.100	0.004	0.0155	0.0004	0.37	0.047	0.002	97.1	4.1	99.2	2.6	65	85	-2.2	-0.5
64	98	28	0.33	105	1.881	0.073	0.1837	0.0069	0.56	0.074	0.002	1077	25	1085	37	1029	69	-0.7	-1.5
65	155	59	0.38	169	4.166	0.100	0.2957	0.0067	0.66	0.103	0.002	1665	21	1669	33	1668	40	-0.2	0.0
66	249	76	0.30	267	4.296	0.110	0.3048	0.0070	0.79	0.104	0.002	1695	22	1714	34	1686	37	-1.1	-0.8
67	256	27	0.11	262	0.509	0.019	0.0665	0.0020	0.39	0.055	0.002	416	13	415	12	424	83	0.2	0.1
68	239	65	0.24	254	4.287	0.120	0.2954	0.0076	0.80	0.105	0.002	1691	23	1667	38	1714	38	1.4	1.2
69	453	181	0.38	496	0.085	0.005	0.0130	0.0005	0.27	0.048	0.003	84.3	4.4	83	3	150	110	1.7	0.3
70	279	143	0.46	313	4.290	0.120	0.2986	0.0070	0.77	0.105	0.002	1688	24	1684	35	1717	37	0.2	0.9
71	80	37	0.48	89	3.251	0.110	0.2594	0.0065	0.56	0.091	0.003	1468	25	1486	33	1460	54	-1.2	-0.8
72	95	48	0.49	106	0.014	0.005	0.0018	0.0002	0.04	0.060	0.021	14.3	4.6	11.5	1.2	130	530	19.6	0.6
73	103	30	0.30	110	4.240	0.140	0.2965	0.0077	0.63	0.104	0.003	1681	26	1672	38	1698	47	0.5	0.7
74	299	101	0.34	323	4.236	0.110	0.2925	0.0062	0.72	0.104	0.002	1681	21	1653	31	1699	38	1.7	1.5
75	119	120	0.97	147	0.041	0.007	0.0062	0.0003	0.08	0.048	0.008	40.5	6.4	39.7	1.9	170	270	2.0	0.1
76	871	129	0.15	901	3.015	0.110	0.2377	0.0086	0.74	0.091	0.003	1408	28	1373	45	1457	51	2.5	1.9
77	105	45	0.45	115	0.044	0.008	0.0063	0.0005	-0.01	0.057	0.012	43.5	7.8	40.9	2.7	230	370	6.0	0.3
78	252	127	0.50	282	1.866	0.053	0.1817	0.0039	0.37	0.076	0.002	1071	19	1076	21	1098	46	-0.5	1.0
79	82	30	0.37	89	0.012	0.005	0.0020	0.0003	0.02	0.051	0.025	12	5	12.7	1.7	-20	630	-10.4	-0.2
80	202	132	0.65	233	0.031	0.004	0.0044	0.0003	0.29	0.053	0.008	30.7	4.3	28.4	1.8	340	300	7.5	0.5
81	214	77	0.35	232	0.087	0.007	0.0122	0.0005	0.20	0.052	0.005	84.7	6.7	77.9	3.3	230	170	8.0	1.0
82	297	59	0.20	311	4.311	0.110	0.3016	0.0067	0.58	0.103	0.002	1695	21	1698	33	1681	42	-0.2	-0.5
83	443	173	0.37	484	0.077	0.005	0.0120	0.0005	0.55	0.047	0.003	74.8	4.2	76.7	3.1	56	100	-2.5	-0.5
84	45	33	0.73	53	0.088	0.015	0.0101	0.0010	0.29	0.057	0.011	85	14	64.6	6.3	560	350	24.0	1.5
85	**97**	**34**	**0.35**	**105**	**0.013**	**0.006**	**0.0015**	**0.0003**	**0.13**	**0.052**	**0.027**	**12.8**	**6.3**	**9.8**	**1.6**	**520**	**870**	**23.4**	**0.5**
86	80	29	0.38	87	0.008	0.004	0.0017	0.0002	-0.14	0.053	0.030	7.6	3.6	10.6	1.3	-560	720	-39.5	-0.8
87	**105**	**49**	**0.48**	**117**	**0.009**	**0.003**	**0.0015**	**0.0001**	**-0.21**	**0.065**	**0.021**	**9.3**	**3.1**	**9.64**	**0.92**	**250**	**530**	**-3.7**	**-0.1**
88	73	28	0.39	80	2.700	0.087	0.2311	0.0066	0.56	0.085	0.002	1327	24	1339	35	1306	54	-0.9	-0.9
89	262	153	0.60	298	0.161	0.008	0.0230	0.0007	0.11	0.050	0.003	151	6.6	146.7	4.1	200	100	2.8	0.7
90	38	18	0.47	43	0.088	0.021	0.0110	0.0008	-0.05	0.058	0.014	84	19	70.8	5.4	470	450	15.7	0.7

Table D-4: Zircon LA-ICP-MS U-Pb Isotopic Data and Ages: HP14-03 (IGSN: IEKHP0300[a]): Calcrete of northwestern Ellis County (452005, 4321496)[b]

					Corrected Isotopic Ratios							Ages (Ma)[j]							
Grain #[c]	U[d] [ppm]	Th[d] [ppm]	Th/U	eU[e] [ppm]	$^{207}Pb/^{235}U$[f]	±2s[g]	$^{206}Pb/^{238}U$[f]	±2s[g]	Rho[h]	$^{207}Pb/^{206}Pb$[i]	±2s[g]	$^{207}Pb/^{235}U$	±2s	$^{206}Pb/^{238}U$	±2s	$^{207}Pb/^{206}Pb$	±2s	Disc. %[k]	Wtd. Disc.[l]
91	679	124	0.20	708	3.143	0.084	0.2468	0.0065	0.60	0.092	0.002	1446	19	1421	33	1469	48	1.7	1.5
92	192	46	0.15	203	0.070	0.006	0.0101	0.0004	0.04	0.050	0.004	68.4	5.5	64.7	2.6	220	160	5.4	0.7
93	548	206	0.36	596	0.039	0.002	0.0058	0.0002	0.12	0.048	0.003	38.5	2.4	37.4	1.2	120	130	2.9	0.5
94	85	51	0.62	97	1.867	0.060	0.1775	0.0041	0.42	0.077	0.002	1069	21	1053	22	1096	58	1.5	2.0
95	312	119	0.39	340	0.106	0.006	0.0160	0.0005	0.36	0.048	0.003	102.1	5.2	102.5	3.2	105	100	-0.4	-0.1
96	526	208	0.39	575	0.094	0.004	0.0142	0.0005	0.24	0.048	0.002	91.4	4.1	90.9	2.9	91	96	0.5	0.1
97	604	28	0.05	611	2.306	0.078	0.1333	0.0045	0.88	0.124	0.003	1212	24	806	25	2011	37	33.5	16.9
98	74	45	0.62	84	1.899	0.056	0.1818	0.0039	0.53	0.076	0.002	1081	20	1076	21	1083	54	0.5	0.3
99	124	16	0.13	128	4.280	0.150	0.3006	0.0088	0.75	0.102	0.003	1684	29	1692	44	1660	46	-0.5	-0.7
100	195	133	0.69	226	0.019	0.003	0.0033	0.0002	0.11	0.044	0.007	19.4	2.8	21.2	1.0	-90	240	-9.3	-0.6
101	225	78	0.35	243	0.102	0.007	0.0162	0.0004	0.36	0.046	0.003	98	6.5	103.3	2.7	30	120	-5.4	-0.8
102	153	64	0.46	168	1.901	0.064	0.1778	0.0044	0.52	0.077	0.002	1079	23	1054	24	1104	58	2.3	2.1
103	334	191	0.61	379	0.503	0.017	0.0673	0.0015	0.36	0.055	0.002	413	12	422	9	398	71	-2.2	-0.8
104	**118**	**63**	**0.53**	**133**	**0.012**	**0.004**	**0.0015**	**0.0002**	**0.04**	**0.065**	**0.024**	**11.6**	**4.1**	**9.7**	**1.0**	**320**	**580**	**16.4**	**0.5**
105	448	85	0.19	468	0.033	0.002	0.0054	0.0002	0.19	0.046	0.004	32.9	2.4	34.4	1.1	50	140	-4.6	-0.6
106	474	165	0.30	513	0.053	0.004	0.0076	0.0003	0.35	0.049	0.004	52.4	3.8	48.7	2.1	150	140	7.1	1.0
107	99	54	0.51	112	1.922	0.052	0.1840	0.0041	0.20	0.075	0.002	1089	19	1088	23	1075	57	0.1	-0.6
108	320	153	0.48	356	0.083	0.005	0.0128	0.0003	0.17	0.047	0.003	81	4.4	81.8	2.2	80	110	-1.0	-0.2
109	229	77	0.33	247	4.350	0.140	0.2991	0.0086	0.72	0.104	0.003	1701	26	1685	43	1715	44	0.9	0.7
110	575	241	0.38	632	0.035	0.002	0.0054	0.0002	0.20	0.047	0.003	34.8	2.1	34.77	0.96	70	110	0.1	0.0
111	119	39	0.32	128	0.034	0.005	0.0051	0.0003	-0.02	0.050	0.007	34.2	4.9	32.7	1.8	160	260	4.4	0.3
112	**372**	**152**	**0.39**	**408**	**0.009**	**0.002**	**0.0015**	**0.0001**	**0.22**	**0.045**	**0.008**	**9.1**	**1.7**	**9.72**	**0.55**	**30**	**300**	**-6.8**	**-0.4**
113	79	39	0.48	88	1.860	0.056	0.1843	0.0037	0.31	0.074	0.002	1064	20	1090	20	1035	63	-2.4	-2.8
114	73	35	0.47	81	1.901	0.064	0.1813	0.0043	0.42	0.076	0.002	1080	23	1076	24	1092	58	0.4	0.7
115	219	72	0.33	236	1.878	0.053	0.1803	0.0046	0.52	0.076	0.002	1072	19	1068	25	1086	52	0.4	0.7
116	123	88	0.70	144	0.090	0.010	0.0062	0.0003	0.21	0.105	0.012	86.3	9.2	39.6	2.0	1630	210	54.1	5.1
117	102	72	0.68	119	0.163	0.019	0.0234	0.0010	0.48	0.049	0.005	152	16	149.1	6.6	220	220	1.9	0.2
118	240	94	0.37	262	4.180	0.110	0.2926	0.0070	0.71	0.104	0.002	1668	21	1657	35	1693	38	0.7	1.0
119	20	21	1.02	25	2.660	0.110	0.2309	0.0070	0.09	0.085	0.004	1310	32	1342	37	1303	96	-2.4	-1.1
120	124	45	0.37	135	1.850	0.048	0.1784	0.0037	0.44	0.075	0.002	1064	17	1060	21	1073	48	0.4	0.6

Table D-4: Zircon LA-ICP-MS U-Pb Isotopic Data and Ages: HP14-03 (IGSN: IEKHP0300[a]): Calcrete of northwestern Ellis County (452005, 4321496)[b]

					Corrected Isotopic Ratios							Ages (Ma)[j]							
Grain #[c]	U[d] [ppm]	Th[d] [ppm]	Th/U	eU[e] [ppm]	$^{207}Pb/^{235}U$[f]	±2s[g]	$^{206}Pb/^{238}U$[f]	±2s[g]	Rho[h]	$^{207}Pb/^{206}Pb$[i]	±2s[g]	$^{207}Pb/^{235}U$	±2s	$^{206}Pb/^{238}U$	±2s	$^{207}Pb/^{206}Pb$	±2s	Disc. %[k]	Wtd. Disc.[l]
121	**182**	**123**	**0.60**	**211**	**0.010**	**0.004**	**0.0015**	**0.0001**	**0.01**	**0.052**	**0.029**	**9.7**	**3.5**	**9.66**	**0.90**	**140**	**560**	**0.4**	**0.0**
122	135	73	0.55	152	1.836	0.047	0.1798	0.0035	0.57	0.076	0.002	1061	17	1065	19	1092	48	-0.4	1.4
123	87	36	0.42	95	0.012	0.005	0.0017	0.0002	0.11	0.060	0.027	12.1	4.7	10.8	1.2	40	680	10.7	0.3
124	**3215**	**1797**	**0.57**	**3637**	**0.010**	**0.001**	**0.0014**	**0.0000**	**0.15**	**0.049**	**0.003**	**9.67**	**0.56**	**9.08**	**0.28**	**150**	**120**	**6.1**	**1.1**
125	**103**	**54**	**0.54**	**116**	**0.011**	**0.006**	**0.0014**	**0.0002**	**-0.01**	**0.067**	**0.037**	**10.5**	**5.6**	**9.0**	**1.1**	**-170**	**890**	**14.3**	**0.3**
126	19	20	1.06	23	2.657	0.096	0.2313	0.0077	0.23	0.084	0.004	1316	26	1344	40	1271	81	-2.1	-1.8
127	218	27	0.11	224	3.158	0.079	0.2505	0.0050	0.63	0.093	0.002	1447	20	1441	26	1476	42	0.4	1.3

[a]International Geo Sample Number (IGSN) registered in the SESAR database
[b]All locations reported as UTM coordinates using Zone 14 NAD 27
[c]Emboldened rows indicate the youngest measured concordant grains
[d]U and Th concentrations and Th/U ratios calculated relative to the GJ-1 zircon standard ID-TIMS values using 287 ± 76 ppm for U and 8.4 ± 2.6 ppm for Th (Jackson et al., 2004)
[e]Equivalent U defined by the equation: eU = U ppm + 0.235*Th ppm
[f]Corrected for U-Pb fractionation and background and normalized to the GJ-1 zircon standard ID-TIMS values: $^{207}Pb/^{235}U = 0.8093 \pm 0.0009$ and $^{206}Pb/^{238}U = 0.09761 \pm 0.00011$ (Jackson et al., 2004)
[g]Propagated uncertainty of internal uncertainties (2 SE) and within run reproducibility of GJ-1 (2 SE)
[h]Uncertainty correlation between $^{206}Pb/^{238}U$ and $^{207}Pb/^{235}U$ uncertainties
[i]Corrected for background and Pb isotopic fractionation using the GJ-1 zircon standard ID-TIMS value: $^{207}Pb/^{206}Pb = 0.06014 \pm 0.00001$ (Jackson et al., 2004)
[j]U-Pb ages calculated relative to the GJ-1 zircon standard
[k]Discordance defined as $[(^{207}Pb/^{235}U_{age} - ^{206}Pb/^{238}U_{age})/(^{207}Pb/^{235}U_{age})]*100$
[l]Uncertainty weighted age difference defined as $(^{207}Pb/^{235}U_{age} - ^{206}Pb/^{238}U_{age})/(^{207}Pb/^{235}U_{age\ uncertainty})$ for grains with $^{206}Pb/^{238}U$ ages <850 Ma and $(^{207}Pb/^{206}Pb_{age} - ^{206}Pb/^{238}U_{age})/(^{206}Pb/^{238}U_{age\ uncertainty})$ for grains with $^{206}Pb/^{238}U$ ages ≥850 Ma

Table D-5: Zircon LA-ICP-MS U-Pb Isotopic Data and Ages: HP14-06 (IGSN: IEKHP0600[a]): Bentonite of the Calvert mine, Norton County (435374, 4410586)[b]

					Corrected Isotopic Ratios							Ages (Ma)[j]							
Grain #[c]	U[d] [ppm]	Th[d] [ppm]	Th/U	eU[e] [ppm]	$^{207}Pb/^{235}U$[f]	±2s[g]	$^{206}Pb/^{238}U$[f]	±2s[g]	Rho[h]	$^{207}Pb/^{206}Pb$[i]	±2s[g]	$^{207}Pb/^{235}U$	±2s	$^{206}Pb/^{238}U$	±2s	$^{207}Pb/^{206}Pb$	±2s	Disc. %[k]	Wtd. Disc.[l]
1	**180**	**94**	**0.52**	**202**	**0.016**	**0.006**	**0.0018**	**0.0002**	**-0.39**	**0.057**	**0.022**	**17.3**	**5.8**	**11.7**	**1.4**	**530**	**680**	**32.4**	**1.0**
2	**186**	**102**	**0.53**	**210**	**0.012**	**0.003**	**0.0019**	**0.0001**	**-0.24**	**0.048**	**0.014**	**11.5**	**3.4**	**12.46**	**0.85**	**-180**	**410**	**-8.3**	**-0.3**
3	602	226	0.37	655	0.037	0.002	0.0057	0.0002	0.15	0.045	0.003	36.4	2.4	36.4	1.1	30	120	0.0	0.0
4	59	22	0.36	64	1.909	0.066	0.1847	0.0053	0.43	0.076	0.002	1085	24	1091	29	1091	58	-0.6	0.0
5	467	141	0.29	500	4.940	0.140	0.3092	0.0084	0.68	0.112	0.002	1808	24	1735	41	1832	34	4.0	2.4
6	**157**	**88**	**0.58**	**177**	**0.011**	**0.003**	**0.0017**	**0.0002**	**-0.05**	**0.062**	**0.017**	**11.1**	**2.9**	**10.9**	**1.0**	**60**	**410**	**1.8**	**0.1**
7	**180**	**101**	**0.55**	**204**	**0.015**	**0.004**	**0.0020**	**0.0002**	**0.17**	**0.050**	**0.013**	**14.8**	**3.6**	**12.8**	**1.0**	**310**	**400**	**13.5**	**0.6**
8	919	270	0.30	983	0.026	0.002	0.0039	0.0001	-0.02	0.049	0.004	26.3	1.9	25.14	0.84	200	170	4.4	0.6
9	139	89	0.64	160	2.044	0.046	0.1930	0.0035	0.47	0.076	0.002	1129	15	1137	19	1095	39	-0.7	-2.2
10	204	198	0.95	251	0.039	0.004	0.0055	0.0003	0.07	0.049	0.006	38.5	4.0	35.4	1.8	230	210	8.1	0.8
11	49	58	1.16	63	0.034	0.010	0.0054	0.0004	0.17	0.054	0.015	33.5	9.7	34.5	2.8	0	450	-3.0	-0.1
12	109	45	0.41	120	0.070	0.008	0.0102	0.0004	0.22	0.048	0.006	67.9	7.8	65.2	2.7	150	200	4.0	0.3
13	365	193	0.52	411	0.089	0.004	0.0134	0.0004	0.10	0.048	0.003	86.0	4.1	86.0	2.2	100	100	0.0	0.0
14	**166**	**92**	**0.53**	**188**	**0.013**	**0.003**	**0.0019**	**0.0002**	**0.41**	**0.045**	**0.012**	**12.7**	**3.4**	**11.9**	**1.1**	**120**	**380**	**6.3**	**0.2**
15	**149**	**74**	**0.48**	**166**	**0.013**	**0.004**	**0.0018**	**0.0002**	**0.12**	**0.050**	**0.015**	**13.2**	**3.8**	**11.9**	**1.1**	**70**	**460**	**9.8**	**0.3**
16	**196**	**115**	**0.58**	**223**	**0.012**	**0.003**	**0.0018**	**0.0002**	**0.01**	**0.056**	**0.017**	**11.7**	**3.2**	**11.3**	**1.1**	**290**	**460**	**3.4**	**0.1**
17	**148**	**78**	**0.51**	**166**	**0.010**	**0.004**	**0.0019**	**0.0002**	**-0.05**	**0.047**	**0.018**	**10.5**	**3.9**	**12.1**	**1.1**	**-90**	**530**	**-15.2**	**-0.4**
18	**175**	**101**	**0.58**	**198**	**0.013**	**0.003**	**0.0019**	**0.0001**	**0.34**	**0.050**	**0.012**	**12.9**	**2.9**	**12.4**	**0.8**	**220**	**360**	**4.1**	**0.2**
19	**119**	**51**	**0.42**	**131**	**0.015**	**0.005**	**0.0020**	**0.0002**	**-0.15**	**0.052**	**0.022**	**15.0**	**4.9**	**12.6**	**1.5**	**180**	**540**	**16.0**	**0.5**
20	**183**	**92**	**0.50**	**205**	**0.013**	**0.003**	**0.0019**	**0.0002**	**-0.03**	**0.052**	**0.013**	**13.3**	**3.2**	**12.3**	**1.1**	**160**	**420**	**7.5**	**0.3**
21	108	41	0.33	117	0.072	0.008	0.0115	0.0005	0.14	0.050	0.006	71.1	7.7	74	3	130	210	-4.1	-0.4
22	**197**	**113**	**0.57**	**224**	**0.014**	**0.003**	**0.0020**	**0.0001**	**0.11**	**0.053**	**0.012**	**14.0**	**2.9**	**12.62**	**0.77**	**210**	**350**	**9.9**	**0.5**
23	162	66	0.39	178	2.125	0.091	0.1890	0.0120	0.73	0.082	0.004	1160	31	1115	66	1229	89	3.9	1.7
24	**182**	**106**	**0.59**	**207**	**0.012**	**0.003**	**0.0017**	**0.0001**	**0.07**	**0.054**	**0.014**	**11.7**	**3.0**	**10.91**	**0.75**	**170**	**430**	**6.8**	**0.3**
26	352	113	0.32	379	4.463	0.088	0.3102	0.0064	0.71	0.105	0.001	1724	17	1744	31	1705	22	-1.2	-1.3
27	**200**	**88**	**0.44**	**221**	**0.017**	**0.004**	**0.0020**	**0.0001**	**-0.05**	**0.061**	**0.016**	**17.2**	**4.2**	**12.72**	**0.90**	**220**	**480**	**26.0**	**1.1**
28	**106**	**41**	**0.38**	**115**	**0.013**	**0.005**	**0.0019**	**0.0002**	**-0.12**	**0.056**	**0.021**	**13.1**	**4.5**	**12.34**	**0.97**	**-220**	**520**	**5.8**	**0.2**
29	225	61	0.27	239	1.897	0.043	0.1838	0.0045	0.68	0.075	0.001	1079	15	1090	24	1073	35	-1.0	-0.7
30	225	89	0.40	246	0.034	0.004	0.0049	0.0002	0.26	0.051	0.006	33.8	4.1	31.7	1.5	220	220	6.2	0.5
31	81	36	0.44	90	0.017	0.006	0.0022	0.0002	0.16	0.056	0.023	16.8	6.0	14.4	1.4	-40	600	14.3	0.4
32	**123**	**64**	**0.52**	**138**	**0.012**	**0.004**	**0.0017**	**0.0002**	**0.01**	**0.055**	**0.022**	**11.8**	**4.1**	**11.0**	**1.2**	**170**	**600**	**6.8**	**0.2**
33	**109**	**49**	**0.45**	**121**	**0.018**	**0.006**	**0.0019**	**0.0003**	**-0.15**	**0.071**	**0.026**	**17.7**	**6.2**	**12.4**	**1.8**	**470**	**680**	**29.9**	**0.9**
34	483	209	0.43	532	3.207	0.076	0.2561	0.0063	0.76	0.090	0.001	1457	19	1474	31	1426	29	-1.2	-1.5
35	**264**	**144**	**0.55**	**298**	**0.013**	**0.002**	**0.0018**	**0.0001**	**-0.03**	**0.055**	**0.010**	**13.3**	**2.3**	**11.69**	**0.88**	**350**	**300**	**12.1**	**0.7**

Table D-5: Zircon LA-ICP-MS U-Pb Isotopic Data and Ages: HP14-06 (IGSN: IEKHP0600[a]): Bentonite of the Calvert mine, Norton County (435374, 4410586)[b]

					Corrected Isotopic Ratios							Ages (Ma)[j]							
Grain #[c]	U[d] [ppm]	Th[d] [ppm]	Th/U	eU[e] [ppm]	^{207}Pb/^{235}U[f]	±2s[g]	^{206}Pb/^{238}U[f]	±2s[g]	Rho[h]	^{207}Pb/^{206}Pb[i]	±2s[g]	^{207}Pb/^{235}U	±2s	^{206}Pb/^{238}U	±2s	^{207}Pb/^{206}Pb	±2s	Disc. %[k]	Wtd. Disc.[l]
36	**179**	**87**	**0.49**	**199**	**0.013**	**0.003**	**0.0018**	**0.0001**	**0.03**	**0.058**	**0.016**	**13.0**	**3.1**	**11.65**	**0.93**	**60**	**390**	**10.4**	**0.4**
37	38	22	0.61	43	2.025	0.076	0.1908	0.0049	0.28	0.077	0.003	1124	25	1125	27	1123	71	-0.1	-0.1
38	81	41	0.51	91	3.159	0.085	0.2541	0.0048	0.44	0.090	0.002	1447	21	1459	25	1425	42	-0.8	-1.4
39	**169**	**86**	**0.51**	**189**	**0.013**	**0.003**	**0.0017**	**0.0001**	**-0.03**	**0.055**	**0.014**	**13.4**	**3.2**	**10.78**	**0.77**	**100**	**420**	**19.6**	**0.8**
40	**207**	**104**	**0.48**	**232**	**0.010**	**0.002**	**0.0018**	**0.0001**	**-0.06**	**0.051**	**0.013**	**10.3**	**2.4**	**11.35**	**0.74**	**-50**	**380**	**-10.2**	**-0.4**
41	**129**	**48**	**0.37**	**140**	**0.014**	**0.004**	**0.0019**	**0.0002**	**-0.03**	**0.058**	**0.020**	**13.6**	**4.2**	**12.4**	**1.2**	**-150**	**510**	**8.8**	**0.3**
42	**156**	**74**	**0.47**	**174**	**0.011**	**0.003**	**0.0017**	**0.0002**	**0.11**	**0.053**	**0.016**	**11**	**3**	**11.06**	**0.97**	**60**	**430**	**-0.5**	**0.0**
43	**147**	**64**	**0.44**	**162**	**0.010**	**0.004**	**0.0019**	**0.0002**	**0.03**	**0.043**	**0.016**	**10.4**	**4.0**	**12.1**	**1.1**	**-60**	**540**	**-16.3**	**-0.4**
44	**140**	**65**	**0.44**	**155**	**0.013**	**0.004**	**0.0019**	**0.0002**	**0.07**	**0.053**	**0.016**	**13.0**	**3.7**	**12.4**	**1.1**	**100**	**460**	**4.6**	**0.2**
45	**123**	**61**	**0.49**	**138**	**0.017**	**0.006**	**0.0017**	**0.0002**	**-0.23**	**0.075**	**0.028**	**16.4**	**5.7**	**10.8**	**1.3**	**780**	**730**	**34.1**	**1.0**
46	**167**	**81**	**0.46**	**186**	**0.011**	**0.003**	**0.0018**	**0.0002**	**0.00**	**0.046**	**0.015**	**11.3**	**3.2**	**11.9**	**1.0**	**-130**	**450**	**-5.3**	**-0.2**
47	663	178	0.26	705	0.036	0.003	0.0053	0.0002	0.27	0.049	0.004	35.7	2.5	33.9	1.1	130	140	5.0	0.7
48	107	70	0.66	124	0.039	0.007	0.0056	0.0003	-0.07	0.050	0.010	39.6	7.2	36.3	1.8	100	330	8.3	0.5
49	**99**	**42**	**0.39**	**109**	**0.012**	**0.005**	**0.0018**	**0.0002**	**-0.07**	**0.052**	**0.030**	**12**	**5**	**11.4**	**1.3**	**-500**	**870**	**7.3**	**0.2**
50	98	38	0.38	106	2.435	0.078	0.2087	0.0053	0.32	0.083	0.003	1254	24	1221	28	1291	63	2.6	2.5
51	**121**	**58**	**0.47**	**134**	**0.014**	**0.005**	**0.0018**	**0.0003**	**-0.06**	**0.068**	**0.026**	**14.4**	**5.0**	**11.8**	**1.7**	**380**	**700**	**18.1**	**0.5**
52	87	54	0.64	100	2.073	0.077	0.1890	0.0069	0.63	0.079	0.003	1141	24	1115	37	1156	60	2.3	1.1
53	**111**	**49**	**0.44**	**122**	**0.014**	**0.004**	**0.0018**	**0.0002**	**-0.06**	**0.064**	**0.020**	**14.4**	**3.7**	**11.6**	**1.2**	**320**	**480**	**19.4**	**0.8**
54	**134**	**55**	**0.41**	**147**	**0.012**	**0.003**	**0.0018**	**0.0001**	**-0.17**	**0.055**	**0.017**	**11.5**	**3.3**	**11.30**	**0.84**	**30**	**440**	**1.7**	**0.1**
55	**147**	**83**	**0.56**	**166**	**0.017**	**0.005**	**0.0019**	**0.0002**	**-0.02**	**0.060**	**0.019**	**17.3**	**4.4**	**12**	**1**	**570**	**530**	**30.6**	**1.2**
56	625	43	0.06	635	0.062	0.003	0.0095	0.0002	0.22	0.047	0.002	60.6	3.3	61.0	1.5	50	98	-0.7	-0.1
57	**136**	**65**	**0.48**	**151**	**0.017**	**0.004**	**0.0019**	**0.0002**	**0.07**	**0.058**	**0.016**	**16.8**	**4.1**	**12.46**	**0.97**	**320**	**430**	**25.8**	**1.1**
58	**178**	**87**	**0.49**	**198**	**0.012**	**0.003**	**0.0017**	**0.0001**	**0.02**	**0.053**	**0.016**	**12**	**3**	**11.21**	**0.83**	**-60**	**460**	**6.6**	**0.2**
59	**224**	**117**	**0.52**	**252**	**0.013**	**0.003**	**0.0018**	**0.0001**	**0.10**	**0.052**	**0.012**	**12.5**	**2.8**	**11.64**	**0.85**	**110**	**370**	**6.9**	**0.3**
60	281	129	0.46	311	0.018	0.003	0.0024	0.0001	0.03	0.051	0.008	17.8	2.9	15.61	0.93	220	300	12.3	0.8
61	725	439	0.43	828	0.036	0.002	0.0056	0.0002	0.16	0.048	0.003	35.8	1.9	35.9	1.0	90	110	-0.3	-0.1
62	136	41	0.30	146	1.889	0.061	0.1782	0.0047	0.53	0.076	0.002	1078	22	1056	26	1122	59	2.0	2.5
63	150	67	0.44	166	3.098	0.079	0.2504	0.0047	0.62	0.090	0.001	1433	20	1440	24	1420	27	-0.5	-0.8
64	**139**	**73**	**0.53**	**156**	**0.016**	**0.005**	**0.0018**	**0.0002**	**0.37**	**0.068**	**0.024**	**16.6**	**5.3**	**11.7**	**1.6**	**480**	**640**	**29.5**	**0.9**
65	**142**	**56**	**0.40**	**155**	**0.012**	**0.004**	**0.0018**	**0.0002**	**0.02**	**0.053**	**0.019**	**12.4**	**3.9**	**11.37**	**0.96**	**-120**	**530**	**8.3**	**0.3**
66	**142**	**63**	**0.45**	**157**	**0.012**	**0.005**	**0.0018**	**0.0002**	**-0.01**	**0.059**	**0.024**	**11.6**	**4.5**	**11.7**	**1.3**	**-80**	**570**	**-0.9**	**0.0**
67	**133**	**60**	**0.45**	**147**	**0.016**	**0.004**	**0.0020**	**0.0002**	**0.18**	**0.056**	**0.016**	**16.3**	**4.3**	**12.6**	**1.0**	**250**	**460**	**22.7**	**0.9**
68	**179**	**90**	**0.48**	**200**	**0.012**	**0.003**	**0.0019**	**0.0002**	**0.05**	**0.054**	**0.017**	**11.7**	**3.2**	**11.88**	**0.93**	**-50**	**440**	**-1.5**	**-0.1**
69	100	55	0.54	113	0.766	0.028	0.0908	0.0020	0.32	0.060	0.002	577	16	560	12	616	72	2.9	1.1

Table D-5: Zircon LA-ICP-MS U-Pb Isotopic Data and Ages: HP14-06 (IGSN: IEKHP0600[a]): Bentonite of the Calvert mine, Norton County (435374, 4410586)[b]

					Corrected Isotopic Ratios							Ages (Ma)[j]							
Grain #[c]	U[d] [ppm]	Th[d] [ppm]	Th/U	eU[e] [ppm]	$^{207}Pb/^{235}U$[f]	±2s[g]	$^{206}Pb/^{238}U$[f]	±2s[g]	Rho[h]	$^{207}Pb/^{206}Pb$[i]	±2s[g]	$^{207}Pb/^{235}U$	±2s	$^{206}Pb/^{238}U$	±2s	$^{207}Pb/^{206}Pb$	±2s	Disc. %[k]	Wtd. Disc.[l]
70	112	44	0.38	122	0.012	0.004	0.0017	0.0002	-0.05	0.062	0.025	12.3	4.2	11	1	-10	560	10.6	0.3
71	125	49	0.40	136	0.012	0.004	0.0017	0.0002	-0.08	0.057	0.021	11.5	4.1	10.9	1.2	80	570	5.2	0.1
72	188	50	0.26	200	1.950	0.046	0.1837	0.0036	0.63	0.077	0.001	1097	16	1087	20	1124	34	0.9	1.9
73	168	98	0.59	191	0.013	0.004	0.0016	0.0001	-0.04	0.058	0.017	12.7	3.5	10.33	0.86	130	470	18.7	0.7
74	131	57	0.43	144	1.917	0.060	0.1795	0.0053	0.47	0.077	0.002	1085	21	1064	29	1122	58	1.9	2.0
75	110	41	0.36	120	0.016	0.005	0.0019	0.0002	0.03	0.059	0.022	15.7	5.4	12.2	1.4	150	620	22.3	0.6
76	151	77	0.52	169	0.014	0.003	0.0017	0.0002	-0.03	0.059	0.015	14.1	3.1	11.09	0.97	310	430	21.3	1.0
77	121	56	0.47	134	0.012	0.004	0.0018	0.0002	-0.05	0.046	0.016	11.5	3.6	11.5	1.1	-10	460	0.0	0.0
78	69	54	0.79	81	1.906	0.059	0.1820	0.0033	0.38	0.077	0.002	1083	21	1078	18	1107	58	0.5	1.6
79	91	37	0.40	100	1.854	0.063	0.1807	0.0060	0.56	0.073	0.002	1065	23	1070	33	999	58	-0.5	-2.2
80	100	53	0.48	112	0.016	0.005	0.0019	0.0002	-0.02	0.075	0.030	15.5	5.1	11.9	1.2	-170	600	23.2	0.7
81	192	100	0.52	215	0.013	0.003	0.0016	0.0002	-0.14	0.062	0.017	13.0	3.1	10.4	1.1	240	430	20.0	0.8
82	186	100	0.54	209	0.015	0.005	0.0017	0.0001	-0.15	0.058	0.020	14.9	4.6	11.02	0.87	310	590	26.0	0.8
83	100	33	0.32	107	0.011	0.004	0.0019	0.0002	-0.23	0.057	0.020	11	4	12.5	1.3	40	530	-10.6	-0.3
84	145	66	0.45	160	0.014	0.005	0.0018	0.0002	0.19	0.065	0.023	14.4	5.1	11.8	1.4	210	590	18.1	0.5
85	183	88	0.48	203	0.012	0.003	0.0020	0.0001	-0.20	0.049	0.011	11.7	2.5	12.99	0.83	20	330	-11.0	-0.5
86	95	57	0.59	108	1.850	0.060	0.1858	0.0047	0.44	0.074	0.002	1061	22	1098	26	1035	67	-3.5	-2.4
87	214	110	0.52	240	0.015	0.004	0.0017	0.0002	-0.07	0.062	0.017	14.6	3.6	10.8	1.1	480	480	26.0	1.1
88	148	89	0.60	169	1.855	0.045	0.1811	0.0034	0.49	0.076	0.002	1066	16	1073	19	1085	43	-0.7	0.6
89	502	475	0.98	614	0.169	0.008	0.0241	0.0005	0.19	0.050	0.002	158.3	6.6	153.7	3.4	203	88	2.9	0.7
90	165	83	0.50	184	0.018	0.006	0.0020	0.0002	0.09	0.068	0.024	18.1	5.5	13.2	1.4	520	580	27.1	0.9
91	133	77	0.58	151	0.011	0.003	0.0019	0.0002	-0.14	0.050	0.014	11.4	3.1	12.04	0.97	90	430	-5.6	-0.2
92	105	54	0.51	118	0.011	0.004	0.0020	0.0002	-0.18	0.052	0.018	11	4	12.6	1.4	-30	520	-16.7	-0.5
93	176	84	0.49	196	1.913	0.042	0.1868	0.0028	0.44	0.075	0.001	1084	15	1104	15	1068	35	-1.8	-2.4
94	174	100	0.58	197	0.012	0.004	0.0018	0.0001	-0.10	0.057	0.017	12.3	3.5	11.65	0.80	-30	460	5.3	0.2
95	126	74	0.60	143	0.515	0.021	0.0668	0.0017	0.48	0.057	0.002	420	14	417	10	484	72	0.7	0.2
96	191	99	0.52	214	0.013	0.003	0.0017	0.0001	-0.02	0.061	0.017	13.3	3.3	10.81	0.91	240	440	18.7	0.8
97	163	95	0.59	185	0.012	0.003	0.0017	0.0001	-0.09	0.047	0.015	11.8	3.3	11.10	0.81	-20	470	5.9	0.2
98	183	100	0.54	207	0.014	0.003	0.0019	0.0001	0.04	0.057	0.014	14.0	3.3	11.99	0.83	220	420	14.4	0.6
99	121	44	0.36	132	0.042	0.010	0.0052	0.0004	-0.18	0.059	0.014	43.0	9.5	33.4	2.5	380	430	22.3	1.0
100	118	44	0.37	129	0.013	0.004	0.0019	0.0002	0.07	0.049	0.017	13.0	3.8	12.3	1.2	130	490	5.4	0.2
101	202	112	0.55	229	0.013	0.003	0.0020	0.0002	0.06	0.047	0.012	12.6	2.7	12.56	0.98	-120	340	0.3	0.0
102	85	70	0.83	101	0.032	0.007	0.0040	0.0003	0.06	0.057	0.013	32	7	25.7	2.1	230	370	19.7	0.9
103	182	97	0.52	205	0.012	0.003	0.0019	0.0002	0.08	0.046	0.013	12.3	2.9	11.89	0.94	150	410	3.3	0.1

Table D-5: Zircon LA-ICP-MS U-Pb Isotopic Data and Ages: HP14-06 (IGSN: IEKHP0600[a]): Bentonite of the Calvert mine, Norton County (435374, 4410586)[b]

					Corrected Isotopic Ratios							Ages (Ma)[j]							
Grain #[c]	U[d] [ppm]	Th[d] [ppm]	Th/U	eU[e] [ppm]	$^{207}Pb/^{235}U$[f]	±2s[g]	$^{206}Pb/^{238}U$[f]	±2s[g]	Rho[h]	$^{207}Pb/^{206}Pb$[i]	±2s[g]	$^{207}Pb/^{235}U$	±2s	$^{206}Pb/^{238}U$	±2s	$^{207}Pb/^{206}Pb$	±2s	Disc. %[k]	Wtd. Disc.[l]
104	228	131	0.58	259	0.013	0.003	0.0018	0.0001	-0.11	0.055	0.011	13.2	2.6	11.47	0.72	260	360	13.1	0.7
105	212	111	0.52	238	0.013	0.003	0.0018	0.0001	0.06	0.055	0.012	13.2	2.8	11.4	0.9	230	370	13.6	0.6
106	73	32	0.42	80	0.086	0.017	0.0114	0.0005	0.24	0.052	0.009	83	16	72.8	3.1	230	330	12.3	0.6
107	171	88	0.52	192	0.013	0.003	0.0018	0.0001	0.26	0.050	0.012	12.5	3.0	11.64	0.84	-30	380	6.9	0.3
108	326	15	0.05	330	4.370	0.120	0.3029	0.0086	0.79	0.103	0.002	1704	24	1704	43	1675	34	0.0	-0.7
109	283	180	0.63	325	0.012	0.002	0.0018	0.0001	0.04	0.048	0.009	12.4	2.3	11.84	0.77	130	310	4.5	0.2
110	186	111	0.58	212	0.014	0.004	0.0017	0.0002	0.01	0.054	0.018	13.5	3.8	10.7	1.0	290	530	20.7	0.7
111	309	129	0.42	340	0.081	0.004	0.0119	0.0004	0.06	0.049	0.003	78.5	4.1	76.4	2.3	140	110	2.7	0.5
112	188	119	0.62	216	0.015	0.003	0.0018	0.0002	0.19	0.060	0.015	14.8	3.3	11.5	1.0	380	430	22.3	1.0
113	159	68	0.43	175	0.017	0.005	0.0018	0.0002	0.03	0.068	0.022	17.4	5.2	11.6	1.4	670	590	33.3	1.1
114	156	81	0.49	175	0.013	0.004	0.0019	0.0002	0.08	0.056	0.017	13.4	4.2	12.1	1.3	30	510	9.7	0.3
115	159	74	0.45	176	0.013	0.004	0.0018	0.0002	-0.06	0.056	0.018	12.9	3.8	11.3	1.1	280	510	12.4	0.4
116	121	72	0.59	138	1.925	0.059	0.1867	0.0037	0.51	0.075	0.002	1094	21	1103	20	1069	48	-0.8	-1.7
117	117	45	0.38	127	0.016	0.005	0.0019	0.0002	0.14	0.062	0.023	15.8	4.5	12.0	1.2	160	530	24.1	0.8
118	119	62	0.52	134	0.012	0.004	0.0016	0.0002	0.02	0.066	0.022	11.9	4.1	10.5	1.1	160	580	11.8	0.3
119	318	208	0.67	367	0.192	0.009	0.0282	0.0006	0.18	0.050	0.002	179.2	7.4	179.3	3.7	183	95	-0.1	0.0
120	106	71	0.65	123	1.963	0.052	0.1872	0.0040	0.38	0.076	0.002	1103	18	1105	22	1107	49	-0.2	0.1
121	116	49	0.43	127	0.013	0.004	0.0018	0.0002	0.18	0.058	0.017	13.0	4.2	11.5	1.0	30	450	11.5	0.4
122	232	115	0.49	259	0.012	0.003	0.0017	0.0002	-0.01	0.053	0.013	12.2	2.8	10.85	0.94	250	400	11.1	0.5
123	199	106	0.54	224	0.011	0.003	0.0020	0.0001	-0.15	0.047	0.013	10.7	3.1	12.84	0.87	20	420	-20.0	-0.7
124	79	28	0.35	86	0.019	0.007	0.0019	0.0003	0.02	0.075	0.032	19.6	6.8	12.4	1.8	530	740	36.7	1.1
125	140	66	0.47	156	0.012	0.004	0.0019	0.0002	0.01	0.061	0.022	12.1	3.6	12.1	1.0	-70	480	0.0	0.0
126	101	44	0.45	111	1.925	0.050	0.1820	0.0036	0.25	0.077	0.002	1090	17	1080	20	1126	53	0.9	2.3
127	128	51	0.39	140	0.016	0.005	0.0018	0.0002	0.01	0.054	0.021	15.4	5.3	11.6	1.2	250	620	24.7	0.7
128	200	85	0.41	220	0.073	0.009	0.0102	0.0005	0.00	0.052	0.006	71.6	8.3	65.1	2.9	230	230	9.1	0.8
129	112	83	0.75	132	0.040	0.006	0.0058	0.0003	-0.11	0.049	0.008	40.6	5.9	37.4	1.9	200	270	7.9	0.5
130	145	64	0.41	160	0.016	0.006	0.0019	0.0002	0.08	0.059	0.023	16	6	12.01	0.97	30	600	24.9	0.7
131	176	97	0.56	198	0.015	0.004	0.0019	0.0002	0.03	0.060	0.016	14.6	3.6	11.91	0.97	370	450	18.4	0.7
132	97	43	0.43	107	0.034	0.008	0.0023	0.0003	0.08	0.119	0.031	33.4	7.5	14.8	1.7	1450	510	55.7	2.5
133	144	65	0.45	159	0.012	0.004	0.0018	0.0002	-0.22	0.049	0.016	12.1	3.6	11.72	0.98	-110	470	3.1	0.1
134	166	69	0.42	182	0.013	0.003	0.0019	0.0002	0.02	0.061	0.017	13.4	3.2	11.9	1.2	180	450	11.2	0.5
135	210	120	0.57	238	0.012	0.003	0.0017	0.0001	-0.12	0.056	0.013	12.3	2.7	11.11	0.84	240	400	9.7	0.4
136	200	107	0.54	225	0.013	0.003	0.0019	0.0001	0.11	0.050	0.012	12.6	2.8	12.25	0.79	-20	350	2.8	0.1
137	191	84	0.44	211	0.013	0.003	0.0018	0.0002	-0.09	0.060	0.015	13.3	3.0	11.59	0.95	180	440	12.9	0.6

Table D-5: Zircon LA-ICP-MS U-Pb Isotopic Data and Ages: HP14-06 (IGSN: IEKHP0600[a]): Bentonite of the Calvert mine, Norton County (435374, 4410586)[b]

					Corrected Isotopic Ratios							Ages (Ma)[j]							
Grain #[c]	U[d] [ppm]	Th[d] [ppm]	Th/U	eU[e] [ppm]	$^{207}Pb/^{235}U$[f]	±2s[g]	$^{206}Pb/^{238}U$[f]	±2s[g]	Rho[h]	$^{207}Pb/^{206}Pb$[i]	±2s[g]	$^{207}Pb/^{235}U$	±2s	$^{206}Pb/^{238}U$	±2s	$^{207}Pb/^{206}Pb$	±2s	Disc. %[k]	Wtd. Disc.[l]
138	398	177	0.44	440	0.037	0.003	0.0054	0.0002	0.25	0.049	0.004	36.6	2.7	34.9	1.3	170	150	4.6	0.6
139	360	242	0.67	417	0.030	0.003	0.0042	0.0002	-0.03	0.053	0.007	29.6	3.3	26.9	1.3	270	240	9.1	0.8
140	178	101	0.57	201	0.015	0.004	0.0018	0.0002	-0.15	0.060	0.017	14.8	3.8	11.8	1.2	370	500	20.3	0.8
141	113	44	0.39	123	0.046	0.007	0.0057	0.0004	0.09	0.056	0.010	45	7	36.9	2.5	360	310	17.8	1.1
142	418	255	0.60	478	0.012	0.002	0.0018	0.0001	0.13	0.050	0.009	11.7	2.0	11.72	0.61	100	280	-0.2	0.0
143	186	90	0.48	207	0.013	0.003	0.0018	0.0001	-0.10	0.054	0.012	12.8	2.7	11.51	0.87	200	370	10.1	0.5
144	66	48	0.71	77	0.029	0.008	0.0049	0.0003	0.19	0.039	0.011	29.8	7.8	31.3	2.2	-220	390	-5.0	-0.2
145	140	74	0.52	157	0.014	0.006	0.0018	0.0001	0.11	0.071	0.026	14.2	5.5	11.38	0.92	110	660	19.9	0.5
146	155	77	0.48	173	0.013	0.003	0.0018	0.0002	0.06	0.058	0.015	12.9	3.1	11.6	1.1	250	410	10.1	0.4
147	192	113	0.59	219	0.010	0.003	0.0018	0.0001	-0.03	0.051	0.014	10.3	2.8	11.50	0.87	-120	400	-11.7	-0.4
148	119	49	0.41	130	0.013	0.004	0.0017	0.0002	-0.04	0.055	0.021	12.5	4.3	10.7	1.1	-100	570	14.4	0.4
149	113	36	0.32	121	0.015	0.004	0.0018	0.0002	0.26	0.052	0.020	14.6	4.4	11.7	1.2	-50	520	19.9	0.7
150	238	128	0.53	268	0.011	0.002	0.0018	0.0001	0.30	0.047	0.009	11.5	2.3	11.66	0.72	50	320	-1.4	-0.1
151	246	128	0.51	276	0.013	0.003	0.0018	0.0002	-0.11	0.052	0.014	13.2	3.0	11.49	0.99	120	420	13.0	0.6
152	124	57	0.46	137	4.283	0.100	0.2982	0.0051	0.53	0.104	0.002	1688	19	1682	25	1702	32	0.4	0.8
153	101	66	0.66	116	1.870	0.053	0.1823	0.0037	0.34	0.074	0.002	1068	19	1079	20	1043	54	-1.0	-1.8
154	182	84	0.46	202	0.014	0.004	0.0020	0.0002	0.15	0.053	0.015	14.2	3.4	13.0	1.1	170	440	8.5	0.4
155	355	164	0.48	394	0.044	0.011	0.0055	0.0005	0.37	0.057	0.013	44	10	35.4	3.0	350	430	19.5	0.9
156	179	96	0.53	201	0.012	0.003	0.0019	0.0002	0.16	0.045	0.012	12.0	3.1	12.47	0.96	-210	390	-3.9	-0.2
157	329	258	0.78	390	0.029	0.003	0.0047	0.0002	-0.06	0.047	0.005	29.2	2.5	30.0	1.2	40	180	-2.7	-0.3
158	130	110	0.84	156	0.029	0.005	0.0041	0.0004	-0.10	0.057	0.012	29.2	5.2	26.3	2.2	260	350	9.9	0.6
159	137	56	0.40	150	0.011	0.003	0.0019	0.0002	-0.04	0.051	0.016	10.7	3.4	12.1	1.1	-110	440	-13.1	-0.4
160	189	88	0.46	210	0.013	0.003	0.0017	0.0001	-0.13	0.055	0.016	12.5	3.3	11.10	0.92	10	460	11.2	0.4
161	379	333	0.86	457	0.049	0.003	0.0062	0.0002	0.24	0.058	0.004	48.9	3.1	40.1	1.4	480	140	18.0	2.8
162	74	24	0.32	80	4.490	0.120	0.3137	0.0063	0.41	0.104	0.003	1731	22	1758	31	1699	45	-1.6	-1.9
163	146	63	0.42	161	0.013	0.006	0.0021	0.0002	-0.14	0.043	0.023	12.6	5.9	13.5	1.3	-160	690	-7.1	-0.2
164	123	41	0.32	132	2.434	0.088	0.1867	0.0049	0.38	0.096	0.003	1250	26	1103	26	1534	67	11.8	16.6
165	469	121	0.25	497	0.093	0.005	0.0138	0.0004	0.32	0.049	0.002	90.6	4.5	88.2	2.4	185	99	2.6	0.5
166	302	176	0.60	343	0.039	0.005	0.0056	0.0002	-0.04	0.050	0.006	38.3	4.4	35.8	1.6	210	220	6.5	0.6
167	127	70	0.54	144	0.018	0.005	0.0019	0.0002	0.26	0.061	0.020	18.1	4.8	11.9	1.3	400	530	34.3	1.3
168	164	85	0.51	184	0.016	0.005	0.0019	0.0002	0.17	0.057	0.017	16	5	12.0	1.2	340	510	25.0	0.8
169	120	76	0.64	138	0.008	0.004	0.0016	0.0002	0.14	0.040	0.021	7.9	3.7	10.2	1.1	-620	600	-29.1	-0.6
170	129	52	0.39	141	0.016	0.005	0.0019	0.0002	0.22	0.058	0.018	15.8	4.6	12.4	1.0	420	500	21.5	0.7
171	107	42	0.39	117	0.017	0.005	0.0020	0.0002	-0.03	0.066	0.021	17.1	5.4	12.8	1.3	360	570	25.1	0.8

Table D-5: Zircon LA-ICP-MS U-Pb Isotopic Data and Ages: HP14-06 (IGSN: IEKHP0600[a]): Bentonite of the Calvert mine, Norton County (435374, 4410586)[b]

					Corrected Isotopic Ratios							Ages (Ma)[j]							
Grain #[c]	U[d] [ppm]	Th[d] [ppm]	Th/U	eU[e] [ppm]	$^{207}Pb/^{235}U^f$	±2s[g]	$^{206}Pb/^{238}U^f$	±2s[g]	Rho[h]	$^{207}Pb/^{206}Pb^i$	±2s[g]	$^{207}Pb/^{235}U$	±2s	$^{206}Pb/^{238}U$	±2s	$^{207}Pb/^{206}Pb$	±2s	Disc. %[k]	Wtd. Disc.[l]
172	45	18	0.40	49	1.820	0.081	0.1751	0.0052	0.50	0.077	0.003	1049	29	1039	28	1105	86	1.0	2.4
173	**210**	**110**	**0.51**	**236**	**0.011**	**0.003**	**0.0017**	**0.0001**	**-0.28**	**0.047**	**0.012**	**11.7**	**2.7**	**10.93**	**0.76**	**10**	**390**	**6.6**	**0.3**
174	173	138	0.78	206	0.081	0.006	0.0119	0.0004	0.19	0.050	0.004	79.1	5.5	76.3	2.6	230	150	3.5	0.5
175	213	77	0.36	231	4.410	0.120	0.2989	0.0091	0.76	0.107	0.002	1715	22	1684	45	1748	32	1.8	1.4
176	**151**	**53**	**0.34**	**163**	**0.015**	**0.004**	**0.0020**	**0.0003**	**0.01**	**0.068**	**0.022**	**15**	**4**	**12.9**	**2.0**	**560**	**540**	**14.0**	**0.5**
177	**141**	**51**	**0.36**	**153**	**0.014**	**0.004**	**0.0019**	**0.0002**	**-0.02**	**0.063**	**0.021**	**13.6**	**4.1**	**11.9**	**1.2**	**250**	**530**	**12.5**	**0.4**
178	123	51	0.40	135	2.067	0.066	0.1959	0.0057	0.62	0.077	0.002	1134	22	1152	31	1094	51	-1.6	-1.9
179	51	33	0.63	58	1.910	0.083	0.1787	0.0045	0.21	0.077	0.003	1085	30	1059	25	1124	81	2.4	2.6
180	**190**	**107**	**0.56**	**215**	**0.013**	**0.003**	**0.0018**	**0.0002**	**0.00**	**0.051**	**0.015**	**12.6**	**3.2**	**11.5**	**1.0**	**140**	**450**	**8.7**	**0.3**
181	**129**	**50**	**0.36**	**141**	**0.016**	**0.004**	**0.0020**	**0.0002**	**0.11**	**0.052**	**0.014**	**15.6**	**4.1**	**12.90**	**0.97**	**130**	**450**	**17.3**	**0.7**
182	**137**	**62**	**0.44**	**151**	**0.011**	**0.003**	**0.0019**	**0.0002**	**-0.06**	**0.044**	**0.015**	**10.5**	**3.4**	**12.1**	**1.0**	**-110**	**430**	**-15.2**	**-0.5**
183	**147**	**66**	**0.44**	**163**	**0.016**	**0.005**	**0.0018**	**0.0002**	**-0.01**	**0.056**	**0.019**	**15.8**	**5.1**	**11.7**	**1.3**	**290**	**570**	**25.9**	**0.8**
184	**215**	**124**	**0.58**	**244**	**0.014**	**0.003**	**0.0018**	**0.0001**	**0.09**	**0.057**	**0.014**	**13.5**	**3.1**	**11.58**	**0.92**	**270**	**440**	**14.2**	**0.6**
185	216	134	0.62	247	0.055	0.005	0.0080	0.0002	0.33	0.049	0.004	54	5	51.2	1.5	190	170	5.2	0.6
186	**137**	**62**	**0.44**	**152**	**0.019**	**0.005**	**0.0021**	**0.0002**	**0.30**	**0.060**	**0.016**	**18.9**	**4.6**	**13.5**	**1.3**	**640**	**420**	**28.6**	**1.2**
187	**147**	**64**	**0.44**	**162**	**0.018**	**0.006**	**0.0021**	**0.0002**	**0.20**	**0.061**	**0.021**	**18.2**	**5.9**	**13.4**	**1.4**	**210**	**570**	**26.4**	**0.8**
188	761	142	0.19	794	0.094	0.003	0.0126	0.0003	0.22	0.055	0.002	91.3	3.2	80.7	1.6	386	86	11.6	3.3
189	**155**	**82**	**0.53**	**174**	**0.015**	**0.004**	**0.0018**	**0.0002**	**0.22**	**0.061**	**0.020**	**14.7**	**4.3**	**11.7**	**1.1**	**220**	**520**	**20.4**	**0.7**
190	154	60	0.36	168	0.035	0.005	0.0051	0.0002	0.01	0.051	0.007	35.2	4.6	32.6	1.4	200	230	7.4	0.6
191	53	16	0.29	56	1.923	0.067	0.1823	0.0044	0.36	0.075	0.003	1092	23	1079	24	1071	68	1.2	-0.3
192	**163**	**86**	**0.53**	**183**	**0.013**	**0.004**	**0.0019**	**0.0002**	**-0.10**	**0.050**	**0.014**	**13.2**	**3.5**	**12.5**	**1.1**	**10**	**440**	**5.3**	**0.2**
193	**140**	**65**	**0.47**	**155**	**0.011**	**0.004**	**0.0018**	**0.0002**	**-0.02**	**0.046**	**0.016**	**11.2**	**3.6**	**11.4**	**1.0**	**-160**	**480**	**-1.8**	**-0.1**
194	**156**	**66**	**0.43**	**171**	**0.014**	**0.004**	**0.0018**	**0.0002**	**0.04**	**0.056**	**0.017**	**13.9**	**3.8**	**11.57**	**0.97**	**340**	**490**	**16.8**	**0.6**
195	**117**	**48**	**0.41**	**128**	**0.012**	**0.004**	**0.0019**	**0.0002**	**-0.02**	**0.059**	**0.021**	**11.7**	**3.8**	**12.2**	**1.3**	**10**	**550**	**-4.3**	**-0.1**
196	**270**	**143**	**0.53**	**304**	**0.014**	**0.003**	**0.0018**	**0.0001**	**0.12**	**0.055**	**0.011**	**13.8**	**2.7**	**11.86**	**0.80**	**210**	**340**	**14.1**	**0.7**
197	**129**	**51**	**0.39**	**141**	**0.014**	**0.005**	**0.0017**	**0.0002**	**-0.13**	**0.064**	**0.024**	**13.9**	**4.5**	**11.2**	**1.3**	**180**	**550**	**19.4**	**0.6**
198	137	76	0.56	155	0.029	0.005	0.0047	0.0003	-0.11	0.049	0.008	28.7	4.4	30.0	1.9	40	270	-4.5	-0.3
199	113	99	0.90	136	0.036	0.006	0.0057	0.0003	-0.01	0.047	0.008	35.6	5.8	36.3	2.0	70	280	-2.0	-0.1
200	200	52	0.26	212	3.220	0.081	0.2493	0.0050	0.54	0.092	0.002	1460	19	1434	26	1483	37	1.8	1.9
201	**173**	**96**	**0.55**	**196**	**0.011**	**0.003**	**0.0018**	**0.0001**	**0.01**	**0.045**	**0.012**	**11**	**3**	**11.45**	**0.87**	**0**	**410**	**-4.1**	**-0.2**
202	259	117	0.45	287	0.031	0.003	0.0049	0.0002	0.22	0.048	0.005	31.1	3.1	31.2	1.4	130	180	-0.3	0.0
203	**97**	**37**	**0.38**	**106**	**0.016**	**0.006**	**0.0017**	**0.0002**	**-0.12**	**0.076**	**0.035**	**16.1**	**6.2**	**10.8**	**1.3**	**110**	**770**	**32.9**	**0.9**
204	**180**	**93**	**0.52**	**202**	**0.013**	**0.003**	**0.0017**	**0.0002**	**0.10**	**0.057**	**0.015**	**12.6**	**3.4**	**10.81**	**0.96**	**180**	**460**	**14.2**	**0.5**
205	72	34	0.47	80	0.070	0.010	0.0115	0.0005	-0.05	0.048	0.007	69.2	8.8	73.9	3.4	80	250	-6.8	-0.5

Table D-5: Zircon LA-ICP-MS U-Pb Isotopic Data and Ages: HP14-06 (IGSN: IEKHP0600[a]): Bentonite of the Calvert mine, Norton County (435374, 4410586)[b]

					Corrected Isotopic Ratios							Ages (Ma)[j]							
Grain #[c]	U[d] [ppm]	Th[d] [ppm]	Th/U	eU[e] [ppm]	$^{207}Pb/^{235}U$[f]	±2s[g]	$^{206}Pb/^{238}U$[f]	±2s[g]	Rho[h]	$^{207}Pb/^{206}Pb$[i]	±2s[g]	$^{207}Pb/^{235}U$	±2s	$^{206}Pb/^{238}U$	±2s	$^{207}Pb/^{206}Pb$	±2s	Disc. %[k]	Wtd. Disc.[l]
206	**217**	**113**	**0.52**	**243**	**0.013**	**0.003**	**0.0017**	**0.0001**	**0.17**	**0.055**	**0.012**	**12.6**	**2.6**	**11.05**	**0.87**	**260**	**360**	**12.3**	**0.6**
207	64	13	0.20	67	0.234	0.020	0.0319	0.0012	0.12	0.053	0.005	212	16	202.2	7.4	270	170	4.6	0.6
208	**231**	**116**	**0.50**	**258**	**0.014**	**0.003**	**0.0018**	**0.0001**	**0.03**	**0.056**	**0.014**	**13.8**	**3.3**	**11.77**	**0.90**	**190**	**410**	**14.7**	**0.6**
209	251	162	0.64	289	0.030	0.003	0.0047	0.0002	0.08	0.047	0.005	30.2	2.9	30.2	1.1	110	180	0.0	0.0
210	89	54	0.62	102	0.036	0.006	0.0053	0.0003	0.13	0.050	0.009	35.3	5.6	33.7	2.0	230	280	4.5	0.3
211	185	52	0.30	197	1.883	0.046	0.1813	0.0032	0.51	0.076	0.001	1073	16	1074	17	1088	38	-0.1	0.8
212	286	92	0.33	307	0.101	0.006	0.0147	0.0004	0.21	0.050	0.003	97.5	5.8	94.1	2.7	160	120	3.5	0.6
213	182	86	0.46	202	0.018	0.004	0.0018	0.0002	0.13	0.068	0.016	17.6	3.9	11.58	0.96	510	450	34.2	1.5
214	123	77	0.62	141	0.040	0.009	0.0051	0.0004	-0.10	0.059	0.013	41	9	32.8	2.5	540	410	20.0	0.9
215	**99**	**48**	**0.48**	**110**	**0.013**	**0.004**	**0.0018**	**0.0002**	**0.07**	**0.068**	**0.025**	**13.3**	**4.3**	**11.8**	**1.5**	**250**	**610**	**11.3**	**0.3**
216	104	88	0.82	124	1.909	0.050	0.1828	0.0047	0.40	0.076	0.002	1082	18	1082	26	1108	53	0.0	1.0
217	**192**	**247**	**1.27**	**250**	**0.008**	**0.004**	**0.0018**	**0.0001**	**-0.14**	**0.049**	**0.020**	**7.6**	**3.8**	**11.61**	**0.74**	**-250**	**520**	**-52.8**	**-1.1**
218	**152**	**73**	**0.48**	**169**	**0.013**	**0.003**	**0.0017**	**0.0002**	**0.17**	**0.053**	**0.015**	**13.0**	**3.3**	**11.1**	**1.0**	**250**	**440**	**14.6**	**0.6**
219	**79**	**36**	**0.46**	**87**	**0.013**	**0.006**	**0.0019**	**0.0002**	**-0.18**	**0.067**	**0.031**	**12.5**	**5.6**	**12.0**	**1.4**	**40**	**700**	**4.0**	**0.1**
220	59	36	0.59	68	2.089	0.071	0.1879	0.0042	0.23	0.080	0.002	1142	23	1110	23	1188	61	2.8	3.4
221	**214**	**115**	**0.54**	**241**	**0.009**	**0.002**	**0.0018**	**0.0001**	**-0.07**	**0.041**	**0.010**	**8.7**	**2.3**	**11.44**	**0.55**	**-320**	**340**	**-31.5**	**-1.2**
222	93	107	1.15	118	0.038	0.007	0.0058	0.0003	-0.09	0.047	0.008	37.6	6.3	37.0	2.2	110	280	1.6	0.1
223	1053	84	0.08	1073	4.433	0.087	0.3093	0.0060	0.82	0.104	0.001	1717	16	1736	30	1691	19	-1.1	-1.5
225	**100**	**34**	**0.34**	**108**	**0.011**	**0.006**	**0.0016**	**0.0002**	**0.15**	**0.055**	**0.028**	**10.9**	**5.5**	**10.2**	**1.4**	**-140**	**740**	**6.4**	**0.1**
226	406	196	0.50	452	0.045	0.004	0.0062	0.0003	-0.11	0.052	0.006	44.1	4.2	39.7	1.8	230	190	10.0	1.0
227	**237**	**127**	**0.52**	**267**	**0.013**	**0.002**	**0.0020**	**0.0001**	**0.02**	**0.051**	**0.010**	**13.5**	**2.4**	**12.70**	**0.82**	**130**	**330**	**5.9**	**0.3**
228	358	160	0.45	396	0.028	0.002	0.0043	0.0002	-0.07	0.050	0.005	28.7	2.2	27.3	1.2	150	180	4.9	0.6
229	**121**	**69**	**0.57**	**137**	**0.014**	**0.004**	**0.0019**	**0.0002**	**-0.03**	**0.055**	**0.018**	**13.8**	**3.8**	**12.4**	**1.2**	**220**	**480**	**10.1**	**0.4**
230	75	36	0.47	83	0.086	0.012	0.0121	0.0006	0.00	0.051	0.007	84	11	77.8	4.1	150	230	7.4	0.6
231	**154**	**80**	**0.52**	**173**	**0.015**	**0.004**	**0.0018**	**0.0002**	**0.08**	**0.049**	**0.014**	**15.3**	**3.6**	**11.42**	**0.95**	**270**	**450**	**25.4**	**1.1**
232	408	85	0.21	428	0.040	0.003	0.0066	0.0002	-0.07	0.045	0.003	40.0	2.8	42.5	1.2	-10	140	-6.3	-0.9
233	358	31	0.08	365	3.109	0.066	0.2511	0.0044	0.72	0.091	0.001	1433	16	1444	23	1442	26	-0.8	-0.1
234	**202**	**87**	**0.43**	**223**	**0.012**	**0.003**	**0.0016**	**0.0001**	**0.12**	**0.055**	**0.015**	**11.9**	**2.9**	**10.31**	**0.79**	**370**	**440**	**13.4**	**0.5**
235	474	201	0.44	521	3.310	0.130	0.2191	0.0051	0.33	0.108	0.004	1482	29	1276	27	1759	70	13.9	17.9
236	**115**	**49**	**0.42**	**127**	**0.014**	**0.005**	**0.0017**	**0.0001**	**-0.13**	**0.067**	**0.022**	**13.7**	**4.9**	**10.9**	**0.9**	**340**	**620**	**20.4**	**0.6**
237	**156**	**59**	**0.38**	**170**	**0.016**	**0.005**	**0.0017**	**0.0002**	**0.22**	**0.067**	**0.024**	**15.9**	**4.7**	**11.1**	**1.2**	**480**	**570**	**30.2**	**1.0**
238	228	124	0.54	257	0.039	0.006	0.0052	0.0003	0.31	0.054	0.008	38.6	5.9	33.6	1.8	310	280	13.0	0.8
239	92	54	0.60	104	1.921	0.054	0.1812	0.0034	0.54	0.077	0.002	1091	18	1073	19	1112	47	1.6	2.1
240	**189**	**103**	**0.53**	**213**	**0.012**	**0.002**	**0.0018**	**0.0001**	**-0.04**	**0.051**	**0.011**	**11.9**	**2.4**	**11.33**	**0.92**	**-10**	**340**	**4.8**	**0.2**

Table D-5: Zircon LA-ICP-MS U-Pb Isotopic Data and Ages: HP14-06 (IGSN: IEKHP0600[a]): Bentonite of the Calvert mine, Norton County (435374, 4410586)[b]

Grain #[c]	U[d] [ppm]	Th[d] [ppm]	Th/U	eU[e] [ppm]	Corrected Isotopic Ratios							Ages (Ma)[j]						Disc. %[k]	Wtd. Disc.[l]
					$^{207}Pb/^{235}U$[f]	±2s[g]	$^{206}Pb/^{238}U$[f]	±2s[g]	Rho[h]	$^{207}Pb/^{206}Pb$[i]	±2s[g]	$^{207}Pb/^{235}U$	±2s	$^{206}Pb/^{238}U$	±2s	$^{207}Pb/^{206}Pb$	±2s		
241	**81**	**28**	**0.34**	**88**	**0.014**	**0.007**	**0.0019**	**0.0003**	**-0.06**	**0.063**	**0.032**	**14.1**	**6.8**	**12.5**	**1.7**	**0**	**760**	**11.3**	**0.2**
242	343	150	0.43	378	0.030	0.003	0.0043	0.0002	0.09	0.051	0.005	29.7	2.9	27.7	1.0	160	190	6.9	0.7
243	**124**	**62**	**0.50**	**139**	**0.012**	**0.004**	**0.0020**	**0.0002**	**0.09**	**0.047**	**0.020**	**12.4**	**4.1**	**12.6**	**1.3**	**-230**	**490**	**-1.6**	**0.0**
244	**121**	**48**	**0.38**	**132**	**0.013**	**0.004**	**0.0017**	**0.0002**	**0.41**	**0.052**	**0.016**	**13**	**4**	**11.1**	**1.1**	**70**	**470**	**14.6**	**0.5**
245	**182**	**89**	**0.48**	**203**	**0.017**	**0.004**	**0.0020**	**0.0002**	**-0.04**	**0.059**	**0.015**	**16.9**	**4.1**	**13.1**	**1.0**	**370**	**450**	**22.5**	**0.9**
246	83	54	0.62	95	0.081	0.009	0.0115	0.0006	0.13	0.049	0.005	78.2	8.5	73.8	3.6	150	200	5.6	0.5
247	243	140	0.56	276	0.246	0.010	0.0347	0.0008	0.18	0.051	0.002	223	8	220	5	232	91	1.4	0.4
248	**480**	**274**	**0.50**	**544**	**0.011**	**0.002**	**0.0019**	**0.0001**	**0.31**	**0.047**	**0.006**	**11.5**	**1.6**	**12.03**	**0.65**	**140**	**230**	**-4.6**	**-0.3**
249	**140**	**65**	**0.46**	**156**	**0.013**	**0.003**	**0.0018**	**0.0001**	**0.18**	**0.055**	**0.014**	**12.7**	**3.3**	**11.25**	**0.92**	**180**	**430**	**11.4**	**0.4**
250	693	6	0.01	695	4.363	0.094	0.3035	0.0062	0.75	0.105	0.001	1707	18	1707	31	1717	25	0.0	0.3
251	**169**	**88**	**0.50**	**190**	**0.012**	**0.003**	**0.0019**	**0.0002**	**0.00**	**0.044**	**0.011**	**11.6**	**2.7**	**12.12**	**0.94**	**-120**	**360**	**-4.5**	**-0.2**
252	**113**	**47**	**0.42**	**124**	**0.012**	**0.004**	**0.0019**	**0.0002**	**0.00**	**0.052**	**0.019**	**12.5**	**4.6**	**12.3**	**1.1**	**-90**	**550**	**1.6**	**0.0**
253	**127**	**46**	**0.37**	**138**	**0.014**	**0.003**	**0.0020**	**0.0002**	**0.12**	**0.049**	**0.014**	**13.7**	**3.4**	**12.74**	**0.97**	**20**	**420**	**7.0**	**0.3**
254	174	81	0.46	193	0.043	0.006	0.0022	0.0002	0.34	0.155	0.021	42.9	5.4	13.9	1.2	2230	240	67.6	5.4
255	**155**	**72**	**0.47**	**172**	**0.015**	**0.005**	**0.0018**	**0.0002**	**0.00**	**0.061**	**0.021**	**15.2**	**4.8**	**11.59**	**0.94**	**150**	**570**	**23.8**	**0.8**
256	639	255	0.40	699	0.098	0.004	0.0149	0.0004	0.31	0.048	0.002	94.6	3.7	95.4	2.5	102	76	-0.8	-0.2
257	237	149	0.61	272	0.041	0.004	0.0062	0.0003	0.07	0.048	0.005	41.5	3.8	39.6	1.8	120	180	4.6	0.5
258	**138**	**49**	**0.37**	**149**	**0.015**	**0.004**	**0.0017**	**0.0001**	**0.07**	**0.060**	**0.018**	**15**	**4**	**11.11**	**0.92**	**300**	**480**	**25.9**	**1.0**
259	821	442	0.53	925	0.028	0.002	0.0043	0.0001	0.20	0.047	0.003	27.5	1.6	27.41	0.84	110	120	0.3	0.1
260	**171**	**89**	**0.51**	**192**	**0.014**	**0.003**	**0.0018**	**0.0001**	**-0.08**	**0.055**	**0.014**	**13.5**	**3.1**	**11.73**	**0.83**	**30**	**400**	**13.1**	**0.6**
261	55	25	0.46	61	0.045	0.010	0.0056	0.0005	-0.03	0.055	0.015	44	10	35.9	3.2	520	470	18.4	0.8
262	53	25	0.49	58	1.972	0.082	0.1806	0.0057	0.37	0.079	0.004	1103	28	1070	31	1179	91	3.0	3.5
263	553	292	0.54	622	0.047	0.003	0.0070	0.0002	0.07	0.048	0.003	46.5	3.0	44.8	1.2	150	140	3.7	0.6
264	79	31	0.40	86	1.891	0.057	0.1801	0.0041	0.46	0.077	0.002	1075	20	1067	22	1102	51	0.7	1.6
265	136	45	0.34	146	0.673	0.021	0.0817	0.0016	0.02	0.059	0.002	522	13	506	9	574	80	3.1	1.2
266	**98**	**41**	**0.42**	**108**	**0.015**	**0.004**	**0.0019**	**0.0002**	**-0.02**	**0.052**	**0.019**	**14.6**	**4.4**	**12.5**	**1.3**	**180**	**480**	**14.4**	**0.5**
267	**160**	**81**	**0.49**	**179**	**0.017**	**0.005**	**0.0019**	**0.0002**	**0.03**	**0.063**	**0.018**	**17.3**	**4.5**	**12.4**	**1.0**	**540**	**510**	**28.3**	**1.1**
268	280	142	0.50	314	0.048	0.004	0.0073	0.0002	0.08	0.049	0.004	47.8	4.0	46.6	1.5	150	160	2.5	0.3
269	60	41	0.70	69	1.918	0.058	0.1818	0.0039	0.42	0.076	0.002	1087	20	1076	21	1086	55	1.0	0.5
270	32	33	1.03	39	0.039	0.019	0.0054	0.0007	-0.09	0.073	0.031	38	18	34.8	4.3	120	740	8.4	0.2
271	177	54	0.28	190	4.400	0.110	0.3044	0.0084	0.71	0.104	0.002	1710	22	1711	42	1696	38	-0.1	-0.4
272	73	36	0.46	82	1.908	0.062	0.1826	0.0044	0.26	0.076	0.002	1083	21	1081	24	1099	58	0.2	0.8
273	**120**	**49**	**0.42**	**131**	**0.013**	**0.004**	**0.0018**	**0.0002**	**0.23**	**0.050**	**0.017**	**12.9**	**3.9**	**11.5**	**1.1**	**150**	**460**	**10.9**	**0.4**
274	53	19	0.36	57	4.350	0.160	0.3090	0.0100	0.73	0.103	0.003	1700	30	1733	51	1676	49	-1.9	-1.1

Table D-5: Zircon LA-ICP-MS U-Pb Isotopic Data and Ages: HP14-06 (IGSN: IEKHP0600[a]): Bentonite of the Calvert mine, Norton County (435374, 4410586)[b]

					Corrected Isotopic Ratios							Ages (Ma)[j]							
Grain #[c]	U[d] [ppm]	Th[d] [ppm]	Th/U	eU[e] [ppm]	$^{207}Pb/^{235}U$[f]	±2s[g]	$^{206}Pb/^{238}U$[f]	±2s[g]	Rho[h]	$^{207}Pb/^{206}Pb$[i]	±2s[g]	$^{207}Pb/^{235}U$	±2s	$^{206}Pb/^{238}U$	±2s	$^{207}Pb/^{206}Pb$	±2s	Disc. %[k]	Wtd. Disc.[l]
275	**107**	**40**	**0.37**	**116**	**0.014**	**0.005**	**0.0017**	**0.0002**	**-0.04**	**0.068**	**0.027**	**13.8**	**5.3**	**11.0**	**1.2**	**170**	**650**	**20.3**	**0.5**
276	**256**	**181**	**0.70**	**298**	**0.013**	**0.003**	**0.0017**	**0.0001**	**0.06**	**0.052**	**0.011**	**13.3**	**2.7**	**11.13**	**0.61**	**150**	**330**	**16.3**	**0.8**
277	104	122	1.18	133	0.022	0.005	0.0021	0.0002	0.15	0.080	0.016	22.2	5.0	13.7	1.4	1010	400	38.3	1.7
278	208	70	0.32	225	0.062	0.006	0.0098	0.0003	0.07	0.047	0.005	60.6	5.4	63.1	2.2	60	180	-4.1	-0.5
279	**199**	**95**	**0.47**	**222**	**0.012**	**0.004**	**0.0018**	**0.0002**	**0.00**	**0.049**	**0.013**	**11.6**	**3.2**	**11.74**	**0.97**	**-150**	**370**	**-1.2**	**0.0**
280	**235**	**101**	**0.44**	**259**	**0.014**	**0.004**	**0.0018**	**0.0002**	**0.00**	**0.058**	**0.015**	**14.1**	**3.5**	**11.38**	**0.96**	**300**	**460**	**19.3**	**0.8**
281	**186**	**92**	**0.50**	**207**	**0.014**	**0.003**	**0.0018**	**0.0001**	**0.05**	**0.058**	**0.013**	**14.5**	**3.2**	**11.40**	**0.88**	**260**	**400**	**21.4**	**1.0**
282	242	133	0.55	273	0.034	0.008	0.0021	0.0002	0.11	0.107	0.027	33.3	7.5	13.3	1.0	1530	470	60.1	2.7
283	183	97	0.54	206	1.891	0.051	0.1813	0.0044	0.42	0.076	0.002	1076	18	1073	24	1089	53	0.3	0.7
284	79	29	0.41	85	4.141	0.094	0.2976	0.0061	0.49	0.102	0.002	1662	19	1678	30	1652	32	-1.0	-0.9
285	277	181	0.49	320	0.038	0.004	0.0055	0.0002	0.18	0.050	0.005	37.6	3.4	35.6	1.4	180	180	5.3	0.6
286	**212**	**112**	**0.51**	**238**	**0.014**	**0.003**	**0.0018**	**0.0002**	**0.06**	**0.057**	**0.013**	**14**	**3**	**11.59**	**0.93**	**470**	**410**	**17.2**	**0.8**
287	208	152	0.73	244	0.046	0.004	0.0072	0.0002	0.00	0.047	0.004	45.2	3.8	46.3	1.5	70	170	-2.4	-0.3
288	86	50	0.58	97	1.908	0.053	0.1806	0.0034	0.27	0.077	0.002	1084	19	1070	18	1118	47	1.3	2.7
289	93	38	0.40	102	2.290	0.067	0.2042	0.0054	0.54	0.081	0.002	1207	21	1197	29	1212	51	0.8	0.5
290	**219**	**124**	**0.56**	**248**	**0.012**	**0.002**	**0.0017**	**0.0001**	**0.18**	**0.050**	**0.011**	**11.6**	**2.4**	**10.91**	**0.79**	**80**	**370**	**5.9**	**0.3**
291	132	75	0.57	149	3.197	0.072	0.2510	0.0043	0.45	0.093	0.002	1455	18	1443	22	1478	33	0.8	1.6
292	**185**	**105**	**0.56**	**210**	**0.016**	**0.006**	**0.0017**	**0.0002**	**-0.35**	**0.081**	**0.035**	**15.5**	**5.5**	**10.8**	**1.3**	**380**	**670**	**30.3**	**0.9**
293	**97**	**31**	**0.33**	**104**	**0.018**	**0.005**	**0.0020**	**0.0002**	**0.05**	**0.080**	**0.033**	**17.9**	**5.4**	**12.6**	**1.4**	**330**	**660**	**29.6**	**1.0**
294	**231**	**110**	**0.48**	**257**	**0.014**	**0.004**	**0.0019**	**0.0002**	**-0.03**	**0.062**	**0.019**	**14.4**	**4.3**	**12.3**	**1.4**	**270**	**560**	**14.6**	**0.5**
295	38	25	0.64	44	1.096	0.089	0.0680	0.0023	0.27	0.117	0.009	751	42	424	14	1880	150	43.5	7.8
296	**217**	**110**	**0.52**	**242**	**0.014**	**0.004**	**0.0018**	**0.0001**	**-0.03**	**0.064**	**0.019**	**13.8**	**4.1**	**11.44**	**0.90**	**410**	**550**	**17.1**	**0.6**
297	317	161	0.51	355	0.037	0.003	0.0056	0.0002	0.13	0.047	0.004	37.2	3.2	35.8	1.0	130	160	3.9	0.5
298	**122**	**60**	**0.49**	**136**	**0.016**	**0.006**	**0.0017**	**0.0002**	**0.23**	**0.066**	**0.024**	**16**	**6**	**10.7**	**1.5**	**500**	**630**	**33.1**	**0.9**
299	**127**	**52**	**0.41**	**139**	**0.018**	**0.005**	**0.0019**	**0.0001**	**0.17**	**0.058**	**0.018**	**17.4**	**4.8**	**11.98**	**0.86**	**160**	**510**	**31.1**	**1.1**
300	**117**	**43**	**0.36**	**127**	**0.013**	**0.004**	**0.0020**	**0.0002**	**-0.17**	**0.050**	**0.017**	**12.9**	**3.9**	**13.0**	**1.3**	**120**	**490**	**-0.8**	**0.0**
301	437	239	0.51	493	0.037	0.003	0.0055	0.0002	0.26	0.049	0.004	36.9	2.6	35.5	1.3	140	140	3.8	0.5
302	96	49	0.51	107	1.900	0.059	0.1822	0.0042	0.59	0.076	0.002	1078	21	1078	23	1087	47	0.0	0.4
303	315	182	0.56	358	3.137	0.065	0.2489	0.0044	0.58	0.091	0.001	1444	16	1432	23	1446	30	0.8	0.6
304	99	15	0.16	102	0.079	0.009	0.0115	0.0005	-0.01	0.053	0.007	76.6	8.7	73.6	3.4	290	230	3.9	0.3
305	**115**	**52**	**0.45**	**127**	**0.019**	**0.007**	**0.0018**	**0.0003**	**0.12**	**0.077**	**0.033**	**18.8**	**6.4**	**11.4**	**1.7**	**950**	**650**	**39.4**	**1.2**
306	171	82	0.50	190	1.842	0.044	0.1762	0.0033	0.43	0.076	0.002	1059	16	1046	18	1074	40	1.2	1.6
307	46	22	0.47	51	1.845	0.072	0.1790	0.0051	0.37	0.076	0.003	1061	25	1061	28	1111	78	0.0	1.8
308	100	48	0.48	111	3.101	0.077	0.2471	0.0056	0.43	0.091	0.002	1431	19	1426	28	1452	44	0.3	0.9

Table D-5: Zircon LA-ICP-MS U-Pb Isotopic Data and Ages: HP14-06 (IGSN: IEKHP0600[a]): Bentonite of the Calvert mine, Norton County (435374, 4410586)[b]

					Corrected Isotopic Ratios							Ages (Ma)[j]							
Grain #[c]	U[d] [ppm]	Th[d] [ppm]	Th/U	eU[e] [ppm]	$^{207}Pb/^{235}U$[f]	±2s[g]	$^{206}Pb/^{238}U$[f]	±2s[g]	Rho[h]	$^{207}Pb/^{206}Pb$[i]	±2s[g]	$^{207}Pb/^{235}U$	±2s	$^{206}Pb/^{238}U$	±2s	$^{207}Pb/^{206}Pb$	±2s	Disc. %[k]	Wtd. Disc.[l]
309	127	73	0.56	144	1.837	0.049	0.1755	0.0035	0.41	0.076	0.002	1057	18	1042	19	1100	48	1.4	3.1
310	169	91	0.54	191	1.896	0.045	0.1818	0.0039	0.47	0.077	0.002	1083	16	1076	21	1109	46	0.6	1.6
311	306	132	0.41	337	4.223	0.097	0.2948	0.0056	0.70	0.103	0.002	1676	19	1664	28	1670	26	0.7	0.2
312	120	52	0.45	133	4.305	0.094	0.3009	0.0057	0.53	0.103	0.002	1692	18	1695	28	1679	29	-0.2	-0.6
313	**191**	**88**	**0.46**	**211**	**0.013**	**0.003**	**0.0017**	**0.0001**	**0.08**	**0.055**	**0.013**	**13.3**	**3.1**	**11.01**	**0.83**	**350**	**420**	**17.2**	**0.7**
314	432	256	0.60	492	0.042	0.004	0.0060	0.0002	0.34	0.051	0.005	41.7	3.9	38.8	1.5	240	180	7.0	0.7
315	174	58	0.32	188	4.346	0.110	0.3009	0.0066	0.64	0.105	0.002	1701	21	1694	33	1717	32	0.4	0.7

[a]International Geo Sample Number (IGSN) registered in the SESAR database
[b]All locations reported as UTM coordinates using Zone 14 NAD 27
[c]Emboldened rows indicate the youngest measured concordant grains
[d]U and Th concentrations and Th/U ratios calculated relative to the GJ-1 zircon standard ID-TIMS values using 287 ± 76 ppm for U and 8.4 ± 2.6 ppm for Th (Jackson et al., 2004)
[e]Equivalent U defined by the equation: eU = U ppm + 0.235*Th ppm
[f]Corrected for U-Pb fractionation and background and normalized to the GJ-1 zircon standard ID-TIMS values: $^{207}Pb/^{235}U = 0.8093 \pm 0.0009$ and $^{206}Pb/^{238}U = 0.09761 \pm 0.00011$ (Jackson et al., 2004)
[g]Propagated uncertainty of internal uncertainties (2 SE) and within run reproducibility of GJ-1 (2 SE)
[h]Uncertainty correlation between $^{206}Pb/^{238}U$ and $^{207}Pb/^{235}U$ uncertainties
[i]Corrected for background and Pb isotopic fractionation using the GJ-1 zircon standard ID-TIMS value: $^{207}Pb/^{206}Pb = 0.06014 \pm 0.00001$ (Jackson et al., 2004)
[j]U-Pb ages calculated relative to the GJ-1 zircon standard
[k]Discordance defined as $[(^{207}Pb/^{235}U_{age} - ^{206}Pb/^{238}U_{age})/(^{207}Pb/^{235}U_{age})]*100$
[l]Uncertainty weighted age difference defined as $(^{207}Pb/^{235}U_{age} - ^{206}Pb/^{238}U_{age})/(^{207}Pb/^{235}U_{age\ uncertainty})$ for grains with $^{206}Pb/^{238}U$ ages <850 Ma and $(^{207}Pb/^{206}Pb_{age} - ^{206}Pb/^{238}U_{age})/(^{206}Pb/^{238}U_{age\ uncertainty})$ for grains with $^{206}Pb/^{238}U$ ages ≥850 Ma

Table D-6: Zircon LA-ICP-MS U-Pb Isotopic Data and Ages: HP14-07 (IGSN: IEKHP0700[a]): Vitric ash of the Calvert mine, Norton County (435540, 4410579)[b]

Grain #[c]	U[d] [ppm]	Th[d] [ppm]	Th/U	eU[e] [ppm]	Corrected Isotopic Ratios $^{207}Pb/^{235}U$[f]	±2s[g]	$^{206}Pb/^{238}U$[f]	±2s[g]	Rho[h]	$^{207}Pb/^{206}Pb$[i]	±2s[g]	Ages (Ma)[j] $^{207}Pb/^{235}U$	±2s	$^{206}Pb/^{238}U$	±2s	$^{207}Pb/^{206}Pb$	±2s	Disc. %[k]	Wtd. Disc.[l]
1	252	170	0.56	292	0.014	0.003	0.0019	0.0001	-0.03	0.054	0.012	14.2	2.9	12.04	0.79	230	370	15.2	0.7
2	61	34	0.56	69	0.015	0.006	0.0022	0.0003	-0.01	0.058	0.027	15	6	14.4	1.7	-10	590	4.6	0.1
3	105	48	0.46	116	0.019	0.004	0.0019	0.0002	0.07	0.079	0.019	18.9	4.2	12.2	1.0	780	460	35.4	1.6
4	114	172	1.50	154	0.014	0.004	0.0018	0.0001	0.02	0.054	0.015	14.0	3.7	11.39	0.84	270	410	18.6	0.7
5	150	84	0.50	170	0.011	0.003	0.0019	0.0002	-0.04	0.050	0.016	11.2	3.1	12.4	1.1	-240	410	-10.7	-0.4
6	113	42	0.38	122	0.013	0.004	0.0019	0.0002	-0.15	0.054	0.019	12.6	3.9	12.3	1.3	120	520	2.4	0.1
7	243	133	0.57	274	0.013	0.002	0.0018	0.0001	-0.06	0.056	0.011	13.4	2.4	11.63	0.86	350	340	13.2	0.7
8	201	101	0.48	225	0.013	0.003	0.0019	0.0001	-0.22	0.055	0.012	13.2	2.6	12.03	0.82	300	370	8.9	0.5
9	143	76	0.52	161	0.011	0.003	0.0018	0.0002	0.05	0.051	0.015	11	3	11.8	1.1	-110	400	-7.3	-0.3
10	127	53	0.43	139	0.011	0.003	0.0018	0.0002	-0.06	0.047	0.016	11.3	3.3	11.5	1.1	10	460	-1.8	-0.1
11	192	97	0.52	215	0.021	0.003	0.0018	0.0001	0.07	0.084	0.013	20.7	3.0	11.81	0.61	1060	290	42.9	3.0
12	106	41	0.39	116	0.013	0.004	0.0020	0.0002	-0.03	0.046	0.016	13.1	4.3	13	1	-180	480	0.8	0.0
13	253	144	0.57	286	0.012	0.002	0.0018	0.0001	-0.08	0.053	0.009	12.1	1.9	11.55	0.59	320	290	4.5	0.3
14	245	131	0.50	276	0.012	0.002	0.0018	0.0001	0.11	0.056	0.010	12.4	2.2	11.74	0.80	330	310	5.3	0.3
15	228	122	0.54	257	0.011	0.002	0.0017	0.0001	0.06	0.056	0.012	11.3	2.3	11.23	0.77	150	360	0.6	0.0
16	166	76	0.42	184	0.012	0.003	0.0019	0.0002	0.12	0.051	0.011	11.7	2.7	11.91	0.95	130	350	-1.8	-0.1
17	280	96	0.35	302	0.052	0.003	0.0077	0.0002	0.15	0.048	0.003	51.2	2.6	49.7	1.3	140	110	2.9	0.6
18	140	68	0.43	156	0.013	0.004	0.0017	0.0001	-0.10	0.053	0.016	12.9	3.6	11.21	0.91	180	460	13.1	0.5
19	136	64	0.46	152	0.012	0.003	0.0017	0.0001	-0.13	0.052	0.014	11.8	3.3	11.17	0.83	90	440	5.3	0.2
20	100	33	0.33	108	0.012	0.004	0.0018	0.0002	-0.12	0.053	0.018	11.9	3.6	11.4	1.1	20	450	4.2	0.1
21	138	58	0.42	152	0.012	0.003	0.0019	0.0002	-0.03	0.050	0.013	12.3	3.3	11.92	0.97	90	440	3.1	0.1
22	202	112	0.56	228	0.015	0.006	0.0017	0.0002	-0.25	0.065	0.026	14.7	5.6	10.7	1.2	190	660	27.2	0.7
23	205	103	0.51	229	0.013	0.003	0.0017	0.0002	0.03	0.055	0.015	12.8	3.3	11.13	0.98	270	450	13.0	0.5
24	136	53	0.38	149	0.013	0.003	0.0018	0.0002	-0.08	0.055	0.016	13.0	3.4	11.45	0.98	-10	470	11.9	0.5
25	112	50	0.44	124	0.010	0.004	0.0018	0.0002	0.10	0.040	0.019	10.1	4.1	11.55	0.99	-290	550	-14.4	-0.4
26	95	31	0.33	102	0.016	0.009	0.0018	0.0002	-0.02	0.072	0.034	12.6	5.6	11.8	1.2	-200	640	6.3	0.1
27	135	67	0.45	151	0.014	0.005	0.0019	0.0002	0.15	0.060	0.020	14.0	5.0	12.0	1.2	170	580	14.3	0.4
28	124	56	0.43	137	0.014	0.004	0.0018	0.0001	0.20	0.051	0.013	13.7	3.5	11.47	0.72	210	410	16.3	0.6
29	99	43	0.44	109	0.012	0.005	0.0019	0.0002	-0.08	0.056	0.029	11.8	4.9	12.0	1.5	-140	610	-1.7	0.0
30	79	28	0.35	86	0.011	0.004	0.0018	0.0002	0.01	0.056	0.023	10.9	4.0	11.7	1.3	30	590	-7.3	-0.2
31	97	37	0.39	106	0.015	0.005	0.0021	0.0004	0.28	0.054	0.017	15.3	4.5	13.4	2.3	360	500	12.4	0.4
32	112	37	0.33	121	0.013	0.004	0.0019	0.0002	0.14	0.049	0.017	12.5	4.0	12.1	1.1	-10	490	3.2	0.1
33	180	101	0.57	204	0.013	0.003	0.0019	0.0001	-0.20	0.051	0.012	12.9	2.8	12.09	0.83	120	380	6.3	0.3
34	93	36	0.38	102	0.015	0.008	0.0019	0.0002	0.23	0.058	0.028	14.5	7.6	12.1	1.5	130	810	16.6	0.3

Table D-6: Zircon LA-ICP-MS U-Pb Isotopic Data and Ages: HP14-07 (IGSN: IEKHP0700[a]): Vitric ash of the Calvert mine, Norton County (435540, 4410579)[b]

					Corrected Isotopic Ratios							Ages (Ma)[j]							
Grain #[c]	U[d] [ppm]	Th[d] [ppm]	Th/U	eU[e] [ppm]	$^{207}Pb/^{235}U$[f]	±2s[g]	$^{206}Pb/^{238}U$[f]	±2s[g]	Rho[h]	$^{207}Pb/^{206}Pb$[i]	±2s[g]	$^{207}Pb/^{235}U$	±2s	$^{206}Pb/^{238}U$	±2s	$^{207}Pb/^{206}Pb$	±2s	Disc. %[k]	Wtd. Disc.[l]
35	**213**	**107**	**0.51**	**238**	**0.013**	**0.003**	**0.0018**	**0.0001**	**-0.04**	**0.048**	**0.010**	**13.0**	**2.5**	**11.43**	**0.76**	**210**	**340**	**12.1**	**0.6**
36	214	114	0.55	241	0.015	0.003	0.0017	0.0002	0.15	0.068	0.017	15.4	3.4	11.1	1.2	640	440	27.9	1.3
37	**102**	**37**	**0.36**	**111**	**0.013**	**0.004**	**0.0019**	**0.0002**	**-0.05**	**0.051**	**0.015**	**12.7**	**3.5**	**12.1**	**1.1**	**210**	**450**	**4.7**	**0.2**
38	**155**	**85**	**0.55**	**175**	**0.010**	**0.003**	**0.0018**	**0.0001**	**0.18**	**0.046**	**0.012**	**10.1**	**2.6**	**11.50**	**0.85**	**-100**	**390**	**-13.9**	**-0.5**
39	**174**	**96**	**0.55**	**197**	**0.015**	**0.003**	**0.0020**	**0.0002**	**-0.13**	**0.055**	**0.013**	**14.8**	**3.0**	**12.9**	**1.2**	**300**	**400**	**12.8**	**0.6**
40	**252**	**147**	**0.58**	**286**	**0.013**	**0.002**	**0.0018**	**0.0001**	**0.06**	**0.053**	**0.009**	**12.7**	**2.1**	**11.77**	**0.75**	**280**	**310**	**7.3**	**0.4**
41	**159**	**71**	**0.43**	**176**	**0.013**	**0.003**	**0.0019**	**0.0001**	**0.06**	**0.052**	**0.011**	**13.6**	**2.8**	**12.17**	**0.86**	**80**	**360**	**10.5**	**0.5**
42	**198**	**100**	**0.52**	**222**	**0.012**	**0.002**	**0.0018**	**0.0001**	**-0.08**	**0.047**	**0.010**	**11.5**	**2.4**	**11.49**	**0.80**	**20**	**340**	**0.1**	**0.0**
43	227	127	0.55	257	0.015	0.003	0.0017	0.0001	0.00	0.068	0.012	15.4	2.7	10.95	0.72	670	330	28.9	1.6
44	**199**	**115**	**0.57**	**226**	**0.012**	**0.003**	**0.0017**	**0.0001**	**-0.14**	**0.058**	**0.013**	**12.5**	**2.7**	**11.12**	**0.70**	**360**	**390**	**11.0**	**0.5**
45	153	63	0.41	168	0.019	0.004	0.0019	0.0002	-0.06	0.082	0.018	18.6	3.6	11.9	1.0	900	440	36.0	1.9
46	**218**	**113**	**0.53**	**244**	**0.014**	**0.003**	**0.0019**	**0.0001**	**0.10**	**0.057**	**0.014**	**14.4**	**3.4**	**12.13**	**0.93**	**330**	**480**	**15.8**	**0.7**
47	**202**	**108**	**0.54**	**227**	**0.013**	**0.003**	**0.0017**	**0.0001**	**0.06**	**0.052**	**0.012**	**12.7**	**2.6**	**11.13**	**0.81**	**260**	**370**	**12.4**	**0.6**
48	**211**	**102**	**0.47**	**235**	**0.014**	**0.002**	**0.0019**	**0.0002**	**0.11**	**0.053**	**0.009**	**14.2**	**2.4**	**12.29**	**0.97**	**360**	**320**	**13.5**	**0.8**
49	**117**	**55**	**0.47**	**129**	**0.014**	**0.004**	**0.0019**	**0.0002**	**-0.14**	**0.061**	**0.020**	**14.1**	**4.2**	**12.2**	**1.1**	**290**	**550**	**13.5**	**0.5**
50	**145**	**65**	**0.43**	**160**	**0.012**	**0.003**	**0.0019**	**0.0001**	**0.01**	**0.048**	**0.015**	**12.3**	**3.3**	**12.34**	**0.80**	**-50**	**450**	**-0.3**	**0.0**
51	**171**	**76**	**0.45**	**189**	**0.009**	**0.003**	**0.0018**	**0.0002**	**-0.05**	**0.048**	**0.017**	**9.5**	**3.0**	**11.39**	**0.98**	**-140**	**480**	**-19.9**	**-0.6**
52	**189**	**95**	**0.48**	**211**	**0.014**	**0.003**	**0.0019**	**0.0001**	**0.04**	**0.056**	**0.013**	**13.8**	**2.9**	**11.92**	**0.93**	**240**	**390**	**13.6**	**0.6**
53	**124**	**47**	**0.37**	**135**	**0.011**	**0.003**	**0.0019**	**0.0002**	**-0.16**	**0.051**	**0.015**	**11.5**	**3.0**	**12.14**	**0.94**	**-150**	**400**	**-5.6**	**-0.2**
54	**126**	**64**	**0.50**	**141**	**0.012**	**0.003**	**0.0020**	**0.0002**	**-0.30**	**0.054**	**0.016**	**12.2**	**3.2**	**12.9**	**1.1**	**40**	**470**	**-5.7**	**-0.2**
55	**139**	**78**	**0.56**	**158**	**0.014**	**0.005**	**0.0018**	**0.0002**	**-0.10**	**0.053**	**0.019**	**13.7**	**4.5**	**11.37**	**0.99**	**100**	**560**	**17.0**	**0.5**
56	164	81	0.50	183	0.025	0.005	0.0019	0.0002	0.01	0.107	0.023	25.8	5.0	11.9	1.2	1340	450	53.9	2.8
57	196	102	0.51	220	0.032	0.004	0.0020	0.0001	0.12	0.122	0.017	32.1	4.3	12.60	0.88	1910	260	60.7	4.5
58	**216**	**115**	**0.53**	**243**	**0.013**	**0.003**	**0.0017**	**0.0001**	**-0.02**	**0.058**	**0.014**	**12.8**	**2.8**	**10.68**	**0.62**	**400**	**430**	**16.6**	**0.8**
59	**93**	**29**	**0.31**	**100**	**0.015**	**0.004**	**0.0017**	**0.0002**	**0.15**	**0.056**	**0.021**	**14.7**	**4.3**	**11.1**	**1.1**	**70**	**570**	**24.5**	**0.8**
60	**144**	**68**	**0.47**	**160**	**0.012**	**0.003**	**0.0019**	**0.0001**	**-0.09**	**0.045**	**0.014**	**11.5**	**3.3**	**12.11**	**0.85**	**-160**	**420**	**-5.3**	**-0.2**
61	**79**	**32**	**0.41**	**87**	**0.015**	**0.005**	**0.0020**	**0.0002**	**0.10**	**0.057**	**0.024**	**15.3**	**5.3**	**13.0**	**1.3**	**-240**	**640**	**15.0**	**0.4**
62	**124**	**47**	**0.39**	**135**	**0.012**	**0.004**	**0.0018**	**0.0001**	**0.18**	**0.047**	**0.015**	**12.3**	**3.6**	**11.6**	**0.85**	**-110**	**460**	**5.7**	**0.2**
63	**139**	**80**	**0.58**	**158**	**0.014**	**0.003**	**0.0019**	**0.0002**	**-0.11**	**0.058**	**0.014**	**14.4**	**3.2**	**12.3**	**1.0**	**330**	**420**	**14.6**	**0.7**
64	**179**	**104**	**0.57**	**203**	**0.014**	**0.003**	**0.0017**	**0.0001**	**0.07**	**0.057**	**0.016**	**13.7**	**3.3**	**11.02**	**0.75**	**250**	**450**	**19.6**	**0.8**
65	**188**	**101**	**0.55**	**212**	**0.014**	**0.003**	**0.0018**	**0.0001**	**0.15**	**0.057**	**0.012**	**13.9**	**2.8**	**11.51**	**0.74**	**360**	**370**	**17.2**	**0.9**
66	47	23	0.51	52	0.045	0.011	0.0021	0.0003	0.21	0.185	0.047	44	11	13.6	1.8	2130	570	69.1	2.8
67	**169**	**78**	**0.43**	**187**	**0.014**	**0.004**	**0.0018**	**0.0002**	**-0.22**	**0.062**	**0.018**	**13.9**	**3.9**	**11.7**	**1.0**	**310**	**480**	**15.8**	**0.6**
68	**78**	**35**	**0.45**	**86**	**0.015**	**0.006**	**0.0017**	**0.0002**	**0.04**	**0.064**	**0.034**	**14.7**	**6.0**	**10.6**	**1.3**	**40**	**740**	**27.9**	**0.7**

Table D-6: Zircon LA-ICP-MS U-Pb Isotopic Data and Ages: HP14-07 (IGSN: IEKHP0700[a]): Vitric ash of the Calvert mine, Norton County (435540, 4410579)[b]

Grain #[c]	U[d] [ppm]	Th[d] [ppm]	Th/U	eU[e] [ppm]	Corrected Isotopic Ratios							Ages (Ma)[j]						Disc. %[k]	Wtd. Disc.[l]
					^{207}Pb/^{235}U[f]	±2s[g]	^{206}Pb/^{238}U[f]	±2s[g]	Rho[h]	^{207}Pb/^{206}Pb[i]	±2s[g]	^{207}Pb/^{235}U	±2s	^{206}Pb/^{238}U	±2s	^{207}Pb/^{206}Pb	±2s		
69	169	78	0.43	187	0.009	0.003	0.0017	0.0001	0.04	0.049	0.014	8.9	2.6	10.96	0.86	-90	400	-23.1	-0.8
70	156	71	0.41	173	0.021	0.005	0.0018	0.0002	0.10	0.087	0.024	20.6	5.1	11.8	1.1	1030	520	42.7	1.7
71	302	121	0.44	330	0.013	0.002	0.0019	0.0001	0.16	0.053	0.009	13.0	1.9	12.01	0.67	350	280	7.6	0.5
72	120	44	0.36	130	0.010	0.003	0.0018	0.0002	-0.06	0.046	0.015	10.2	3.2	11.7	1.0	-80	460	-14.7	-0.5
73	88	34	0.39	96	0.015	0.006	0.0019	0.0003	-0.11	0.054	0.031	14.5	5.9	12.4	2.0	-30	760	14.5	0.4
74	98	40	0.40	108	0.012	0.004	0.0019	0.0002	0.17	0.044	0.019	12.4	3.9	12.5	1.2	-200	520	-0.8	0.0
75	197	106	0.52	222	0.012	0.003	0.0019	0.0002	0.04	0.044	0.011	12.0	2.8	12.07	0.98	-20	380	-0.6	0.0
76	140	48	0.34	151	0.013	0.003	0.0018	0.0002	-0.06	0.056	0.016	12.5	3.3	11.3	1.0	150	480	9.6	0.4
77	69	30	0.43	76	0.019	0.006	0.0022	0.0002	0.27	0.057	0.018	18.6	5.6	13.9	1.4	210	550	25.3	0.8
78	509	464	0.90	618	0.013	0.002	0.0019	0.0001	-0.02	0.054	0.008	13.0	1.8	11.92	0.49	310	280	8.3	0.6
79	229	111	0.48	255	0.013	0.003	0.0018	0.0001	-0.10	0.052	0.010	12.9	2.5	11.46	0.65	60	320	11.2	0.6
80	234	126	0.52	263	0.012	0.003	0.0017	0.0002	0.03	0.052	0.012	11.8	2.8	10.7	1.0	230	390	9.3	0.4
81	176	86	0.49	196	0.014	0.003	0.0019	0.0001	-0.10	0.054	0.013	14.0	3.1	12.35	0.82	200	390	11.8	0.5
82	177	85	0.47	197	0.012	0.004	0.0019	0.0002	-0.09	0.047	0.016	12.1	3.8	11.9	1.1	70	510	1.7	0.1
83	115	43	0.38	125	0.014	0.004	0.0019	0.0002	-0.12	0.056	0.015	13.9	3.9	12.0	1.2	330	460	13.7	0.5
84	96	39	0.41	105	0.024	0.006	0.0019	0.0002	0.19	0.104	0.028	24.0	5.5	12.2	1.2	860	540	49.2	2.1
85	150	77	0.50	168	0.015	0.003	0.0019	0.0001	-0.04	0.057	0.012	14.6	3.0	12.11	0.86	260	370	17.1	0.8
86	197	112	0.57	223	0.013	0.003	0.0017	0.0001	-0.03	0.058	0.014	13.1	3.0	10.7	0.82	350	420	18.3	0.8
87	173	89	0.50	194	0.032	0.004	0.0019	0.0001	0.27	0.137	0.020	32.2	4.2	12.13	0.85	1960	290	62.3	4.8
88	193	102	0.52	217	0.011	0.002	0.0018	0.0001	0.01	0.055	0.012	11.3	2.2	11.58	0.80	100	340	-2.5	-0.1
89	109	41	0.38	118	0.017	0.005	0.0018	0.0002	0.13	0.069	0.025	16.7	5.0	11.8	1.4	490	590	29.3	1.0
90	249	141	0.57	282	0.012	0.002	0.0018	0.0001	-0.06	0.053	0.011	12.1	2.2	11.52	0.68	190	330	4.8	0.3
91	133	56	0.43	147	0.016	0.003	0.0018	0.0001	0.02	0.071	0.016	16.0	3.4	11.58	0.88	530	420	27.6	1.3
92	173	91	0.53	194	0.014	0.003	0.0018	0.0002	0.07	0.058	0.014	13.8	3.1	11.65	0.94	220	390	15.6	0.7
93	197	114	0.57	224	0.013	0.003	0.0017	0.0001	0.13	0.057	0.014	12.5	3.1	10.83	0.87	270	440	13.4	0.5
94	106	40	0.37	116	0.014	0.005	0.0019	0.0002	0.04	0.052	0.022	13.5	4.8	12.5	1.3	-200	540	7.4	0.2
95	140	60	0.43	154	0.017	0.005	0.0018	0.0002	-0.04	0.067	0.021	16.6	5.0	11.3	1.2	530	580	31.9	1.1
96	221	136	0.62	253	0.013	0.002	0.0018	0.0001	-0.15	0.055	0.011	12.8	2.2	11.66	0.77	270	340	8.9	0.5
97	146	81	0.55	165	0.077	0.009	0.0024	0.0002	0.24	0.239	0.031	74.7	8.5	15.5	1.3	3030	220	79.3	7.0
98	141	66	0.42	157	0.013	0.003	0.0019	0.0002	0.06	0.060	0.016	13.3	3.3	12.4	1.0	170	430	6.8	0.3
99	113	41	0.35	122	0.012	0.004	0.0019	0.0002	-0.01	0.059	0.023	11.7	3.8	12.2	1.1	-80	500	-4.3	-0.1
100	194	102	0.52	218	0.012	0.003	0.0018	0.0001	-0.04	0.049	0.011	12.2	2.6	11.47	0.78	170	390	6.0	0.3
101	107	38	0.34	115	0.014	0.006	0.0021	0.0002	0.36	0.055	0.024	14.3	6.0	13.4	1.6	-110	630	6.3	0.2
102	203	107	0.48	228	0.011	0.002	0.0017	0.0001	-0.10	0.045	0.011	11.0	2.3	10.91	0.75	120	360	0.8	0.0

Table D-6: Zircon LA-ICP-MS U-Pb Isotopic Data and Ages: HP14-07 (IGSN: IEKHP0700[a]): Vitric ash of the Calvert mine, Norton County (435540, 4410579)[b]

					Corrected Isotopic Ratios							Ages (Ma)[j]							
Grain #[c]	U[d] [ppm]	Th[d] [ppm]	Th/U	eU[e] [ppm]	$^{207}Pb/^{235}U$[f]	±2s[g]	$^{206}Pb/^{238}U$[f]	±2s[g]	Rho[h]	$^{207}Pb/^{206}Pb$[i]	±2s[g]	$^{207}Pb/^{235}U$	±2s	$^{206}Pb/^{238}U$	±2s	$^{207}Pb/^{206}Pb$	±2s	Disc. %[k]	Wtd. Disc.[l]
103	**114**	**45**	**0.37**	**124**	**0.015**	**0.004**	**0.0019**	**0.0002**	**-0.01**	**0.055**	**0.016**	**14.8**	**3.8**	**12.3**	**1.0**	**190**	**470**	**17.2**	**0.7**
104	**116**	**59**	**0.49**	**130**	**0.015**	**0.004**	**0.0019**	**0.0002**	**0.10**	**0.060**	**0.019**	**15.2**	**4.4**	**12.2**	**1.2**	**190**	**530**	**19.7**	**0.7**
105	**212**	**108**	**0.48**	**237**	**0.011**	**0.003**	**0.0017**	**0.0001**	**-0.08**	**0.050**	**0.011**	**11.4**	**2.5**	**11.01**	**0.66**	**100**	**360**	**3.4**	**0.2**
106	**208**	**113**	**0.53**	**235**	**0.014**	**0.003**	**0.0019**	**0.0001**	**0.04**	**0.060**	**0.013**	**14.2**	**2.9**	**12.51**	**0.93**	**300**	**390**	**11.9**	**0.6**
107	**158**	**78**	**0.47**	**177**	**0.011**	**0.003**	**0.0017**	**0.0001**	**0.05**	**0.045**	**0.014**	**11.1**	**3.1**	**11.07**	**0.88**	**30**	**440**	**0.3**	**0.0**
108	99	53	0.53	111	0.068	0.008	0.0023	0.0002	0.10	0.240	0.033	68.6	7.9	14.8	1.2	2960	250	78.4	6.8
109	137	53	0.39	149	0.032	0.005	0.0018	0.0001	0.13	0.122	0.021	31.6	5.3	11.54	0.78	1730	400	63.5	3.8
110	**208**	**115**	**0.54**	**235**	**0.011**	**0.002**	**0.0018**	**0.0001**	**0.24**	**0.044**	**0.009**	**10.8**	**2.3**	**11.77**	**0.65**	**-80**	**320**	**-9.0**	**-0.4**
111	**107**	**48**	**0.43**	**118**	**0.013**	**0.004**	**0.0019**	**0.0002**	**0.11**	**0.051**	**0.018**	**13.1**	**4.1**	**12.0**	**1.1**	**20**	**520**	**8.4**	**0.3**
112	**231**	**118**	**0.50**	**259**	**0.010**	**0.002**	**0.0018**	**0.0001**	**0.10**	**0.043**	**0.008**	**10.0**	**1.9**	**11.7**	**0.75**	**-100**	**280**	**-17.0**	**-0.9**
113	**154**	**78**	**0.48**	**172**	**0.012**	**0.004**	**0.0019**	**0.0001**	**-0.04**	**0.051**	**0.015**	**12.3**	**3.8**	**11.88**	**0.88**	**60**	**460**	**3.4**	**0.1**
114	**178**	**101**	**0.53**	**202**	**0.011**	**0.003**	**0.0019**	**0.0001**	**-0.06**	**0.047**	**0.013**	**10.7**	**2.7**	**12.21**	**0.92**	**-140**	**380**	**-14.1**	**-0.6**
115	**154**	**64**	**0.39**	**169**	**0.013**	**0.003**	**0.0017**	**0.0002**	**0.15**	**0.049**	**0.015**	**12.6**	**3.3**	**11.15**	**0.97**	**100**	**430**	**11.5**	**0.4**
116	**162**	**70**	**0.44**	**178**	**0.011**	**0.002**	**0.0018**	**0.0001**	**0.06**	**0.046**	**0.012**	**10.6**	**2.3**	**11.62**	**0.89**	**-60**	**380**	**-9.6**	**-0.4**
117	207	108	0.52	233	0.046	0.006	0.0020	0.0002	0.09	0.175	0.024	45.0	5.5	13.16	0.96	2510	250	70.8	5.8
118	**151**	**61**	**0.41**	**165**	**0.012**	**0.003**	**0.0018**	**0.0001**	**-0.03**	**0.051**	**0.012**	**11.7**	**2.9**	**11.38**	**0.92**	**20**	**400**	**2.7**	**0.1**
119	**135**	**56**	**0.41**	**148**	**0.011**	**0.003**	**0.0018**	**0.0002**	**0.05**	**0.045**	**0.014**	**11.1**	**3.4**	**11.82**	**0.95**	**-50**	**440**	**-6.5**	**-0.2**
120	138	65	0.47	153	0.050	0.006	0.0024	0.0002	0.05	0.180	0.026	48.9	5.7	15.4	1.4	2380	280	68.5	5.9
121	**193**	**97**	**0.49**	**216**	**0.015**	**0.003**	**0.0019**	**0.0002**	**0.03**	**0.060**	**0.014**	**15.4**	**3.2**	**11.9**	**1.2**	**390**	**420**	**22.7**	**1.1**
122	**180**	**96**	**0.51**	**202**	**0.015**	**0.004**	**0.0019**	**0.0002**	**-0.09**	**0.064**	**0.018**	**15.1**	**3.8**	**12.1**	**1.2**	**220**	**440**	**19.9**	**0.8**
123	**192**	**97**	**0.47**	**215**	**0.013**	**0.003**	**0.0018**	**0.0002**	**0.18**	**0.056**	**0.014**	**12.8**	**2.7**	**11.67**	**0.96**	**150**	**380**	**8.8**	**0.4**
124	**199**	**116**	**0.58**	**226**	**0.013**	**0.002**	**0.0018**	**0.0001**	**0.07**	**0.055**	**0.011**	**12.8**	**2.4**	**11.30**	**0.67**	**200**	**330**	**11.7**	**0.6**
125	**123**	**49**	**0.39**	**135**	**0.016**	**0.005**	**0.0021**	**0.0002**	**-0.03**	**0.051**	**0.017**	**16.2**	**4.8**	**13.3**	**1.2**	**150**	**500**	**17.9**	**0.6**

[a]International Geo Sample Number (IGSN) registered in the SESAR database
[b]All locations reported as UTM coordinates using Zone 14 NAD 27
[c]Emboldened rows indicate the youngest measured concordant grains
[d]U and Th concentrations and Th/U ratios calculated relative to the GJ-1 zircon standard ID-TIMS values using 287 ± 76 ppm for U and 8.4 ± 2.6 ppm for Th (Jackson et al., 2004)
[e]Equivalent U defined by the equation: eU = U ppm + 0.235*Th ppm
[f]Corrected for U-Pb fractionation and background and normalized to the GJ-1 zircon standard ID-TIMS values: $^{207}Pb/^{235}U = 0.8093 \pm 0.0009$ and $^{206}Pb/^{238}U = 0.09761 \pm 0.00011$ (Jackson et al., 2004)
[g]Propagated uncertainty of internal uncertainties (2 SE) and within run reproducibility of GJ-1 (2 SE)
[h]Uncertainty correlation between $^{206}Pb/^{238}U$ and $^{207}Pb/^{235}U$ uncertainties
[i]Corrected for background and Pb isotopic fractionation using the GJ-1 zircon standard ID-TIMS value: $^{207}Pb/^{206}Pb = 0.06014 \pm 0.00001$ (Jackson et al., 2004)
[j]U-Pb ages calculated relative to the GJ-1 zircon standard
[k]Discordance defined as $[(^{207}Pb/^{235}U_{age} - ^{206}Pb/^{238}U_{age})/(^{207}Pb/^{235}U_{age})]*100$
[l]Uncertainty weighted age difference defined as $(^{207}Pb/^{235}U_{age} - ^{206}Pb/^{238}U_{age})/(^{207}Pb/^{235}U_{age\ uncertainty})$ for grains with $^{206}Pb/^{238}U$ ages <850 Ma and $(^{207}Pb/^{206}Pb_{age} - ^{206}Pb/^{238}U_{age})/(^{206}Pb/^{238}U_{age\ uncertainty})$ for grains with $^{206}Pb/^{238}U$ ages ≥850 Ma

Table D-7: Zircon LA-ICP-MS U-Pb Isotopic Data and Ages: HP14-05b (IGSN: IEKHP05b0[a]): Vitric ash of the Calvert mine, Norton County (435361, 4410678)[b]

					Corrected Isotopic Ratios							Ages (Ma)[j]							
Grain #[c]	U[d] [ppm]	Th[d] [ppm]	Th/U	eU[e] [ppm]	$^{207}Pb/^{235}U$[f]	±2s[g]	$^{206}Pb/^{238}U$[f]	±2s[g]	Rho[h]	$^{207}Pb/^{206}Pb$[i]	±2s[g]	$^{207}Pb/^{235}U$	±2s	$^{206}Pb/^{238}U$	±2s	$^{207}Pb/^{206}Pb$	±2s	Disc. %[k]	Wtd. Disc.[l]
1	89	53	0.60	101	4.114	0.069	0.2964	0.0036	0.64	0.100	0.002	1656	14	1673	18	1627	29	-1.0	-2.6
2	144	79	0.55	163	0.015	0.003	0.0017	0.0001	0.15	0.064	0.012	14.6	2.6	10.98	0.61	440	330	24.8	1.4
3	140	53	0.38	152	0.021	0.003	0.0018	0.0001	0.05	0.082	0.012	21.4	2.6	11.45	0.68	1160	270	46.5	3.8
4	828	478	0.58	940	0.050	0.004	0.0054	0.0002	0.19	0.067	0.005	49.2	3.5	34.8	1.2	810	150	29.3	4.1
5	121	104	0.86	145	1.006	0.038	0.0979	0.0026	0.46	0.075	0.003	704	19	602	15	1055	67	14.5	5.4
6	168	60	0.36	182	0.017	0.003	0.0017	0.0001	0.31	0.078	0.015	16.7	3.2	11.18	0.85	740	360	33.1	1.7
7	155	82	0.53	174	0.031	0.003	0.0019	0.0001	0.11	0.117	0.013	30.9	3.4	12.29	0.61	1950	220	60.2	5.5
8	279	191	0.68	324	0.395	0.010	0.0538	0.0010	0.65	0.053	0.001	337.1	7.5	337.7	6.1	337	48	-0.2	-0.1
9	227	92	0.41	249	0.015	0.002	0.0020	0.0001	0.05	0.050	0.007	14.5	2.0	13.16	0.56	190	250	9.2	0.7
10	190	108	0.57	215	0.015	0.002	0.0018	0.0001	0.00	0.064	0.010	15.4	2.2	11.86	0.48	630	290	23.0	1.6
11	155	68	0.44	171	0.019	0.003	0.0018	0.0001	-0.05	0.077	0.011	19.1	2.5	11.64	0.61	960	260	39.1	3.0
12	**190**	**106**	**0.56**	**215**	**0.011**	**0.002**	**0.0017**	**0.0001**	**0.05**	**0.048**	**0.009**	**11.1**	**2.0**	**10.97**	**0.46**	**70**	**300**	**1.2**	**0.1**
13	193	54	0.28	206	1.842	0.029	0.1761	0.0023	0.42	0.076	0.001	1060	10	1045	13	1096	35	1.4	3.9
14	**164**	**86**	**0.52**	**184**	**0.011**	**0.002**	**0.0018**	**0.0001**	**-0.15**	**0.050**	**0.010**	**11.2**	**2.1**	**11.73**	**0.57**	**120**	**300**	**-4.7**	**-0.3**
15	**129**	**73**	**0.57**	**146**	**0.011**	**0.002**	**0.0018**	**0.0001**	**-0.02**	**0.051**	**0.010**	**11.1**	**2.1**	**11.38**	**0.65**	**90**	**310**	**-2.5**	**-0.1**
16	210	108	0.51	235	0.020	0.003	0.0019	0.0001	-0.05	0.081	0.010	20.5	2.5	11.95	0.44	1120	260	41.7	3.4
17	228	130	0.57	259	0.014	0.002	0.0018	0.0001	0.17	0.059	0.007	14.4	1.5	11.45	0.55	470	200	20.5	2.0
18	177	93	0.53	199	0.015	0.002	0.0018	0.0001	0.13	0.063	0.009	15.2	2.0	11.44	0.48	610	250	24.7	1.9
19	211	86	0.41	231	0.019	0.003	0.0019	0.0001	0.16	0.067	0.012	18.6	3.3	11.94	0.93	670	370	35.8	2.0
20	**123**	**44**	**0.36**	**133**	**0.013**	**0.003**	**0.0017**	**0.0001**	**0.03**	**0.057**	**0.015**	**12.6**	**3.1**	**11.17**	**0.68**	**120**	**390**	**11.3**	**0.5**
21	192	95	0.49	214	0.023	0.003	0.0019	0.0001	0.18	0.089	0.012	22.5	3.2	12.04	0.70	1380	270	46.5	3.3
22	**168**	**70**	**0.42**	**184**	**0.011**	**0.002**	**0.0018**	**0.0001**	**0.02**	**0.044**	**0.010**	**11.0**	**2.3**	**11.54**	**0.55**	**30**	**320**	**-4.9**	**-0.2**
23	146	130	0.89	177	1.909	0.035	0.1828	0.0027	0.55	0.075	0.001	1083	12	1082	14	1082	36	0.1	0.0
24	152	92	0.61	174	2.147	0.059	0.1872	0.0033	0.67	0.082	0.002	1162	19	1109	18	1246	42	4.6	7.6
25	123	128	1.04	153	0.064	0.006	0.0055	0.0003	0.19	0.086	0.008	62.8	5.3	35.4	1.8	1200	180	43.6	5.2
26	123	57	0.46	136	0.017	0.003	0.0018	0.0001	0.13	0.071	0.012	17	3	11.63	0.60	780	330	31.6	1.8
27	177	97	0.55	200	0.030	0.004	0.0019	0.0001	-0.06	0.117	0.015	29.6	3.8	12.07	0.58	1810	260	59.2	4.6
30	**389**	**246**	**0.63**	**447**	**0.012**	**0.002**	**0.0018**	**0.0001**	**0.04**	**0.052**	**0.007**	**12.0**	**1.5**	**11.41**	**0.52**	**240**	**250**	**4.9**	**0.4**
31	163	78	0.48	181	0.045	0.004	0.0020	0.0001	-0.07	0.164	0.016	44.1	3.9	12.90	0.57	2220	210	70.7	8.0
32	221	118	0.53	249	0.025	0.003	0.0018	0.0001	0.14	0.100	0.012	24.8	3.0	11.54	0.5	1530	250	53.5	4.4

Table D-7: Zircon LA-ICP-MS U-Pb Isotopic Data and Ages: HP14-05b (IGSN: IEKHP05b0[a]): Vitric ash of the Calvert mine, Norton County (435361, 4410678)[b]

					Corrected Isotopic Ratios							Ages (Ma)[j]							
Grain #[c]	U[d] [ppm]	Th[d] [ppm]	Th/U	eU[e] [ppm]	$^{207}Pb/^{235}U$[f]	±2s[g]	$^{206}Pb/^{238}U$[f]	±2s[g]	Rho[h]	$^{207}Pb/^{206}Pb$[i]	±2s[g]	$^{207}Pb/^{235}U$	±2s	$^{206}Pb/^{238}U$	±2s	$^{207}Pb/^{206}Pb$	±2s	Disc. %[k]	Wtd. Disc.[l]
33	90	47	0.52	101	0.467	0.020	0.0049	0.0003	0.47	0.665	0.037	390	15	31.5	1.6	4661	91	91.9	23.9
34	169	92	0.54	191	0.065	0.008	0.0024	0.0001	0.44	0.205	0.022	63.2	7.6	15.15	0.70	2860	190	76.0	6.3
35	125	73	0.58	142	0.074	0.009	0.0024	0.0001	0.19	0.218	0.026	71.7	8.1	15.57	0.86	2920	210	78.3	6.9
36	**365**	**236**	**0.65**	**420**	**0.012**	**0.001**	**0.0017**	**0.0001**	**0.02**	**0.051**	**0.005**	**12.1**	**1.1**	**10.96**	**0.36**	**290**	**180**	**9.4**	**1.0**
37	104	59	0.57	118	0.133	0.016	0.0025	0.0002	0.47	0.366	0.035	126	15	16.4	1.3	3730	150	87.0	7.3
38	162	84	0.52	182	0.021	0.003	0.0018	0.0001	0.12	0.090	0.012	21.2	2.7	11.75	0.73	1140	290	44.6	3.5
39	188	87	0.46	208	0.033	0.003	0.0020	0.0001	0.01	0.124	0.014	33	3.2	12.91	0.61	1900	220	60.9	6.3
40	77	63	0.82	92	0.245	0.027	0.0035	0.0003	0.70	0.473	0.039	219	22	22.6	1.7	4140	130	89.7	8.9
41	137	79	0.58	156	0.020	0.004	0.0017	0.0001	0.05	0.086	0.016	20.1	3.6	10.83	0.66	1000	380	46.1	2.6
43	170	85	0.50	190	0.021	0.004	0.0018	0.0001	0.01	0.085	0.018	21.1	3.8	11.73	0.76	1190	400	44.4	2.5
44	146	71	0.49	163	0.013	0.003	0.0016	0.0001	0.06	0.058	0.014	13.4	2.6	10.29	0.80	440	410	23.2	1.2
45	138	58	0.42	152	0.024	0.005	0.0018	0.0001	0.47	0.091	0.018	23.9	4.7	11.47	0.73	1180	390	52.0	2.6
46	225	119	0.53	253	0.079	0.006	0.0023	0.0001	0.64	0.247	0.016	77.0	5.6	14.87	0.63	3190	100	80.7	11.1
48	221	117	0.53	248	0.016	0.002	0.0017	0.0001	0.01	0.068	0.009	15.8	1.9	11.14	0.50	660	250	29.5	2.5
49	226	116	0.51	253	0.142	0.006	0.0030	0.0001	0.19	0.361	0.018	134.2	5.3	19.14	0.61	3726	74	85.7	21.7
50	211	106	0.50	236	0.045	0.005	0.0020	0.0001	0.46	0.166	0.018	44.7	4.5	13.09	0.60	2390	200	70.7	7.0
51	547	269	0.49	610	0.021	0.002	0.0017	0.0001	-0.06	0.085	0.008	20.6	1.8	11.01	0.40	1210	200	46.6	5.3
53	87	59	0.68	101	0.735	0.079	0.0080	0.0007	0.96	0.669	0.030	530	42	51.0	4.6	4650	73	90.4	11.4
54	204	110	0.54	230	0.043	0.004	0.0020	0.0001	0.32	0.162	0.014	42.4	3.7	12.62	0.58	2460	150	70.2	8.0
55	196	107	0.55	221	0.073	0.007	0.0023	0.0001	0.47	0.226	0.019	70.6	6.8	14.75	0.70	2980	150	79.1	8.2
56	**136**	**52**	**0.38**	**148**	**0.010**	**0.002**	**0.0017**	**0.0001**	**0.18**	**0.045**	**0.010**	**10.4**	**2.3**	**11.23**	**0.56**	**-50**	**320**	**-8.0**	**-0.4**
57	91	33	0.36	99	0.224	0.021	0.0037	0.0002	0.77	0.451	0.032	202	17	23.8	1.3	4030	110	88.2	10.5
58	**152**	**82**	**0.54**	**171**	**0.011**	**0.002**	**0.0018**	**0.0001**	**-0.01**	**0.050**	**0.009**	**11.3**	**2.1**	**11.36**	**0.47**	**10**	**300**	**-0.5**	**0.0**
59	**133**	**59**	**0.44**	**147**	**0.012**	**0.003**	**0.0017**	**0.0001**	**-0.02**	**0.054**	**0.014**	**12.1**	**3.0**	**11.24**	**0.63**	**140**	**410**	**7.1**	**0.3**
60	99	53	0.54	111	1.964	0.034	0.1879	0.0023	0.53	0.076	0.001	1102	12	1110	12	1096	33	-0.7	-1.2
61	152	34	0.22	160	0.111	0.005	0.0163	0.0003	0.06	0.050	0.002	107	4	104.3	1.9	188	89	2.5	0.6
62	155	64	0.41	170	0.015	0.002	0.0018	0.0001	0.20	0.063	0.009	15.8	2.4	11.74	0.58	470	270	25.7	1.7
63	**158**	**96**	**0.61**	**181**	**0.012**	**0.002**	**0.0019**	**0.0001**	**-0.05**	**0.046**	**0.009**	**11.6**	**2.0**	**11.95**	**0.54**	**50**	**280**	**-3.0**	**-0.2**
64	170	81	0.48	189	0.033	0.004	0.0019	0.0001	0.40	0.126	0.013	32.5	3.6	12.04	0.63	1980	220	63.0	5.7
65	**137**	**64**	**0.47**	**152**	**0.014**	**0.004**	**0.0018**	**0.0001**	**0.13**	**0.053**	**0.017**	**13.8**	**4.1**	**11.73**	**0.64**	**50**	**520**	**15.0**	**0.5**

Table D-7: Zircon LA-ICP-MS U-Pb Isotopic Data and Ages: HP14-05b (IGSN: IEKHP05b0[a]): Vitric ash of the Calvert mine, Norton County (435361, 4410678)[b]

					Corrected Isotopic Ratios							Ages (Ma)[j]							
Grain #[c]	U[d] [ppm]	Th[d] [ppm]	Th/U	eU[e] [ppm]	$^{207}Pb/^{235}U$[f]	±2s[g]	$^{206}Pb/^{238}U$[f]	±2s[g]	Rho[h]	$^{207}Pb/^{206}Pb$[i]	±2s[g]	$^{207}Pb/^{235}U$	±2s	$^{206}Pb/^{238}U$	±2s	$^{207}Pb/^{206}Pb$	±2s	Disc. %[k]	Wtd. Disc.[l]
66	**262**	**174**	**0.66**	**303**	**0.012**	**0.001**	**0.0018**	**0.0001**	**0.05**	**0.047**	**0.006**	**11.6**	**1.4**	**11.35**	**0.35**	**40**	**210**	**2.2**	**0.2**
67	**161**	**87**	**0.54**	**181**	**0.013**	**0.003**	**0.0018**	**0.0001**	**-0.13**	**0.054**	**0.011**	**13.2**	**2.8**	**11.53**	**0.58**	**210**	**340**	**12.7**	**0.6**
68	**114**	**57**	**0.50**	**127**	**0.011**	**0.003**	**0.0017**	**0.0001**	**0.02**	**0.046**	**0.012**	**10.9**	**2.5**	**10.80**	**0.57**	**60**	**340**	**0.9**	**0.0**
69	**163**	**80**	**0.49**	**182**	**0.011**	**0.002**	**0.0017**	**0.0001**	**0.26**	**0.046**	**0.011**	**10.8**	**2.4**	**10.64**	**0.52**	**110**	**350**	**1.5**	**0.1**
70	**182**	**101**	**0.55**	**206**	**0.010**	**0.002**	**0.0017**	**0.0001**	**0.03**	**0.042**	**0.007**	**9.7**	**1.7**	**11.11**	**0.52**	**-230**	**250**	**-14.5**	**-0.8**
71	**86**	**35**	**0.41**	**94**	**0.011**	**0.003**	**0.0018**	**0.0001**	**-0.12**	**0.044**	**0.015**	**11.7**	**3.4**	**11.75**	**0.68**	**-130**	**430**	**-0.4**	**0.0**
72	145	100	0.69	169	1.998	0.040	0.1838	0.0022	0.31	0.079	0.002	1113	14	1088	12	1163	37	2.2	6.3
73	167	90	0.54	188	0.033	0.004	0.0019	0.0001	0.07	0.125	0.016	32.5	3.7	12.44	0.70	1970	230	61.7	5.4
74	128	72	0.56	145	0.016	0.003	0.0017	0.0001	0.09	0.068	0.013	16.3	3.0	11.09	0.68	630	360	32.0	1.7
75	104	69	0.66	120	1.928	0.038	0.1830	0.0027	0.55	0.076	0.001	1091	13	1083	15	1098	35	0.7	1.0
76	121	54	0.45	134	0.017	0.003	0.0018	0.0001	0.15	0.069	0.014	16.7	3.0	11.27	0.73	730	370	32.5	1.8
77	160	89	0.56	181	0.041	0.005	0.0020	0.0001	0.29	0.145	0.015	40.9	4.5	12.84	0.65	2210	210	68.6	6.2
78	129	69	0.53	145	0.025	0.004	0.0018	0.0001	0.01	0.097	0.017	24.6	3.8	11.78	0.55	1370	340	52.1	3.4
79	181	106	0.59	206	0.127	0.010	0.0028	0.0001	-0.03	0.328	0.023	120.3	8.6	17.94	0.78	3518	98	85.1	11.9
80	155	76	0.49	173	0.029	0.004	0.0018	0.0001	0.06	0.123	0.018	29.0	3.8	11.82	0.70	1900	280	59.2	4.5
81	189	84	0.44	209	0.072	0.006	0.0022	0.0001	0.40	0.237	0.018	70.3	5.9	14.43	0.59	3050	130	79.5	9.5
82	375	125	0.33	404	0.045	0.003	0.0056	0.0001	0.20	0.059	0.003	44.1	2.5	35.71	0.76	540	120	19.0	3.4
83	**248**	**143**	**0.58**	**282**	**0.012**	**0.001**	**0.0018**	**0.0001**	**-0.05**	**0.051**	**0.006**	**12.4**	**1.4**	**11.3**	**0.46**	**260**	**220**	**8.9**	**0.8**
84	**216**	**113**	**0.52**	**243**	**0.012**	**0.002**	**0.0017**	**0.0001**	**0.26**	**0.047**	**0.007**	**12.0**	**1.7**	**11.13**	**0.41**	**50**	**230**	**7.2**	**0.5**
85	172	68	0.40	188	0.034	0.006	0.0019	0.0001	0.01	0.127	0.023	33.4	5.7	12.3	0.69	1400	330	63.2	3.7
86	**248**	**126**	**0.51**	**278**	**0.012**	**0.002**	**0.0019**	**0.0001**	**0.18**	**0.046**	**0.007**	**11.6**	**1.7**	**11.96**	**0.43**	**30**	**230**	**-3.1**	**-0.2**
87	**232**	**143**	**0.62**	**266**	**0.012**	**0.002**	**0.0017**	**0.0001**	**-0.16**	**0.055**	**0.008**	**12.2**	**1.8**	**10.97**	**0.45**	**340**	**280**	**10.1**	**0.7**
88	254	146	0.57	288	0.024	0.004	0.0018	0.0001	0.42	0.090	0.012	23.5	3.5	11.84	0.52	1320	270	49.6	3.3
89	**186**	**107**	**0.58**	**211**	**0.012**	**0.002**	**0.0018**	**0.0001**	**0.03**	**0.051**	**0.007**	**12.7**	**1.7**	**11.69**	**0.54**	**200**	**250**	**8.0**	**0.6**
90	145	77	0.53	163	0.026	0.004	0.0019	0.0001	0.17	0.103	0.016	25.6	3.6	12.15	0.70	1540	260	52.5	3.7
91	67	21	0.31	72	4.229	0.075	0.2973	0.0042	0.41	0.105	0.002	1681	14	1677	21	1704	33	0.2	1.3
92	77	35	0.45	85	2.765	0.059	0.2316	0.0038	0.49	0.088	0.002	1347	16	1342	20	1375	39	0.4	1.7
93	154	55	0.36	167	0.068	0.009	0.0023	0.0001	0.62	0.202	0.025	66.5	9.0	14.89	0.78	2580	270	77.6	5.7
94	**215**	**117**	**0.54**	**242**	**0.012**	**0.003**	**0.0017**	**0.0001**	**-0.12**	**0.050**	**0.013**	**11.8**	**2.8**	**10.97**	**0.66**	**260**	**420**	**7.0**	**0.3**
95	**220**	**114**	**0.52**	**247**	**0.012**	**0.002**	**0.0017**	**0.0001**	**-0.07**	**0.052**	**0.009**	**12.1**	**1.9**	**10.83**	**0.50**	**280**	**290**	**10.5**	**0.7**

Table D-7: Zircon LA-ICP-MS U-Pb Isotopic Data and Ages: HP14-05b (IGSN: IEKHP05b0[a]): Vitric ash of the Calvert mine, Norton County (435361, 4410678)[b]

Grain #[c]	U[d] [ppm]	Th[d] [ppm]	Th/U	eU[e] [ppm]	Corrected Isotopic Ratios							Ages (Ma)[j]						Disc. %[k]	Wtd. Disc.[l]
					$^{207}Pb/^{235}U$[f]	±2s[g]	$^{206}Pb/^{238}U$[f]	±2s[g]	Rho[h]	$^{207}Pb/^{206}Pb$[i]	±2s[g]	$^{207}Pb/^{235}U$	±2s	$^{206}Pb/^{238}U$	±2s	$^{207}Pb/^{206}Pb$	±2s		
96	**151**	**70**	**0.46**	**167**	**0.013**	**0.003**	**0.0018**	**0.0001**	**0.05**	**0.053**	**0.010**	**12.7**	**2.5**	**11.31**	**0.58**	**270**	**330**	**10.9**	**0.6**
97	171	73	0.43	188	0.025	0.004	0.0018	0.0001	0.05	0.101	0.016	24.4	3.6	11.57	0.58	1360	320	52.6	3.6
98	123	68	0.55	139	0.035	0.005	0.0020	0.0001	-0.10	0.135	0.020	34.4	4.8	12.75	0.67	2100	270	62.9	4.5
99	**277**	**164**	**0.59**	**316**	**0.012**	**0.001**	**0.0018**	**0.0001**	**0.16**	**0.047**	**0.006**	**11.9**	**1.4**	**11.70**	**0.41**	**60**	**200**	**1.7**	**0.1**
100	**137**	**51**	**0.37**	**149**	**0.012**	**0.003**	**0.0017**	**0.0001**	**0.07**	**0.045**	**0.012**	**12.4**	**3.0**	**11.17**	**0.60**	**220**	**380**	**9.9**	**0.4**
101	**177**	**90**	**0.51**	**198**	**0.014**	**0.003**	**0.0019**	**0.0001**	**0.34**	**0.058**	**0.012**	**14.1**	**3.0**	**12.05**	**0.52**	**340**	**370**	**14.5**	**0.7**

[a]International Geo Sample Number (IGSN) registered in the SESAR database
[b]All locations reported as UTM coordinates using Zone 14 NAD 27
[c]Emboldened rows indicate the youngest measured concordant grains
[d]U and Th concentrations and Th/U ratios calculated relative to the GJ-1 zircon standard ID-TIMS values using 287 ± 76 ppm for U and 8.4 ± 2.6 ppm for Th (Jackson et al., 2004)
[e]Equivalent U defined by the equation: eU = U ppm + 0.235*Th ppm
[f]Corrected for U-Pb fractionation and background and normalized to the GJ-1 zircon standard ID-TIMS values: $^{207}Pb/^{235}U = 0.8093 \pm 0.0009$ and $^{206}Pb/^{238}U = 0.09761 \pm 0.00011$ (Jackson et al., 2004)
[g]Propagated uncertainty of internal uncertainties (2 SE) and within run reproducibility of GJ-1 (2 SE)
[h]Uncertainty correlation between $^{206}Pb/^{238}U$ and $^{207}Pb/^{235}U$ uncertainties
[i]Corrected for background and Pb isotopic fractionation using the GJ-1 zircon standard ID-TIMS value: $^{207}Pb/^{206}Pb = 0.06014 \pm 0.00001$ (Jackson et al., 2004)
[j]U-Pb ages calculated relative to the GJ-1 zircon standard
[k]Discordance defined as $[(^{207}Pb/^{235}U_{age} - ^{206}Pb/^{238}U_{age})/(^{207}Pb/^{235}U_{age})]*100$
[l]Uncertainty weighted age difference defined as $(^{207}Pb/^{235}U_{age} - ^{206}Pb/^{238}U_{age})/(^{207}Pb/^{235}U_{age\ uncertainty})$ for grains with $^{206}Pb/^{238}U$ ages <850 Ma and $(^{207}Pb/^{206}Pb_{age} - ^{206}Pb/^{238}U_{age})/(^{206}Pb/^{238}U_{age\ uncertainty})$ for grains with $^{206}Pb/^{238}U$ ages ≥850 Ma

Table D-8: Zircon LA-ICP-MS U-Pb Isotopic Data and Ages: HP14-08 (IGSN: IEKHP0800[a]): Calcrete near Almena, Norton County (439726, 4415082)[b]

					Corrected Isotopic Ratios							Ages (Ma)[j]							
Grain #[c]	U[d] [ppm]	Th[d] [ppm]	Th/U	eU[e] [ppm]	$^{207}Pb/^{235}U$[f]	±2s[g]	$^{206}Pb/^{238}U$[f]	±2s[g]	Rho[h]	$^{207}Pb/^{206}Pb$[i]	±2s[g]	$^{207}Pb/^{235}U$	±2s	$^{206}Pb/^{238}U$	±2s	$^{207}Pb/^{206}Pb$	±2s	Disc. %[k]	Wtd. Disc.[l]
1	306	112	0.38	332	1.839	0.048	0.1774	0.0040	0.70	0.076	0.002	1058	17	1055	22	1088	42	0.3	1.5
2	401	364	0.92	487	0.039	0.002	0.0059	0.0002	0.10	0.049	0.003	39.2	2.3	38.1	1.1	120	120	2.8	0.5
3	57	22	0.37	62	0.085	0.010	0.0117	0.0005	0.01	0.054	0.007	81.9	9.1	74.6	3.3	260	220	8.9	0.8
4	144	57	0.38	157	1.863	0.058	0.1773	0.0049	0.60	0.075	0.002	1066	20	1052	27	1085	53	1.3	1.2
5	117	53	0.46	129	3.068	0.090	0.2485	0.0058	0.67	0.090	0.002	1423	23	1430	30	1434	48	-0.5	0.1
6	947	113	0.05	974	4.259	0.098	0.2962	0.0061	0.78	0.104	0.002	1684	19	1671	30	1687	33	0.8	0.5
7	237	13	0.05	240	4.280	0.110	0.2982	0.0060	0.76	0.105	0.002	1687	21	1682	29	1705	37	0.3	0.8
8	328	94	0.29	350	1.906	0.044	0.1820	0.0034	0.65	0.076	0.002	1082	16	1078	19	1089	40	0.4	0.6
9	350	107	0.30	375	4.347	0.120	0.2987	0.0071	0.71	0.106	0.002	1703	22	1684	35	1739	39	1.1	1.6
10	95	39	0.42	104	2.103	0.069	0.1968	0.0048	0.33	0.077	0.003	1156	23	1158	26	1132	69	-0.2	-1.0
11	108	54	0.52	121	3.111	0.077	0.2464	0.0051	0.49	0.091	0.002	1437	19	1419	26	1451	43	1.3	1.2
12	95	47	0.50	105	1.894	0.056	0.1809	0.0041	0.30	0.075	0.002	1076	20	1074	22	1071	59	0.2	-0.1
13	245	119	0.49	273	0.081	0.006	0.0115	0.0004	0.17	0.051	0.004	79.6	5.7	73.6	2.3	220	140	7.5	1.1
14	380	245	0.66	438	0.033	0.003	0.0049	0.0002	-0.05	0.048	0.004	32.9	2.5	31.3	1.1	200	170	4.9	0.6
15	90	56	0.55	103	3.134	0.079	0.2483	0.0046	0.41	0.091	0.002	1439	19	1429	24	1462	40	0.7	1.4
16	**330**	**177**	**0.51**	**372**	**0.016**	**0.002**	**0.0021**	**0.0001**	**0.42**	**0.054**	**0.009**	**16.0**	**2.3**	**13.24**	**0.71**	**390**	**280**	**17.3**	**1.2**
17	462	159	0.35	499	0.092	0.004	0.0139	0.0004	0.08	0.049	0.002	89.6	3.9	88.9	2.2	139	80	0.8	0.2
18	204	103	0.48	228	0.040	0.003	0.0059	0.0003	0.09	0.048	0.005	40.3	3.3	37.6	1.6	200	180	6.7	0.8
19	101	47	0.46	112	1.913	0.060	0.1821	0.0044	0.54	0.076	0.002	1083	21	1078	24	1089	55	0.5	0.5
20	274	86	0.30	294	0.107	0.006	0.0159	0.0004	0.31	0.048	0.003	102.7	5.6	102	3	130	110	0.7	0.1
21	**148**	**65**	**0.42**	**164**	**0.014**	**0.003**	**0.0019**	**0.0001**	**-0.02**	**0.052**	**0.013**	**14.3**	**3.4**	**12.17**	**0.88**	**230**	**460**	**14.9**	**0.6**
22	833	667	0.81	990	0.176	0.006	0.0252	0.0006	0.46	0.050	0.002	164.2	5.2	160.6	3.5	181	67	2.2	0.7
23	75	53	0.72	87	1.872	0.057	0.1815	0.0042	0.48	0.075	0.002	1073	20	1075	23	1090	56	-0.2	0.7
24	103	103	0.98	127	0.039	0.005	0.0058	0.0003	0.22	0.049	0.006	38.5	4.9	37.3	1.9	180	230	3.1	0.2
25	184	61	0.33	198	4.252	0.100	0.2983	0.0061	0.65	0.103	0.002	1682	19	1682	30	1671	37	0.0	-0.4
26	**146**	**67**	**0.45**	**161**	**0.018**	**0.005**	**0.0021**	**0.0002**	**0.04**	**0.068**	**0.021**	**17.5**	**4.8**	**13.6**	**1.1**	**320**	**530**	**22.3**	**0.8**
27	379	103	0.27	403	0.034	0.003	0.0054	0.0002	0.18	0.046	0.004	33.4	2.5	34.7	1.1	30	150	-3.9	-0.5
28	161	60	0.34	175	1.916	0.050	0.1821	0.0036	0.36	0.077	0.002	1085	17	1078	20	1110	52	0.6	1.6
29	108	81	0.72	127	0.039	0.005	0.0055	0.0003	0.13	0.052	0.007	39.0	4.6	35.3	1.8	300	240	9.5	0.8
30	133	47	0.32	144	0.036	0.005	0.0055	0.0003	-0.09	0.050	0.007	36.6	4.6	35.2	1.9	250	250	3.8	0.3

Table D-8: Zircon LA-ICP-MS U-Pb Isotopic Data and Ages: HP14-08 (IGSN: IEKHP0800[a]): Calcrete near Almena, Norton County (439726, 4415082)[b]

					Corrected Isotopic Ratios							Ages (Ma)[j]							
Grain #[c]	U[d] [ppm]	Th[d] [ppm]	Th/U	eU[e] [ppm]	$^{207}Pb/^{235}U$[f]	±2s[g]	$^{206}Pb/^{238}U$[f]	±2s[g]	Rho[h]	$^{207}Pb/^{206}Pb$[i]	±2s[g]	$^{207}Pb/^{235}U$	±2s	$^{206}Pb/^{238}U$	±2s	$^{207}Pb/^{206}Pb$	±2s	Disc. %[k]	Wtd. Disc.[l]
31	647	68	0.11	663	4.387	0.096	0.3031	0.0052	0.73	0.104	0.002	1709	18	1706	26	1694	32	0.2	-0.5
32	**109**	**48**	**0.44**	**120**	**0.014**	**0.004**	**0.0020**	**0.0002**	**-0.01**	**0.052**	**0.016**	**14.3**	**4.3**	**12.9**	**1.0**	**30**	**480**	**9.8**	**0.3**
33	214	405	1.91	309	0.036	0.005	0.0048	0.0003	0.24	0.051	0.007	35.3	5.3	31.1	1.8	300	280	11.9	0.8
34	275	162	0.58	313	0.043	0.004	0.0067	0.0002	0.02	0.047	0.005	42.4	3.9	43.1	1.4	80	170	-1.7	-0.2
35	139	49	0.35	150	4.490	0.130	0.3076	0.0070	0.69	0.106	0.002	1733	23	1728	35	1720	42	0.3	-0.2
36	31	22	0.73	36	4.160	0.140	0.2827	0.0074	0.36	0.103	0.004	1663	27	1610	39	1691	71	3.2	2.1
37	89	53	0.59	102	1.883	0.053	0.1807	0.0033	0.37	0.076	0.002	1077	18	1071	18	1085	54	0.6	0.8
38	69	32	0.48	76	1.791	0.067	0.1741	0.0047	0.62	0.075	0.002	1043	24	1034	26	1064	60	0.9	1.2
39	364	191	0.54	409	0.042	0.003	0.0060	0.0002	0.08	0.048	0.004	41.2	3.3	38.8	1.4	100	150	5.8	0.7
40	**262**	**150**	**0.57**	**297**	**0.015**	**0.003**	**0.0020**	**0.0001**	**0.07**	**0.056**	**0.011**	**15.1**	**2.8**	**12.77**	**0.84**	**230**	**330**	**15.4**	**0.8**
41	155	86	0.56	175	1.943	0.050	0.1819	0.0036	0.28	0.076	0.002	1094	17	1077	19	1080	57	1.6	0.2
42	52	48	0.90	63	0.041	0.009	0.0066	0.0005	0.17	0.047	0.010	39.9	8.5	42.1	3.0	-110	320	-5.5	-0.3
43	61	74	1.22	79	2.751	0.089	0.2289	0.0046	0.37	0.087	0.003	1346	24	1328	24	1374	55	1.3	1.9
44	477	197	0.39	523	0.035	0.003	0.0055	0.0002	0.13	0.046	0.003	34.7	2.5	35.5	1.1	10	130	-2.3	-0.3
45	176	46	0.25	187	0.766	0.024	0.0944	0.0021	0.32	0.059	0.002	576	14	581	12	538	68	-0.9	-0.4
46	443	70	0.15	459	0.302	0.010	0.0416	0.0008	0.32	0.052	0.002	268	8	262.5	5.1	269	73	2.1	0.7
47	**652**	**290**	**0.44**	**720**	**0.013**	**0.001**	**0.0020**	**0.0001**	**0.08**	**0.047**	**0.004**	**12.9**	**1.1**	**12.76**	**0.52**	**80**	**160**	**1.1**	**0.1**
48	343	60	0.17	357	0.035	0.003	0.0054	0.0002	0.11	0.047	0.005	34.3	3.2	34.5	1.4	100	180	-0.6	-0.1
49	510	287	0.57	577	0.083	0.004	0.0127	0.0003	0.31	0.048	0.002	80.9	3.8	81.1	1.9	89	94	-0.2	-0.1
50	89	42	0.47	99	1.904	0.065	0.1811	0.0044	0.42	0.076	0.002	1084	22	1072	24	1079	61	1.1	0.3
51	152	47	0.30	163	0.029	0.005	0.0043	0.0002	0.06	0.050	0.009	29.1	5.3	27.5	1.5	100	320	5.5	0.3
52	105	55	0.52	118	4.240	0.130	0.2911	0.0073	0.42	0.105	0.003	1680	25	1652	35	1717	51	1.7	1.9
53	123	83	0.71	143	3.091	0.071	0.2448	0.0053	0.52	0.091	0.002	1431	18	1411	27	1443	44	1.4	1.2
54	1001	153	0.06	1037	2.280	0.120	0.1685	0.0077	0.95	0.097	0.002	1206	38	1002	43	1559	38	16.9	13.0
55	57	31	0.54	64	1.946	0.069	0.1837	0.0040	0.34	0.076	0.003	1093	24	1087	22	1102	66	0.5	0.7
56	201	59	0.30	215	4.331	0.110	0.2992	0.0061	0.73	0.104	0.002	1701	20	1686	30	1702	35	0.9	0.5
57	**182**	**104**	**0.53**	**206**	**0.012**	**0.003**	**0.0021**	**0.0001**	**-0.03**	**0.048**	**0.013**	**12.2**	**3.1**	**13.37**	**0.92**	**-190**	**370**	**-9.6**	**-0.4**
58	107	35	0.33	115	0.206	0.013	0.0303	0.0007	0.02	0.049	0.003	189	11	192.5	4.5	140	130	-1.9	-0.3
59	115	46	0.45	126	0.077	0.011	0.0113	0.0006	0.20	0.048	0.008	76	10	72.3	4.0	250	250	5.0	0.4
60	408	131	0.32	439	0.045	0.006	0.0061	0.0005	0.24	0.053	0.006	44.7	5.3	38.9	3.0	340	260	13.0	1.1

Table D-8: Zircon LA-ICP-MS U-Pb Isotopic Data and Ages: HP14-08 (IGSN: IEKHP0800[a]): Calcrete near Almena, Norton County (439726, 4415082)[b]

					Corrected Isotopic Ratios							Ages (Ma)[j]							
Grain #[c]	U[d] [ppm]	Th[d] [ppm]	Th/U	eU[e] [ppm]	$^{207}Pb/^{235}U$[f]	±2s[g]	$^{206}Pb/^{238}U$[f]	±2s[g]	Rho[h]	$^{207}Pb/^{206}Pb$[i]	±2s[g]	$^{207}Pb/^{235}U$	±2s	$^{206}Pb/^{238}U$	±2s	$^{207}Pb/^{206}Pb$	±2s	Disc. %[k]	Wtd. Disc.[l]
61	187	45	0.23	198	4.160	0.130	0.2861	0.0078	0.70	0.103	0.003	1663	26	1626	40	1678	47	2.2	1.3
62	100	51	0.49	112	0.080	0.010	0.0114	0.0005	0.07	0.052	0.006	77.9	8.9	73.2	3.0	300	220	6.0	0.5
63	648	207	0.30	697	0.105	0.004	0.0153	0.0003	0.37	0.049	0.002	101.1	3.5	98	2	143	77	3.1	0.9
64	238	99	0.43	261	0.042	0.005	0.0062	0.0003	-0.02	0.050	0.007	41.7	4.5	39.9	1.9	130	220	4.3	0.4
65	304	224	0.73	356	0.021	0.002	0.0032	0.0002	0.05	0.048	0.006	21.8	2.2	20.3	1.2	90	190	6.9	0.7
66	214	37	0.17	223	1.969	0.068	0.1859	0.0069	0.63	0.075	0.003	1104	24	1098	37	1067	66	0.5	-0.8
67	160	57	0.36	173	3.139	0.095	0.2509	0.0065	0.72	0.091	0.002	1443	23	1442	34	1437	46	0.1	-0.1
68	417	202	0.48	464	0.037	0.003	0.0052	0.0002	0.07	0.051	0.005	36.8	3.2	33.7	1.5	190	180	8.4	1.0
69	488	192	0.40	533	0.030	0.003	0.0046	0.0002	0.10	0.046	0.004	30.2	2.8	29.62	0.97	40	160	1.9	0.2
70	133	88	0.67	154	0.035	0.007	0.0051	0.0003	0.25	0.058	0.011	34.5	6.5	32.8	1.8	310	330	4.9	0.3
71	138	80	0.58	157	1.878	0.060	0.1813	0.0038	0.62	0.074	0.002	1071	21	1074	21	1042	51	-0.3	-1.5
72	534	23	0.05	539	0.491	0.015	0.0646	0.0016	0.69	0.055	0.001	408	11	403.6	9.6	413	56	1.0	0.4
73	560	226	0.41	613	0.030	0.002	0.0044	0.0001	0.07	0.050	0.004	29.5	2.1	28.0	0.9	170	150	5.1	0.7
74	1530	1080	0.71	1784	0.079	0.003	0.0119	0.0003	0.30	0.049	0.002	77.6	2.6	76.1	1.7	133	73	1.9	0.6
75	176	97	0.56	199	0.030	0.004	0.0040	0.0002	0.09	0.053	0.008	29.4	4.0	25.8	1.4	360	250	12.2	0.9
76	231	90	0.39	253	1.864	0.052	0.1774	0.0040	0.56	0.075	0.002	1070	18	1052	22	1082	48	1.7	1.4
77	342	127	0.40	372	0.115	0.011	0.0149	0.0007	0.20	0.053	0.006	110	10	95.1	4.7	310	190	13.5	1.5
78	244	103	0.40	268	4.600	0.150	0.3108	0.0081	0.87	0.107	0.002	1747	26	1743	40	1745	35	0.2	0.1
79	521	344	0.61	602	0.078	0.004	0.0118	0.0004	0.04	0.049	0.003	76.6	3.8	75.4	2.3	150	110	1.6	0.3
80	142	93	0.65	164	0.019	0.005	0.0022	0.0003	0.12	0.065	0.018	19.4	4.9	14.4	1.6	490	460	25.8	1.0
81	51	13	0.24	54	17.740	0.490	0.5800	0.0140	0.62	0.218	0.005	2972	27	2946	57	2959	40	0.9	0.2
82	103	28	0.24	110	4.572	0.110	0.3115	0.0072	0.60	0.106	0.002	1742	20	1747	36	1730	41	-0.3	-0.5
83	65	65	1.02	80	0.038	0.007	0.0059	0.0004	-0.03	0.049	0.010	37.1	7.2	37.9	2.4	100	340	-2.2	-0.1
84	858	185	0.18	901	0.078	0.003	0.0122	0.0003	0.36	0.047	0.002	75.8	2.9	78.3	1.9	48	77	-3.3	-0.9
85	104	40	0.37	114	3.046	0.095	0.2436	0.0064	0.66	0.091	0.002	1421	24	1404	33	1436	46	1.2	1.0
86	140	119	0.99	168	3.121	0.088	0.2508	0.0053	0.61	0.090	0.002	1435	22	1446	27	1418	43	-0.8	-1.0
87	88	63	0.69	103	0.073	0.009	0.0110	0.0005	0.24	0.048	0.005	71.3	8.1	70.4	3.4	170	200	1.3	0.1
88	157	85	0.52	177	3.166	0.082	0.2542	0.0058	0.56	0.091	0.002	1449	20	1459	30	1454	43	-0.7	-0.2
89	165	6	0.02	167	2.693	0.076	0.2285	0.0050	0.61	0.085	0.002	1326	20	1326	26	1329	44	0.0	0.1
90	386	87	0.23	406	0.038	0.002	0.0054	0.0002	-0.01	0.050	0.004	37.5	2.3	34.8	1.2	190	140	7.2	1.2

Table D-8: Zircon LA-ICP-MS U-Pb Isotopic Data and Ages: HP14-08 (IGSN: IEKHP0800[a]): Calcrete near Almena, Norton County (439726, 4415082)[b]

Grain #[c]	U[d] [ppm]	Th[d] [ppm]	Th/U	eU[e] [ppm]	Corrected Isotopic Ratios $^{207}Pb/^{235}U$[f]	±2s[g]	$^{206}Pb/^{238}U$[f]	±2s[g]	Rho[h]	$^{207}Pb/^{206}Pb$[i]	±2s[g]	Ages (Ma)[j] $^{207}Pb/^{235}U$	±2s	$^{206}Pb/^{238}U$	±2s	$^{207}Pb/^{206}Pb$	±2s	Disc. %[k]	Wtd. Disc.[l]
91	167	34	0.21	175	3.601	0.100	0.2702	0.0056	0.63	0.098	0.002	1547	22	1544	28	1579	43	0.2	1.3
92	437	128	0.29	467	0.031	0.002	0.0047	0.0002	0.39	0.050	0.004	31.4	2.4	30.4	1.1	210	140	3.2	0.4
93	216	107	0.47	241	0.027	0.004	0.0042	0.0002	-0.03	0.049	0.007	27.3	3.5	27.2	1.5	140	250	0.4	0.0
94	79	107	1.27	104	1.755	0.060	0.1734	0.0044	0.56	0.073	0.002	1026	22	1030	24	1007	61	-0.4	-1.0
95	260	76	0.27	278	0.031	0.003	0.0055	0.0002	0.05	0.043	0.005	31.2	3.2	35.6	1.4	-120	180	-14.1	-1.4
96	390	26	0.05	396	3.092	0.071	0.2481	0.0044	0.68	0.091	0.002	1429	18	1428	23	1456	37	0.1	1.2
97	223	153	0.69	259	0.033	0.004	0.0046	0.0002	0.39	0.051	0.006	33.3	4.0	29.5	1.5	170	210	11.4	0.9
98	165	123	0.74	194	0.034	0.004	0.0049	0.0003	0.24	0.051	0.006	33.7	3.8	31.5	1.8	240	230	6.5	0.6
99	336	29	0.05	343	0.481	0.017	0.0640	0.0016	0.60	0.055	0.001	398	12	399.5	9.6	414	61	-0.4	-0.1
100	223	217	0.96	274	0.174	0.009	0.0255	0.0007	0.22	0.050	0.003	163.6	7.7	162.5	4.7	190	100	0.7	0.1
101	725	134	0.18	756	0.343	0.010	0.0486	0.0011	0.52	0.052	0.002	300.6	8.2	305.7	6.9	289	63	-1.7	-0.6
102	668	292	0.44	737	0.032	0.002	0.0050	0.0002	0.15	0.048	0.003	32.2	1.9	31.82	0.93	110	120	1.2	0.2
103	90	38	0.44	99	1.826	0.057	0.1786	0.0035	0.42	0.074	0.002	1054	20	1059	19	1055	60	-0.5	-0.2
104	574	210	0.37	623	0.031	0.002	0.0044	0.0001	0.29	0.050	0.004	30.5	2.2	28.08	0.85	250	150	7.9	1.1
105	195	88	0.46	215	0.029	0.004	0.0043	0.0002	0.13	0.049	0.006	29.0	3.8	27.9	1.3	180	230	3.8	0.3
106	409	147	0.36	443	0.184	0.007	0.0271	0.0006	0.10	0.050	0.002	172.2	5.9	172.6	3.8	190	80	-0.2	-0.1
107	288	137	0.48	320	0.015	0.002	0.0022	0.0001	0.07	0.051	0.007	15.4	2.1	14.04	0.62	170	260	8.8	0.6
108	139	43	0.31	149	1.949	0.047	0.1850	0.0035	0.34	0.077	0.002	1099	17	1094	19	1105	53	0.5	0.6
109	347	49	0.10	358	3.114	0.086	0.2509	0.0058	0.69	0.090	0.002	1434	21	1442	30	1416	43	-0.6	-0.9
110	77	77	0.95	95	3.021	0.100	0.2500	0.0057	0.45	0.089	0.003	1414	24	1437	30	1395	56	-1.6	-1.4
111	216	70	0.32	232	0.029	0.004	0.0046	0.0002	-0.01	0.047	0.006	29.3	3.7	29.5	1.3	90	220	-0.7	-0.1
112	94	41	0.43	104	0.093	0.009	0.0140	0.0005	-0.06	0.048	0.005	90.3	8.4	89.3	3.4	70	190	1.1	0.1
113	127	51	0.38	139	1.932	0.081	0.1808	0.0053	0.64	0.077	0.002	1089	28	1071	29	1106	58	1.7	1.2
114	280	77	0.27	298	3.057	0.069	0.2490	0.0050	0.57	0.090	0.002	1422	18	1439	27	1424	42	-1.2	-0.6
115	307	119	0.38	335	0.062	0.004	0.0093	0.0003	0.13	0.047	0.003	60.5	3.9	59.6	1.8	90	130	1.5	0.2
116	152	65	0.43	167	4.275	0.098	0.3012	0.0053	0.53	0.104	0.002	1687	19	1697	26	1689	38	-0.6	-0.3
117	841	233	0.27	896	0.036	0.002	0.0057	0.0002	0.29	0.045	0.002	36.1	1.7	36.9	1.0	-7	86	-2.2	-0.5
118	364	149	0.40	399	0.034	0.007	0.0042	0.0003	-0.11	0.059	0.012	33.5	6.4	27.2	1.7	460	400	18.8	1.0
119	692	198	0.29	739	0.037	0.002	0.0056	0.0001	0.04	0.048	0.003	37.3	2.1	36.14	0.91	130	110	3.1	0.6
120	55	45	0.87	66	4.015	0.100	0.2838	0.0068	0.35	0.102	0.003	1640	21	1609	34	1651	54	1.9	1.2

Table D-8: Zircon LA-ICP-MS U-Pb Isotopic Data and Ages: HP14-08 (IGSN: IEKHP0800[a]): Calcrete near Almena, Norton County (439726, 4415082)[b]

Grain #[c]	U[d] [ppm]	Th[d] [ppm]	Th/U	eU[e] [ppm]	Corrected Isotopic Ratios							Ages (Ma)[j]						Disc. %[k]	Wtd. Disc.[l]
					$^{207}Pb/^{235}U$[f]	±2s[g]	$^{206}Pb/^{238}U$[f]	±2s[g]	Rho[h]	$^{207}Pb/^{206}Pb$[i]	±2s[g]	$^{207}Pb/^{235}U$	±2s	$^{206}Pb/^{238}U$	±2s	$^{207}Pb/^{206}Pb$	±2s		
121	392	78	0.19	410	0.240	0.010	0.0346	0.0008	0.29	0.050	0.002	217.7	7.8	219.4	4.8	217	83	-0.8	-0.2
122	149	127	0.86	179	0.023	0.004	0.0031	0.0002	-0.13	0.053	0.010	22.8	3.8	19.7	1.4	290	330	13.6	0.8
123	683	67	0.10	699	0.016	0.002	0.0022	0.0001	0.13	0.051	0.005	15.6	1.6	14.32	0.63	330	190	8.2	0.8
124	220	93	0.43	242	0.252	0.010	0.0366	0.0008	0.26	0.049	0.002	227.9	7.8	231.8	4.8	202	88	-1.7	-0.5
125	1020	263	0.28	1082	0.037	0.003	0.0055	0.0002	0.29	0.048	0.003	36.9	2.6	35.1	1.0	100	120	4.9	0.7
126	325	21	0.06	330	4.244	0.100	0.2958	0.0064	0.70	0.105	0.002	1681	20	1669	32	1706	37	0.7	1.2
127	297	224	0.76	350	1.865	0.050	0.1802	0.0043	0.65	0.076	0.002	1068	18	1068	24	1104	45	0.0	1.5
128	223	54	0.22	236	0.431	0.018	0.0582	0.0013	0.33	0.054	0.002	364	13	364.5	8.2	352	84	-0.1	0.0
129	385	138	0.33	417	0.042	0.003	0.0063	0.0002	0.01	0.051	0.004	41.7	3.2	40.4	1.4	220	170	3.1	0.4

[a]International Geo Sample Number (IGSN) registered in the SESAR database
[b]All locations reported as UTM coordinates using Zone 14 NAD 27
[c]Emboldened rows indicate the youngest measured concordant grains
[d]U and Th concentrations and Th/U ratios calculated relative to the GJ-1 zircon standard ID-TIMS values using 287 ± 76 ppm for U and 8.4 ± 2.6 ppm for Th (Jackson et al., 2004)
[e]Equivalent U defined by the equation: eU = U ppm + 0.235*Th ppm
[f]Corrected for U-Pb fractionation and background and normalized to the GJ-1 zircon standard ID-TIMS values: $^{207}Pb/^{235}U = 0.8093 \pm 0.0009$ and $^{206}Pb/^{238}U = 0.09761 \pm 0.00011$ (Jackson et al., 2004)
[g]Propagated uncertainty of internal uncertainties (2 SE) and within run reproducibility of GJ-1 (2 SE)
[h]Uncertainty correlation between $^{206}Pb/^{238}U$ and $^{207}Pb/^{235}U$ uncertainties
[i]Corrected for background and Pb isotopic fractionation using the GJ-1 zircon standard ID-TIMS value: $^{207}Pb/^{206}Pb = 0.06014 \pm 0.00001$ (Jackson et al., 2004)
[j]U-Pb ages calculated relative to the GJ-1 zircon standard
[k]Discordance defined as $[(^{207}Pb/^{235}U_{age} - ^{206}Pb/^{238}U_{age})/(^{207}Pb/^{235}U_{age})]*100$
[l]Uncertainty weighted age difference defined as $(^{207}Pb/^{235}U_{age} - ^{206}Pb/^{238}U_{age})/(^{207}Pb/^{235}U_{age\ uncertainty})$ for grains with $^{206}Pb/^{238}U$ ages <850 Ma and $(^{207}Pb/^{206}Pb_{age} - ^{206}Pb/^{238}U_{age})/(^{206}Pb/^{238}U_{age\ uncertainty})$ for grains with $^{206}Pb/^{238}U$ ages ≥850 Ma